Mechanism of poly(3-hydroxybutyrate-co-3-hydroxyhexanoate) depolymerization in superheated steam and characterization of the degradation products for biomaterial applications

著者	Dhurga Devi Rajaratanam
その他のタイトル	過熱水蒸気中でのポリ（３－ヒドロキシ酪酸-co-３－ヒドロキシヘキサン酸）の分解機構とバイオマテリアルとしての応用のための分解生成物の特性評価
学位授与年度	平成29年度
学位授与番号	17104甲生工第299号
URL	http://hdl.handle.net/10228/00006933

MECHANISM OF POLY(3-HYDROXYBUTYRATE-CO-3-HYDROXYHEXANOATE) DEPOLYMERIZATION IN SUPERHEATED STEAM AND CHARACTERIZATION OF THE DEGRADATION PRODUCTS FOR BIOMATERIAL APPLICATIONS

by

DHURGA DEVI RAJARATANAM

Graduate School of Life Sciences and Systems Engineering
Kyushu Institute of Technology

ACKNOWLEDGEMENTS

I would like to convey all praise be to Almighty god who gave me the inside, will and guidance towards the completion of the research. The completion of the research works and dissertation would be nearly impossible without the continuous guidance and contribution from the supervisors, fellow research colleagues, friends and family.

First and foremost, I would like to extend my deepest gratitude to my supervisors, Assoc. Prof. Dr. Hidayah Ariffin and Prof. Dr. Haruo Nishida for their kind support, motivation, sacrifice, constructive comments, guidance, enlightening lectures and for numerous invaluable discussions throughout the study. They have been always available to advice and to provide ideal solution to all the problems that I have faced in my research and I truly appreciate all the essential concepts from their perspectives. I also would like to express my heartfelt appreciation to my co-supervisor Prof. Dr. Mohd Ali Hassan for his suggestion and encouragement that greatly eased my study. My deepest appreciation also goes to Prof. Dr. Yoshihito Shirai for his continuous advice and guidance on the completion of dual-degree programme. My extended appreciation also goes to Dr. Nik Mohd Afizan Nik Abd. Rahman for his kind advice and for teaching me the cell culturing techniques of animal cells.

I also would like to express my deepest appreciation to my tutor, Dr. Satoshi Gomi and the fellow laboratory members, Dr. Takayuki Tsukegi, Dr. Reijiro Nogami, Mr. Yuuki Kawasaki, Mr. Taichi Furukawa, Mr. Kunimoto Kazutoshi, Mr. Masayuki Maeda, Mr. Shun Iwakiri, Mr. Tadahide Kitayama, Mr. Hiroshi Fujio, Mr. Fuma Koga, Mr. Rintaro

Hatase and all the academic and non-academic staffs from Kyushu Institute of Technology (KYUTECH) for assisting me during the conduct of experimental works at Japan. I also would like to thank environmental biotechnology research group and animal tissue culture laboratory members of Universiti Putra Malaysia (UPM), especially, Mr. Mohd. Nor Faiz Norrrahim, Mr. Syed Umar Faruq Syed Najmuddin, Ms. Zahiah Mohamed Amin, Ms. Koh May Zie and Ms. Nurliyana Mohd Yusof and others for their help and suggestions during the conduct of experimental works at UPM. I am grateful to all the members of our research group for their continuous support. I also would like to thank Japan Student Services Organization (JASSO) and Ministry of Higher Education Malaysia for the provision of scholarship.

Last but not the least; I owe my sincere gratitude to my parents and brother for their unconditional love, understanding, sacrifice and support throughout my life. Without their blessings and encouragement, this achievement would be impossible.

This list is far from exhaustive; I pray for forgiveness from those I did not mention by name and include them in my heart-felt gratitude.

TABLE OF CONTENTS

LIST OF FIGURES

LIST OF TABLES

LIST OF ABBREVIATIONS

PHA	Polyhydroxyalkanoate
PHB	Polyhydroxybutyrate
PHBHHx	Poly (3-hydroxybutyrate-*co*-3-hydroxyhexanoate)
SHS	Superheated steam
PLA	Poly(lactic acid)
T_c	Crystallization temperature
T_m	Melting temperature
T_g	Glass transition temperature
ΔH_m	Enthalpy of melting
M_w	Weight average molecular weight
M_n	Number average molecular weight
TG	Thermogravimetry
DTG	Differential thermogravimetry
DSC	Differential scanning calorimetry
SEC	Size-exclusion chromatography
NMR	Nuclear magnetic resonance
GPC	Gel Permeation Chromatography
WAXD	Wide Angle X-ray Diffraction
$CDCl_3$	Chloroform-d
TMS	Tetramethylsilane
t	Time

k	Rate constant
MPD	Most probable distribution
PDI	Polydispersity index
E_a	Activation energy
T_{d50}	Half weight loss temperature
A	Pre-exponential factor
$+I$	Inductive effect
$+R$	Resonance effect
PLLA	Poly(L-lactic acid)
MTT	3-(4,5-dimethylthiazol-2-yl)-diphenyl-tetrazolium bromide
NIH	National Institute of Health
DMEM	Dulbecco's modified eagle medium
DMSO	Dimethyl sulfoxide
ATCC	American Type Culture Collection
FBS	Fetal bovine serum

PUBLICATIONS AND CONFERENCES ATTENDED

1. Dhurga Devi Rajaratanam, Hidayah Ariffin, Mohd Ali Hassan and Haruo Nishida, 2016. Changes in diad sequence distribution by preferential chain scission during the thermal hydrolysis of poly(3-hydroxybutyrate-*co*-3-hydroxyhexanoate). *Polymer Journal*. 48, 839-842. Published.

2. Dhurga Devi Rajaratanam, Hidayah Ariffin, Mohd Ali Hassan, Yuki Kawasaki and Haruo Nishida, 2017. Effects of (*R*)-3-Hydroxyhexanoate units on thermal hydrolysis of poly((*R*)-3-hydroxybutylrate-co-(*R*)-3-hydroxyhexanoate)s. *Polymer Degradation and Stability*. 137, 58-66. Published.

3. Dhurga Devi Rajaratanam, Hidayah Ariffin, Mohd Ali Hassan, Nik Mohd Afizan Nik Abd Rahman and Haruo Nishida, 2017. *In vitro* cytotoxicity study of superheated steam hydrolyzed poly(3-hydroxybutyrate-*co*-3-hydroxyhexanoate) oligoesters for biomaterial applications. (Draft in preparation).

4. [Other Publications] Dhurga Devi Rajaratanam, Hidayah Ariffin, Mohd Ali Hassan and Haruo Nishida, 2017. Potential of superheated steam for the production of low molecular weight poly(3-hydroxybutyrate-*co*-3-hydroxyhexanoate). INTROPica, ISSN No.1985-4951, Issue 14 Jan 2017–June 2017.

5. [Poster Presenter] Dhurga Devi Rajaratanam, Hidayah Ariffin, Mohd Ali Hassan and Haruo Nishida, 2015. Evaluation of degradation products and kinetics of poly(3-hydroxybutyrate-*co*-3-hydroxyhexanoate) superheated steam hydrolysis. Asian Congress on Biotechnology (15^{th}–19^{th} November 2015). Istana Hotel, Kuala Lumpur, Malaysia.

6. [Oral Presenter] Dhurga Devi Rajaratanam, Hidayah Ariffin, Mohd Ali Hassan and Haruo Nishida, 2015. Evaluation of degradation products and kinetics of poly(3-hydroxybutyrate-*co*-3-hydroxyhexanoate) superheated steam hydrolysis for the production of biocompatible oligoesters. 3^{rd} International Symposium on Applied Engineering and Sciences (23^{rd}–24^{th} November 2015). Universiti Putra Malaysia, Selangor, Malaysia.

7. [Invited Speaker] Dhurga Devi Rajaratanam, Hidayah Ariffin, Mohd Ali Hassan and Haruo Nishida, 2017. Evaluation of degradation products and kinetics of poly(3-hydroxybutyrate-*co*-3-hydroxyhexanoate) during thermal hydrolysis for the production of biocompatible oligoesters. UPM-KYUTECH Joint Seminar (8^{th} March 2017). Universiti Putra Malaysia, Selangor, Malaysia.

ABSTRACT

Polyhydroxyalkanoates (PHAs) are microbial polyesters produced by wide range of bacteria as an intracellular energy reserve material under substrate limiting and at elevated carbon sources. Poly((*R*)-3-hydroxybutyrate-*co*-(*R*)-3-hydroxyhexanoate) (PHBHHx) is a copolymer in PHA family that is highly favorable due to its biodegradability, flexible mechanical properties, good melt-processability and biocompatibility. However, the intracellularly produced PHAs with high molecular weight (M_w) of 200-3000 kDa makes them undesirable for the production of specialty polymers that require a low, specific range of 1-25 kDa. Therefore, an effective degradation method is necessary to produce oligoesters with desired M_w range to produce specialty polymers for various applications. Thus, the present study aimed at the unprecedented oligoester production using superheated steam (SHS) treatment. The effect of SHS temperature and reaction time on the characteristics of hydrolyzed products were determined for PHBHHxs with different comonomer units, poly((*R*)-3-hydroxybutyrate-*co*-6%-(*R*)-3-hydroxyhexanoate and poly((*R*)-3-hydroxybutyrate-*co*-11%-(*R*)-3-hydroxyhexanoate.

The PHBHHx films that were prepared using compressed molding technique was used for hydrothermal degradation by SHS at the temperature range of 130–190 °C for 600–200 minutes and the M_W reduction was monitored precisely using size-exclusion chromatography (SEC). The obtained SHS hydrolyzed products were analyzed for their changes in chain-end structures, and thermal properties using proton nuclear magnetic

resonance (^{1}H NMR) spectroscopy, thermogravimetric analyzer (TGA) and differential scanning calorimetry (DSC). Based on the chain-end structure analysis, the PHBHHx oligoesters mainly had hydroxyl, crotonoyl and 2-hexenoyl groups. Moreover, the changes in diad sequence distribution during SHS hydrolysis was determined using carbon nuclear magnetic resonance (^{13}C NMR) spectroscopy and thermal degradation was conducted in TGA to clarify the SHS hydrolysis mechanism that resulted in the crotonoyl-chain ends. Based on the thermal degradation behaviors of PHBHHx, it was considered that HHx unit was relatively reactive to thermal β-elimination reaction at higher temperatures and the higher activation energy, E_a values of PHBHHxs during thermal degradation suggest that in the SHS hydrolysis, the β-elimination reaction gradually becomes a preferential mechanism with increased temperature.

The PHBHHx oligoesters with unsaturated chain ends and untreated PHBHHx were further evaluated for their *in vitro* cytotoxicity, using mouse fibroblast cell line NIH 3T3 to be used as a biomaterial. Based on the *in vitro* cytotoxicity results of 24 and 48 hr, the SHS treated PHBHHx oligoesters with unsaturated chain ends were found to be not toxic to the growth of mouse fibroblast NIH 3T3 cell line with cell viability percentage of more than 95%. In order to serve as a potential resorbable medical suture, PHBHHx oligoesters was blended with poly(L-lactic acid) (PLLA). The PHBHHX/PLLA (20:80) blend films were evaluated for their thermal, mechanical and surface wetting properties. The thermal properties measured in TG and DSC showed a good compatibility between PHBHHx oligoesters and PLLA components. The tensile strength of oligo(PHB-*co*-6%HHx)/PLLA and oligo(PHB-*co*-11%HHx)/PLLA were determined as 27 and 34 MPa respectively, which values were close enough to the desirable range of strength of

medical sutures: 37±10 MPa. In general, the current approach of SHS treatment for PHBHHx oligoester production appears to be a cost effective and greener method for the production of fast degrading medical sutures with improved mechanical properties by further consideration of blending method with PLLA.

CHAPTER 1

INTRODUCTION

1.1 Research overview

Biodegradable polymers are one of the interesting areas to be explored and there is a growing interest from the scientific world due to its broad spectrum of applications. According to Hassan *et al*. (2013), total usage of biodegradable polymers is estimated to increase by 13% per year within a time frame of six years (2009-2014). Biodegradable polymers play an important role in the solid waste management as it acts as an alternative to petroleum based applications, enhances chemical recycling as well as used in the production of biodegradable materials for biomedical applications (Parra *et al*., 2006; Djonlagic and Nikolic, 2011; Gumel *et al*., 2013; Montoro *et al*., 2013). Biodegradable polymers are widely used in biomedical field especially for controlled drug delivery as it can eliminate the conventional surgical procedures that commonly used in the drug delivery procedures (Montoro *et al*., 2013). Previously, biodegradable polymers were produced using dual synthesis and blending techniques in order to introduce a simple yet a cost-effective method (Gumel *et al*., 2013).

Polyhydroxyalkanoate (PHA) is a type of biodegradable plastic that could directly contribute to the solid waste management and act as an alternative to the traditional, petroleum based plastics. In general, biodegradable plastics can be divided into three

types as chemically synthesized polymers, starch-based biodegradable plastics and polyhydroxyalkanoates (Khanna and Srivastava, 2005; Hassan *et al*., 2013). Among various types of bioplastics, only PHAs are able to completely degrade under environmental or biological conditions as well as in animal tissues (Khanna and Srivastava, 2005; Chen, 2009). The PHAs which belongs to family of polyesters are being produced by a number of Archaea and many types of Gram-negative bacteria as an intracellular energy reserve material under the condition of substrate limitation as well as excessive carbon source both in aerobic and anaerobic environmental conditions (Prieto *et al*., 2007; Tian *et al*., 2009). Polyhydroxybutyrate (PHB) is the first, most common representative of polyhydroxyalkanoate (PHA) family and it is a homopolymer of 3-hydroxybutyric acid units (Khanna and Srivastava, 2005). Even though PHB biopolymers widely synthesized as renewable feedstocks, it is still considered as a brittle material (Sudesh *et al*., 2000; Hablot *et al*., 2008) which eventually limits its applications. According to Sudesh *et al*. (2000), this can be overcome by incorporating another monomer unit into the existing PHB biopolymer.

Poly (3-hydroxybutyrate-*co*-3-hydroxyhexanoate) (PHBHHx) is a random copolymer of PHA family (Zheng *et al*., 2005) that made up of (*R*)-3HB and (*R*)-3HHx units, having a propyl (C_3H_7) side chain (Sudesh *et al*., 2000). The PHBHHx copolymer exhibits better elastic, biocompatible properties compared to its homopolymer, PHB and make its desirable for biomedical applications (Zheng *et al*, 2005). Moreover, it was reported that the degradation products of PHBHHx (monomers and oligomers) does not results in toxicity effect and immuno-stimulations when it was used as an implant biomaterial (Chen, 2009). This desirable property of PHBHHx makes the oligoester to have wide

applications in biomedical field. Previously it was reported that the PHA oligomers exhibits a significant number of therapeutic as well as nutritional applications (Chen, 2009). In general, oligoesters are low molecular mass polymer or oligomers that contain two or more ester functional repeat units (Scandola *et al*., 2011; Alejandra *et al*., 2012; Ramier *et al*., 2012). Oligoesters can be used to produce specialty polymer that later can be utilized for various applications such as drug carriers, surgical pins as well as surgical sutures (Ravenelle and Marchessault, 2002; Kulkarni *et al*., 2008; Alejandra *et al*., 2012; Ramier *et al*., 2012). Due to the low molecular weight, the oligoesters generally possess higher biodegradation rate in comparison to the polymers which makes them desirable for biomedical applications as abovementioned.

The current trend of oligoesters production is via the utilization of petroleum based polyesters that could deplete by time and the multi-step petrochemical synthesis able to release harmful by-products to the environment. Moreover, Faler (2006) reported that the industrial production of macrocyclic oligoesters from linear polyesters requires usage of expensive equipment due to high viscosity of high molecular weight polyesters as well as several costly ending processes. Therefore, there is a great interest to produce the oligoesters biologically by utilizing a number of degradation methods of polyhydroxyalkanoate (PHA). To date, some of the reported methods that used to degrade the PHA polymers are enzymatic degradation (Sudesh *et al*., 2000; Mudoo *et al*., 2011; Rodriguez-Contreras et al., 2012; Alejandra *et al*., 2012), thermal degradation (Ariffin *et al*., 2010), hydrothermal degradation (Saeki *et al*., 2005) , acid hydrolysis and alkaline hydrolysis (Ramier *et al*., 2012). Therefore, superheated steam (SHS) was

introduced in the present study as an alternative method for the production of PHBHHx oligoesters.

1.2 Problem statement

The biodegradation attribute of PHA is one of the areas of interest as it can broaden the applications of PHA which is currently limited by its original high molecular weight (200 to 3000 kDa) (Sudesh *et al*., 2000; Ravenelle and Marchessault, 2002; Alejandra *et al*., 2012; Rondriguez-Contreras *et al*., 2012). The scientists and researchers around the world diverted their attention to make use of the available degradation technologies in order degrade the PHA polymers to produce oligoesters that can be used to produce specialty polymers for various applications (Gumel *et al*., 2013). To date, the common methods that used to degrade the PHA polymers are enzymatic degradation, thermal degradation, hydrothermal degradation, acid hydrolysis and alkaline hydrolysis (Ramier *et al*., 2012). However, each of the existing methods has its own disadvantage for the oligoester production. Thus, an effective, yet ecofriendly degradation method of PHBHHx is needed to enhance the oligoester production. In that case, hydrolysis procedure with the utilization of superheated steam (SHS), a type of unsaturated steam produced by the addition of heat to saturated steam, which enables the steam's temperature to exceed its boiling point (Bahrin *et al*., 2012) is a remarkable approach to produce the PHBHHx oligoesters.

1.3 Objectives of study

The aim of the present study is to introduce an efficient and eco-friendly degradation method of poly(3-hydroxybutyrate-*co*-3-hydroxyhexanoate) (PHBHHx) in order to produce a biocompatible, low molecular weight PHBHHx in the range of 1,200 to 25,000 Da for various biomedical applications. In designing such a method, it is crucial to identify the key factors that contribute to the controlled depolymerization of PHBHHx. Therefore, the objectives of the present study are:

1) To determine SHS treatment time and temperature for controlled depolymerization of PHBHHx into oligoester and to characterize the produced PHBHHx oligoesters
2) To evaluate the behavior and kinetics of PHBHHx depolymerization in order to identify the degradation mechanism occurring during the SHS treatment
3) To determine the *in vitro* cytotoxicity effect of superheated steam hydrolyzed PHBHHx oligoesters and the characteristics of PHBHHx oligoester/poly(L-lactic acid), PLLA blend for biomaterial applications

1.4 Thesis plan

The research work begins with the literature review on the biodegradable polymers followed by an introduction to the PHAs and its copolymer, PHBHHx which exhibits improved thermal and mechanical properties compare to other type of monomer units in

PHA family. Moreover, the currently existing degradation method for PHA oligoester production was discussed. The theory of PHA degradation mechanism and the factors affecting the degradation mechanism also highlighted. Finally, some of the available applications of PHA based oligomers, PHA applications in biomedical field and the potential application of PHA oligomers in biomedical field were also described.

Chapter 3 introduces SHS hydrolysis as an alternative method for the controlled depolymerization of PHBHHx into oligoesters and the resulted oligoesters were characterized for their structural, physical and thermal properties.

Chapter 4 evaluates the kinetics and degradation behavior of PHBHHx during the thermal hydrolysis. The expected SHS hydrolysis mechanism of PHBHHx was proposed based on the obtained characterization results.

Chapter 5 studies the *in vitro* cytotoxicity effect of SHS treated PHBHHx with low and high percentage of unsaturated chain ends for further biomaterial applications. The potential application for the PHBHHx oligoesters resulted from the SHS treatment also evaluated by blending it with poly(L-lactic acid) (PLLA).

In Chapter 6, the summary and conclusion of the present study were described. The recommendations for the future research also were highlighted.

CHAPTER 2

LITERATURE REVIEW

2.1 Polyhydroxyalkanoate (PHA)

2.1.1 Diversity and polymeric structure of PHA

Polyhydroxyalkanoate (PHA) is the most favorable polymer in the family of bio-based polymer (Figure 2.1) due to its attributes of biodegradable, biocompatible, diverse monomer units as well as nature origin via microbial fermentation (Wang *et al*., 2016). PHA was first discovered in 1923 as poly(3-hydroxybutyrate) (P3HB) by a French microbiologist, Maurice Lemoigne from the intracellular granules of *Bacillus megaterium*, a Gram-positive bacterium (Jendrossek *et al*., 1996; Keshavarz and Roy, 2010; Rai and Roy, 2011). The monomer unit of PHA relies on the type of carbon source that being supplied and choice of bacterial strain introduced during the production phase (Jendrossek *et al*., 1996) as well as the specific reaction site of PHA polymerase towards the incorporation of the monomer unit (Chen, 2010). In general, the PHAs can be classified as short-chain (3 to 5 carbon atoms), medium-chain (6 to 15 carbon atoms) and long-chain (more than 15 carbon atoms) length HAs based on the number of carbon atoms that found in its polymer chain (Reddy *et al*., 2003; Kunasundari and Sudesh, 2011). To date, there are more than 150 monomer units of PHA have been reported (Chen, 2010; Rai and Roy, 2011). The PHA with wide range of hydroxyalkanoate units can be synthesized using more than 75 different genera of both Gram positive and Gram

negative bacteria where the amount of intracelluarly accumulated PHA polymer can be up to 90% of cell dry weight (Reddy *et al*., 2003; Hassan *et al*., 2013). The general structure of PHA is shown in Figure 2.2.

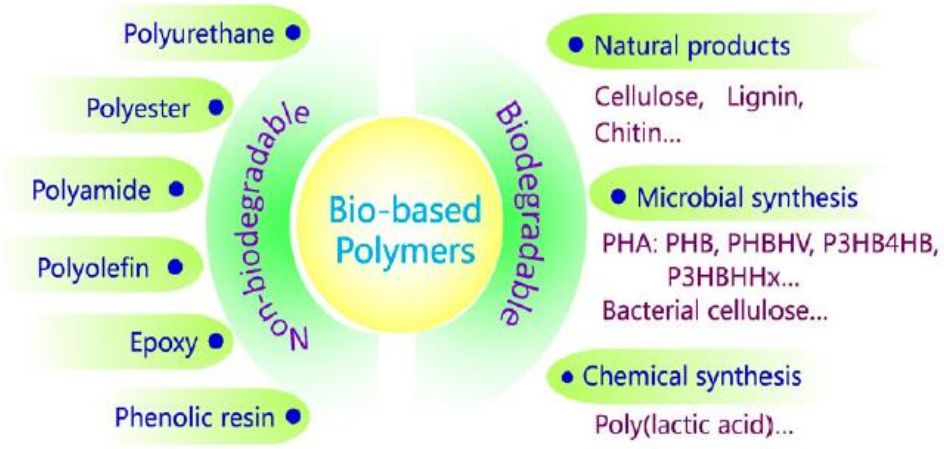

Figure 2.1. General classification of bio-based polymers
Source: Wang *et al.,* (2016)

In addition, PHA can exist as homopolymer or heteropolymer based on the type of monomer present in the polymer chain (Table 2.1). If only a single type of hydroxyalkanoate present as monomer unit, the PHA polymer is categorized as homopolymer such as P(3HB) or P(3HHx). On the other hand, if there is more than one kind of monomer present, the PHA polymer is categorized as heteropolymer such as hydroxybutyrate-*co*-3-hydroxyhexanoate, P(3HB-*co*-3HHx) (Rai and Roy, 2011). The different growth conditions using different bacterial strains able to produce various types of PHA homopolymers, random copolymers as well as block copolymers (Chen, 2010). According to Corre *et al*. (2012), either bacterial fermentation or chemical synthesis can be opt for the production of PHA copolymers with various HA units. It is reported that the type of monomers and the chemical structure of PHA greatly influences its

mechanical and physical properties (Rai and Roy, 2011). The PHA plays an important role as bioplastics, biofuels, bioimplants, foods and feeds as well as controlled drug delivery carriers (Chen, 2010).

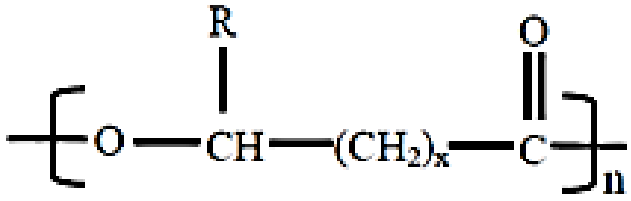

Figure 2.2. General structure of PHA
Source: Loo and Sudesh, (2007)

Table 2.1. The general structure of PHA

Number of 'CH_2' groups (x)	Type of side chain (R)	Type of polyhydroxyalkanoate (PHA)	
1	hydrogen	poly (-3-hydroxypropionate)	P(3HP)
	methyl	poly (-3-hydroxybutyrate)	P(3HB)
	ethyl	poly(3-horoxyvalerate)	P(3HV)
	propyl	poly (-3-hydroxyhexanoate)	P(3HHx)
	pentyl	poly (-3-hydroxyoctanoate)	P(3HO)
	nonyl	poly (-3-hydroxydodecanoate)	P(3HDD)
2	hydrogen	poly (-4-hydroxybutyrate)	P(4HB)
3	hydrogen	poly (-5-hydroxyvalerate)	P(5HV)

(Source: Ojumu *et al*., 2004)

Moreover, the molecular weight of PHAs that being produced intracellularly reported to be in the range of 200 to 3000 kDa (Sudesh *et al*., 2000; Ravenelle and Marchessault, 2002; Ojumu *et al*., 2004; Alejandra *et al*., 2012; Rondriguez-Contreras *et al*., 2012). Some of the common type of PHA producing bacterial strains and the resulted molecular weight is shown in Table 2.2. Based on Table 2.2, it can be seen that most of the bacterial strains produces PHA with high molecular weight. According to Montoro *et al*.

(2013), the mechanical strength, swelling properties, ease of hydrolysis and biodegradation rate of polymer greatly depends on the molecular weight of the PHAs. Therefore, for certain applications such as drug delivery, it's crucial to employ PHA polymers with low molecular weight as polymeric matrixes where it will increase the degradation rate and enables the absorption of target drug by the body (Montoro *et al*., 2013).

Table 2.2. Molecular weight of intracellularly produced PHA using different bacterial strains

Microorganism	Type of PHA	Molecular weight (Mw)	References
Escherichia coli XL1-Blue	P(3HB)	3–11 $\times 10^6$ Da	Zinn *et al*., 2001
Recombinant *Escherichia coli*	P(3HB)	2 $\times 10^7$ Da	Djonlagic and Nikolic, 2011
Cupriavidus necator NCIMB 11599	P(3HB)	848 $\times 10^6$ Da	Zahari *et al*., 2014
Cupriavidus necator DSM 545	P(3HB)	786$\times 10^3$ Da	Cavalheiro *et al*., 2009
Alcaligenes latus ATCC 29174	P(3HB)	507$\times 10^3$ Da	Yezza *et al*., 2007
Cupriavidus necator CCUG 52238^T	P(3HB)	812 $\times 10^3$ Da	Zahari *et al*., 2012
Comamonas sp. EB172	P(3HB-*co*-3HV)	622-838 $\times 10^3$ Da	Zakaria *et al*., 2013
Cupriavidus necator A-04	P(3HB-*co*-3HV-*co*-4HB)	177-1100$\times 10^3$ Da	Chanprateep, 2010
Aeromonas hydrophila 4AK4	P(3HB-*co*-3HHx)	4 $\times 10^5$ Da	Ye *et al*., 2010

2.1.2 Poly(3-hydroxybutyrate-*co*-3-hydroxyhexanoate)

The first and most common form of PHA that widely being used is PHB. However, the application of PHB in biomedical field is slightly limited due to its stiffeness and brittleness (Hablot *et al*., 2008; Rai and Roy, 2011). Recently, scientists reported that the incorporation of a second monomer into the polymer backbone can enhance the flexibility and toughness of the polymer besides decreasing its stiffness (Sudesh *et al*., 2000; Rai and Roy, 2011). Poly(3-hydroxybutyrate-*co*-3-hydroxyhexanoate), P(3HB-*co*-3HHx) is a desirable copolymer in PHA family where the small incorporation of 3HHx unit (5 mol%) into the backbone structure 3HB, significantly reduced the melting temperature from 180 to 155 °C whereby, enhanced the overall thermal and physical properties of the polymer that closely resembles commercial plastics such as PP and low density polyethylene (LDPE) (Loo and Sudesh, 2007). The chemical structure of PHBHHx is shown in Figure 2.3. The random copolymer of PHBHHx copolymer was produced for the first time via *Aeromonas caviaewas* from alkanoic acids with carbon atoms in the range of 12-18 and oil (Doi *et al*., 1995). PHBHHx exhibits estimated mole fraction of HHx in the range of 0-31 mol% (Chen *et al*., 2005b) and reported to have better mechanical properties and processing ability compared to PHB and poly((*R*)-3-hydroxyvalerate) (PHBV) (Wang *et al*., 2004).

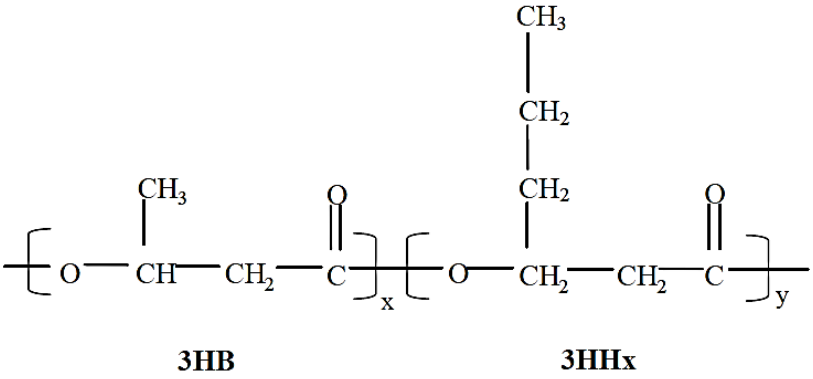

Figure 2.3. Chemical structure of poly(3-hydroxybutyrate-*co*-3-hydroxyhexanoate)

Source: Loo and Sudesh, 2007

2.1.3 Physical, mechanical and thermal properties of PHBHHx

In general, the thermal and mechanical properties of PHBHHx copolymer significantly depend on the content of comonomer unit. The thermal and mechanical properties of PHBHHx for different comonomer content obtained from the previous studies are listed in Table 2.3. Based on Table 2.3, it is obvious that as the content of 3HHx comonomer unit increased, the melting temperature, (T_m), glass transition temperature, (T_g) and enthalpy of melting, (ΔH_m) decreased. Despite of 3HHx content, the PHBHHx showed a relatively low tensile strength and Young's modulus, but exceptionally high elongation to break. Moreover, the lower T_g also indicates the ease of process ability of PHBHHx.

Table 2.3. Thermal and mechanical properties of PHBHHx

Samples	T_g (°C)	T_m (°C)	ΔH_m (J/g)	Tensile strength (MPa)	Young's Modulus (MPa)	Elongation at break (%)	Reference
PHB	4	177	97	43	-	5	Doi *et al*., (1995)
P(3HB-*co*-5%3HH)	0	151	69	-	-	-	
P(3HB-*co*-10%3HH)	-1	127	77	21	-	400	
P(3HB-*co*-15%3HH)	0	115	54	23	-	760	
P(3HB-*co*-17%3HH)	-2	120	34	20	-	850	
P(3HB-*co*-19%3HH)	-4	111	34	-	-	-	
P(3HB-*co*-25%3HH)	-4	52	19	-	-	-	
P(3HB-*co*-12%3HH)	-	-	-	20	-	500	Zhao *et al*., (2003)
P(3HB-*co*-7%3HH)	2	141	48	-	-	-	Cai and Qiu, (2009)
P(3HB-*co*-10%3HH)	3	139	42	-	-	-	
P(3HB-*co*-18%3HH)	1	-	-	-	-	-	
P(3HB-*co*-20%3HH)	-4	108	-	18	370	19	Zhao *et al*., 2012

From table 2.3, it is obvious that the incorporation 3HHx unit in the polymeric backbone structure significantly improved the elongation at break, with at least eighty times and higher compare to the homopolymer, PHB. Therefore, the right proportion of 3HHx unit in the PHBHHx copolymer structure contributes to its low crystallinity, high tensile strength than PHB and other copolymers in the PHA family.

2.1.4 PHA oligomers

Generally, oligomers obtained from microbial polyester, also known as oligoesters that contain two or more ester functional repeat units in its backbone structure (Scandola *et al*., 2011; Alejandra *et al*., 2012; Ramier *et al*., 2012). The weight average molecular weight (M_w) of PHA oligomers are reported to be in the range of 100 to 100, 000 Da, where the preferable range is 1,200 to 25, 000 Da (Scandola *et al*., 2011). Previously it was reported that the PHA oligomers exhibits a significant number of therapeutic as well as nutritional applications (Chen, 2009). Oligoesters can be used to produce specialty polymer that later can be utilized for various applications such as drug carriers, surgical pins as well as surgical sutures (Ravenelle *et al*., 2002; Kulkarni *et al*., 2008; Alejandra *et al*., 2012; Ramier *et al*., 2012). Scandola *et al*. (2011) also have reported that the PHA oligomers have potential applications in the field of controlled delivery, cosmetics, medicine (nano- or microsperes), as well as in households and coatings. Due to the low molecular weight, the oligoesters generally possess higher biodegradation rate in comparison to the polymers which makes them desirable for various applications.

In general, oligoesters can be produced from the polyesters by utilizing biological or conventional chemical synthesis. The current trend of oligoesters production is via the utilization of petroleum based polyesters that could deplete by time and the multi-step petrochemical synthesis able to release harmful by-products to the environment. Moreover, Faler (2006) reported that the industrial production of macrocyclic oligoesters from linear polyesters requires usage of expensive equipment due to high viscosity of high molecular weight polyesters as well as several costly ending processes. Thus, biological way of oligoester production via polyhydroxyalkanoate is a better option as the degradation rate can be controlled to produce the oligoesters of desired molecular weight for various applications.

The PHA oligomers were produced using a number of degradation methods including acid-catalyzed methanolysis, acid-base hydrolysis, enzymatic degradation as well as thermal degradation (Sin *et al*., 2011). Thermal degradation is the most common degradation method used to prepare PHB oligomer from high molecular weight PHB that results in the oligomers having *trans*-crotonate end groups as the main products (Scandola *et al*., 2011). The PHB oligomers with *trans*-crotonate end bear unsaturated double bond in its chemical structure, where it can be further oxidized with hydroxyl, and carboxyl or oxirane groups for further application. Due to the renewability and commercial availability, currently there is a great interest to produce the oligoesters biologically by utilizing a number of degradation methods of polyhydroxyalkanoate (PHA).

2.2 Degradation methods of PHA

Degradation can be defined as a reduction in the molecular weight of a polymer (Ariffin *et al*., 2008). Recently, scientists found that the opposite route which is the degradation of the polymers tend to be more effective than the conventional biodegradable polymer synthesis method in the production of specialty polymers for specific applications (Gumel *et al*., 2013). Moreover, Djonlagic and Nikolic (2011) reported that polymer chain must contain specific groups in order to be biodegraded. Among the different types of polyesters, only PHAs are able to completely degrade under environmental or biological conditions as well as in animal tissues (Khanna and Srivastava, 2005; Chen, 2009). In general polymers can be degraded or modified using a number of technologies such as biodegradation, oxidation, photo degradation, microwave irradiation, ozonization, ultrasonic irradiation as well as high-energy radiation (Gumel *et al*., 2013). To date, some of the reported methods that used to degrade the PHA polymers are enzymatic degradation, thermal degradation, hydrothermal degradation, acid hydrolysis and alkaline hydrolysis (Ramier *et al*., 2012). The enzymatic degradation usually occurs via enzymatic hydrolysis and other degradation methods which include thermal degradation, hydrothermal degradation, acid hydrolysis and alkaline hydrolysis are considered as non-enzymatic degradation methods (Chen, 2009). Currently, both enzymatic and non-enzymatic degradation are commonly used for PHA degradation in order to reduce the high molecular weight for the production of oligomers and monomers for various applications.

2.2.1 Enzymatic degradation

Enzymatic degradation is one of the common degradation techniques that used to degrade the PHA materials. According to Sudesh *et al*. (2000), the morphological analysis by electron microscopy shown that enzymatic degradation of the PHA polymers occurs via surface hydrolysis where the molecular weights of the PHA remain constant throughout the biodegradation process. This statement was supported by Mudhoo *et al*. (2011) which reported that this is mainly due to the physical structure of extracellular enzymes that too large to penetrate deep into the polymer materials. Thus, the enzyme was only able to react at the surface of the polymers and the reaction is considered as surface erosion. Moreover, Sudesh *et al*. (2000) also reported that the rate of enzymatic degradation directly proportional to the percentage of crystallinity in a PHA materials, where the degradation starts at the amorphous region and followed by the crystalline region. Later, Kulkarni *et al*. (2008) also agrees that enzymatic degradation occurs via surface erosion and the rate of water penetration into polymer matrix depends on porosity, crystallinity, hydrophobicity, surface roughness as well as the size of the polymer sample.

Most of the reported studies on PHA depolymerization utilized lipase and PHA depolymerase. The enzymatic degradation of PHA was first demonstrated 30 years ago by utilizing *Bacillus*, *Pseudomonas* and *Streptomyces* bacteria that uses specific type of PHA depolymerase (PHB depolymerase) that formed 3-hydroxybutyric acid as an end-product (Jendrossek *et al*., 1996). In general, PHA depolymerase that secreted from microorganisms can be divided into two subgroups, namely intracellular (i-PHA) and

extracellular (e-PHA) depolymerases (Rodriguez-Contreras *et al*., 2012; Loredo-Trevino *et al*., 2012).

The extracellular depolymerase unable to degrade the intracellular PHA granules while the intracellular depolymerase unable to degrade the extracellular PHA. This is mainly due to the differences in the physical structure of intracellular and extracellular PHA (Jendrossek *et al*., 1996; Mudhoo *et al*., 2011). The e-PHA depolymerase degrades the PHA polymers into monomers or oligomers and the resulted decomposed components will be used by the microorganisms (Rodriguez-Contreras *et al*., 2012). On the other hand, the lipase specificity can be subdivided as regioselectivity, substrate as well as enantioselectivity and among the three classes of specificity, regioselectivity lipases specifically reacts at certain position of the PHA polymers (Rodriguez-Contreras *et al*., 2012). Moreover, *Kaihara et al*. (2005) also reported that poly[(*R*-3-hydroxybutyrate)-*co*-12%(*R*-3-hydroxyvalerate)], P(3HB-*co*-12%3HHx) can be completely degraded into the desired oligomer using lipase. In general, the enzymatic degradation of polymer materials occurs via cleavage of hydrolytically or enzymatically sensitive bonds. However, the shortcoming of this enzymatic degradation for oligoester production is purification of final product prior to application.

2.2.2 Chemical degradation

Acid and alkaline hydrolysis generally can be regarded as chemical degradation. Alkaline hydrolysis is also commonly known as saponification and was first performed by Lemoigne in order to degrade his experimental bacterial biopolymer to reveal the structure of PHB (Alejandra *et al*., 2012). In recent years, Yu and Marchessault (2000) also used acidic and alkaline media conditions to study the structure of PHB. In general, acid-catalyzed hydrolysis results in linear oligomers with hydroxyl and carboxyl groups at their ends that exhibits very low amount of cyclic structures. On the other hand, the alkaline-catalyzed hydrolysis results in oligomers with hydroxyl and ester groups at their ends (Ramier *et al*., 2012).

According to Yu *et al*. (2005), acid and alkaline hydrolysis is possible for PHB where it occurs through random scission of ester bonds that results in soluble and insoluble oligomers as well as monomeric acids as end products (Figure 2.4). The acid and alkaline mechanism of PHB is shown in Figure 2.5. In general, the mechanism is similar to that of an ester. Previously, Yu and Marchessault (2000) reported that during acid hydrolysis (3N HCl, 105 °C), the ester bonds of both crystalline outer layer and non-crystalline inner layer of PHB granules are attacked by the acid. On the other hand, during the alkaline hydrolysis, sodium hydroxide was used to degrade PHB in the presence of methanol. This step yields different fractions of low molecular weight PHBs that exhibits a range of melting points (Yu and Marchessault, 2000). In both cases of acid and alkaline hydrolysis, the reactions are heterogeneous, occurs non-random and it

produces end products of double bonds due to dehydration of hydroxyl end. Moreover, the end products with double bond or crotonate end was mainly formed through transient structure of 6-membered ring state of PHB (Figure 2.6), with the presence of hydroxyl anions that results in the occurrence of simultaneous dehydration of 3-hydroxyl group and hydrolysis of ester bond (Yu *et al*., 2005).

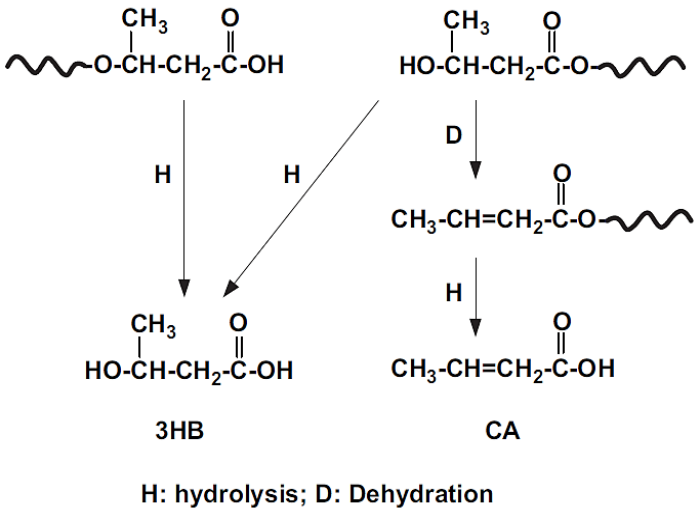

Figure 2.4. Proposed mechanism of PHB hydrolysis in alkaline solution

Source: Yu *et al*. (2005)

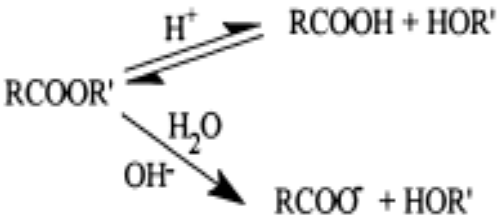

Figure 2.5. Acid and alkaline mechanism of PHB

Source: Yu and Marchessault, (2000)

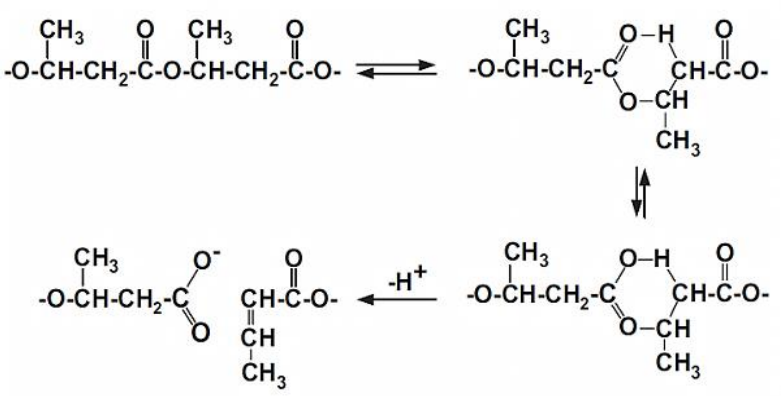

Figure 2.6. Crotonate formation via 6-membered ring transient state of PHB

Source: Yu *et al*. (2005)

However, the shortcoming of this chemical degradation for oligoester production is it involves water immersion and the final product needs further drying prior to application. Moreover, this degradation method also yields crotonate end group oligomers which might be not suitable for biomedical applications.

2.2.3 Thermal degradation

Thermal degradation of any polymer materials conducted at certain temperature range using several thermal analytical procedures such as pyrolysis (Gonzalez *et al*., 2005; Ariffin *et al*., 2010a), microwave-assisted degradation (Ramier *et al*., 2012), thermogravimetry (TG) (Sin *et al*., 2010) and others. The detailed thermal analytical procedures and its heating methods were previously reported by Nishida *et al*. (2010). Based on their studies, it is found that different heating method leads to different

degradation mechanism. In general, a number factors such as molecular weight, moisture content, functional group at the chain end, presence of residual metal compounds as well as hydrolyzed monomer or oligomer units contributes the overall process of thermal degradation regardless of the type of the aliphatic polyesters including (Kim *et al*., 2008).

The poly[(*R*)-3-hydroxybutyric acid] (PHB) is the well-known form of biologically produced polyester with melting and glass transition temperature of 180 °C and 4 °C respectively (Abe, 2006). It was reported that trans/cis-crotonic acids as well as oligomers that consist of dimers and trimers with the existence of crotonyl group at one of the chain end are the main thermal degradation products of PHB (Ariffin *et al*., 2010b). The thermal decomposed polymers are often analyzed using non-isothermal techniques such as differential thermogravitimetry (DTG) and differential scanning calorimetry (DSC). On the other hand, pyrolysis-gas chromatography/mass spectrometry (Py-GC/MS), nuclear magnetic resonance (NMR) and infrared spectroscopy are commonly used to analyze the volatile products (Abe, 2006). Previous studies reported that the presence of $CaCl_2$ and $MgCl_2$ in P[(*R*)-3HB] samples able to stimulate the degradation process but no changes was observed with addition of $ZnCl_2$ (Abe, 2006). The results prove that Ca^{2+} and Mg^{2+} ions actively participate in the thermal degradation process of PHB. This could be mainly due to the nature of Ca^{2+} and Mg^{2+} ions that act as Lewis acids (strong acids) that enables them to interact with carboxyl groups to form double bond of crotonyl group by eliminating a β-hydrogen (Abe, 2006; Ariffin *et al*., 2010b). Moreover, the Cl^- ions (weak base) does take part in the reaction as it unable to

conjugate with the proton of PHB chain. This is mainly due to the Bronsted-Lowry theory, where the stronger the acid, the weaker the base conjugation with the acid (Kawalec *et al*., 2010). Similarly, in the presence $Mg(OH)_2$ as catalyst, the activation energy as well as temperature was lowered (11-14kJ/mol and 40-50 °C respectively) and almost complete transformation of PHB into trans-crotonic acid was achieved (Ariffin *et al.*, 2010b).

Some of the reported thermal degradation mechanisms of PHAs are ß-elimination, ß-elimination in the presence of metal compounds, E1cB degradation mechanism as well as intermolecular transesterification (Table 2.4). The thermal degradation of PHA materials yields various end products. According to Ariffin *et al.* (2010), the thermal degradation of poly[(*R*)-3-hydroxybutyric acid] (PHB) yields CO_2, H_2O, propene, ketene, acetaldehyde, ß-butyrolactone, trans/cis-crotonic acid, 3-butanoic acid (BA), linear oligomers as well as cyclic trimers. However, the main products of thermal degradation of poly[(*R*)-3-hydroxybutyric acid] are either *trans* or *cis* crotonic acids and linear oligomers that consist of dimers and trimers with a crotonyl-end group (Ariffin *et al*., 2010b). On the other hand, Nguyen *et al*. (2001) reported that at moderately low temperature range of 170-200 °C, a well-defined poly(3-hydroxyalkanoates) oligomer with molecular weight range of 500-10000 Da was obtained. The oligomers exhibit an unsaturated end group (trans-alkyl and carboxylic end group).

Table 2.4. Thermal degradation mechanisms of PHA

Mechanisms	Description	End-Products
ß-elimination	- Proceeds based on the structures of pyrolysis products that contains crotonate end-group	1) Crotonyl chain end 2) Oligomers with crotonate end-group such as 3-Butenoic end
ß-elimination in the presence of metal compounds	- Proceeds based on the structures of pyrolysis products that contains crotonate end-group	1) Crotonyl chain end
E1cB degradation	- Proceeds thorough α-deprotonation by carboxylate anion	1) Crotonyl chain end
Intermolecular transesterification	- Proceeds thorough exchange of functional group	1) Cyclic trimer

Source: Nishida *et al*., (2010)

In general, thermal degradation is not suitable for all types of PHA as certain type of biopolymers are very sensitive to the temperature (Hablot *et al*., 2008). For an example, PHB and poly(3-hydroxybutyrate-*co*-3-hydroxyvalerate) (PHBV) exhibits a narrow processing window (Leja and Lewandowicz, 2010) where the degradation occurs very near to the melting point which makes them undesirable for melt processing via random scission process. A number of studies reported the PHA degradation affected by fermentation residues and plasticizers (Hablot *et al*., 2008). This is in agreement with a study conducted by Ramis *et al*. (2004) which reported that thermal degradation of polypropylene or starch-based materials occurs at high temperature range of 200-400 °C leads to chain scission and largely affected by the presence of impurities, such as unsaturation sites, head-to-head units. The presence of metal compounds in thermal degradation favors the production of desired end-product. Studies conducted by Ariffin

et al. (2010b) and Kim *et al*. (2008) shown that the presence of Magnesium (Mg) compounds enhanced the thermal degradation of PHB towards the production of end-product that proceeds through ß-elimination and random chain scission mechanisms respectively.

Previously, mixed mechanism of thermal degradation pathway of PHB was proposed by Ariffin *et al*. (2008). The proposed thermal degradation pathway begins with generation of carboxyl compounds for auto-accelerated degradation where the carboxyl compounds randomly attack ester groups on polymer chains to stimulate the trans-esterification (Nguyen *et al*., 2002; Ariffin *et al*. 2008). Later, the degradation proceeds through *0*th-order weight loss process in the middle stage where kinetically favored scissions occurred at the chain ends of ester group neighbouring the crotonate end group to generate crotonic acid. The expected overall thermal degradation pathway of PHB is shown in Figure 2.7.

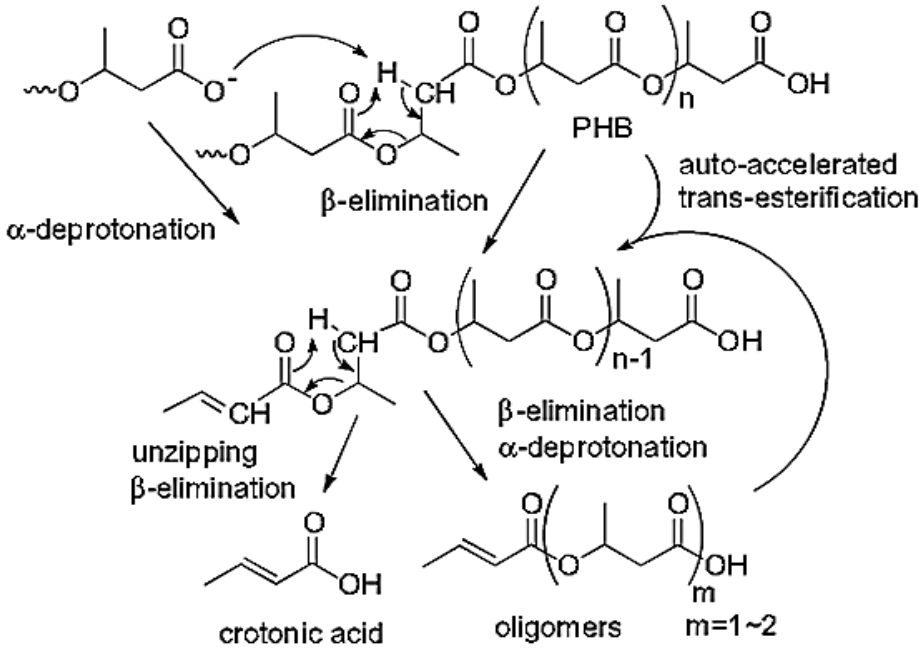

Figure 2.7. Expected thermal degradation pathway of PHB

Source: Ariffin *et al*. (2008)

Thermal degradation is not desirable for oligoesters production that aimed for biomedical applications due to random chain scission that able to produce undesirable products such as crotonic acids that suggested to be toxic to the cell growth (Kaihara *et al*., 2005; Sun *et al*., 2007).

2.2.4 Hydrothermal degradation

Hydrothermal degradation is conducted at high temperature and high pressure in the presence of water (Saeki *et al*., 2005). Thus, it is also known as high temperature and high pressure (HHW) water or supercritical water treatment (Watanabe *et al*., 2009). In the hydrothermal process, the water exhibits various roles such as a solvent, reactant, catalyst as well as a product (Qadariyah *et al*., 2011; Kruse and Dinjus, 2007). This is in agreement with Kruse and Dinjus (2007) findings, where the temperature and density changes the characteristics of hot compressed water (HCW). In the same study they reported that the water tend to act as an acid or base catalyst precursor due to the position of ionic products more than three orders of magnitude compare to its position at ambient conditions when it was subjected to below the critical temperature or at elevated pressure. Previously, study conducted by Mohd-Adnan *et al*. (2008) reported that highly pressurized steam in a temperature range of 100-130 ℃ was able to degrade poly(L-lactic acid) effectively. In a biomass depolymerization study, it was found that water facilitates the degradation process via hydrolysis where the structure of biomass was first break down by hot compressed water and followed by the reaction of water molecules (Kruse and Dinjus, 2007).

According to Saeki *et al*. (2005), the hydrothermal treatment of poly[(*R*)-3-hydroxybutyric acid] resulted in the molecular weight degradation without the formation of any oligomers that proceeded randomly via bulk erosion mechanism. During the bulk erosion, the water molecules can easily penetrate through the polymer matrix and react

with specific bonds that lead to the cleavage at the amorphous phase. Moreover, the hydrothermal treatment conducted at high temperature and high pressure water (180–300 °C, 360 min) as well as involves water immersion. This attributes makes the hydrothermal treatment undesirable for oligoesters production as further drying treatment required for the wet polymeric materials. Moreover, Kaihara *et al*. (2005) also reported the possibility of crotonate end oligomers formation via hydrolytic degradation due to the elimination of water molecules at the hydroxyl terminal of polymer chain. The resulted crotonate end group oligomers also might be toxic to the cells in biomedical applications (Sun *et al*., 2007). The shortcomings of currently existing degradation methods of PHA for oligoester production are summarized in Table 2.5.

Table 2.5. Existing degradation methods of PHA

Degradation methods	Disadvantages of the methods for oligoester production	References
Enzymatic hydrolysis	-Recovery is needed due to solvent immersion (using PHB depolymerases, lipase)	Alejandra *et al*., 2012; Sudesh *et al*., 2000
Thermal degradation	-Occurs randomly- produces undesirable products (Crotonic acid group which might be toxic to cell)	Ramier *et al*., 2012; Ariffin *et al*., 2008; Sun *et al*., 2007
Hydrothermal degradation	-Conducted at high temperature and high pressure water (180–300 °C ,360 min)	Saeki *et al*., 2005
Acid Hydrolysis	-Occurs randomly- produces undesirable products (Crotonic acid group which might be toxic to cell) - Recovery is needed due to solvent immersion	Yu *et al*., 2005; Yu and Marchessault, 2000; Sun et al., 2007
Alkaline hydrolysis	-Occurs randomly- produces undesirable products (Crotonic acid group which might be toxic to cell) - Recovery is needed due to solvent immersion	Yu *et al*., 2005; Yu and Marchessault, 2000; Sun et al., 2007

As shown in Table 2.5, the currently existing degradation methods of PHA has its own shortcomings for the oligoester production. The enzymatic hydrolysis requires further recovery due to solvent immersion (Alejandra *et al*., 2012; Sudesh *et al*., 2000). Also, the most commonly used thermal degradation occurs randomly and the final product, crotonic acid might be toxic to the living cells (Ramier *et al*., 2012; Ariffin *et al*., 2008; Sun *et al*., 2007). Similarly, acid and alkaline hydrolysis also occurs randomly and produces the undesirable final product, crotonic acid and additionally, it requires further drying/recovery due to solvent immersion (Yu *et al*., 2005; Yu and Marchessault, 2000; Sun *et al*., 2007). Finally, the hydrothermal degradation also not preferable for the oligoester production as it involves safety issues, where the treatment is conducted at high temperature (180–300 °C) and high pressure (Saeki *et al*., 2005).

2.3 Degradation mechanisms of PHA

2.3.1 Surface and bulk erosion mechanism

The degradation of biodegradable polymers mainly proceeds via surface or bulk erosion mechanisms (Figure 2.8). Polymer erosion is different from the degradation where the polymer erosion often regarded as physical phenomenon, but degradation process considered being a chemical phenomenon. During the bulk erosion, molecular weight of the polymer reduces significantly but there are no observable changes in its shape and size. In the case of surface erosion, molecular weight of the polymer does not change but thinning of the polymer due to mass loss at the exterior surface is observable (Gajjar and King, 2014). In general, the polymers underwent surface erosion at a constant velocity

throughout the erosion period, but it not possible in the case of bulk erosion (Gopferinch and Langer, 1993; Gopferinch, 1996).

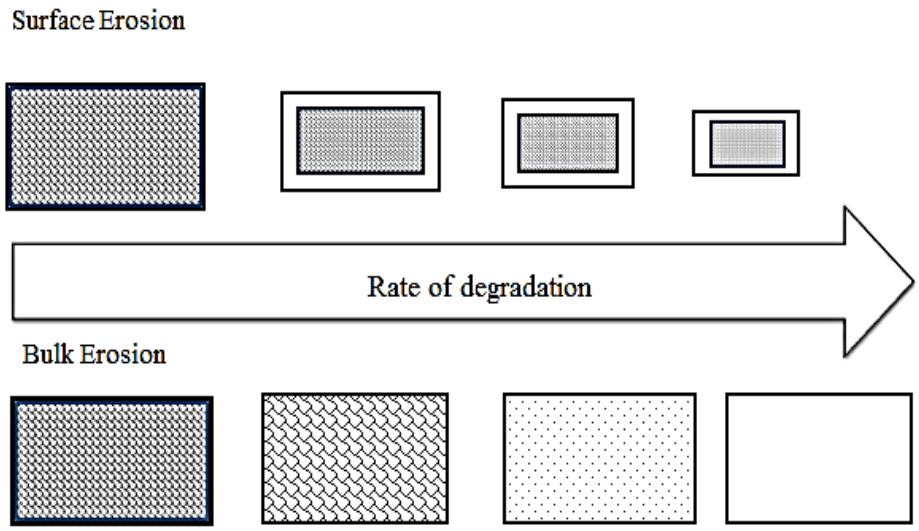

Figure 2.8. Mode of degradation

In an erosion model proposed by Burkersrodaa *et al*., (2002), it was speculated that the erosion mechanism of a polymer matrix mainly depends on the diffuse ability of the water molecules inside the polymer matrix and the degradation rate of the polymer's functional groups. Thus, the bulk erosion occurs when the rate of water diffusion into the polymer matrix faster than the degradation of polymer bonds. However, if the degradation rate of polymer bonds faster, the diffused water will hydrolyze the bonds on the polymer bonds whereby it prevents the diffusion of water into the bulk (Burkersrodaa *et al*., 2002; Lyu and Untereker, 2009).

2.3.2 Theories on hydrolysis kinetics

In general, the polyester underwent hydrolytic degradation via random scission of ester linkages that occurrs on the polymer chain (Lauzier *et al*., 1994). It was reported that the hydrolytic degradation of polyester is an autocatalytic reaction which was induced by their carboxylic end groups (Nishida *et al*., 2000a). The mechanism of polymer hydrolytic degradation will be initiated at amorphous region with the diffusion of water molecules as it unable to penetrate the densely packed crystalline region. At the amorphous region, water molecules will hydrolyze the ester bonds and as the hydrolytic degradation proceeds, the polymer gradually degraded into shorter chain with hydroxyl and carboxylic acid end group (Antheunis *et al*., 2010). At this point, the molecular weight of the polymer decreases due to the hydrolytic degradation, however, the physical properties remained unchanged as the matrix was held together by the crystalline regions (Gajjar and King, 2014).

The hydrolysis of polyester generates shorter chains with hydroxyl and carboxyl end groups that leads to the increased concentration of carboxylic acid end group. Since the hydrolytic degradation of polyester is an autocatalytic reaction, the formed carboxylic acid end groups will further catalyze and accelerate the hydrolysis process as shown in Figure 2.9. As the hydrolytic degradation precedes, the molecular weight of the polymer decreases and at certain point it becomes small enough to diffuse out from the bulk polymer where onset of mass loss occurs (Park, 1995).

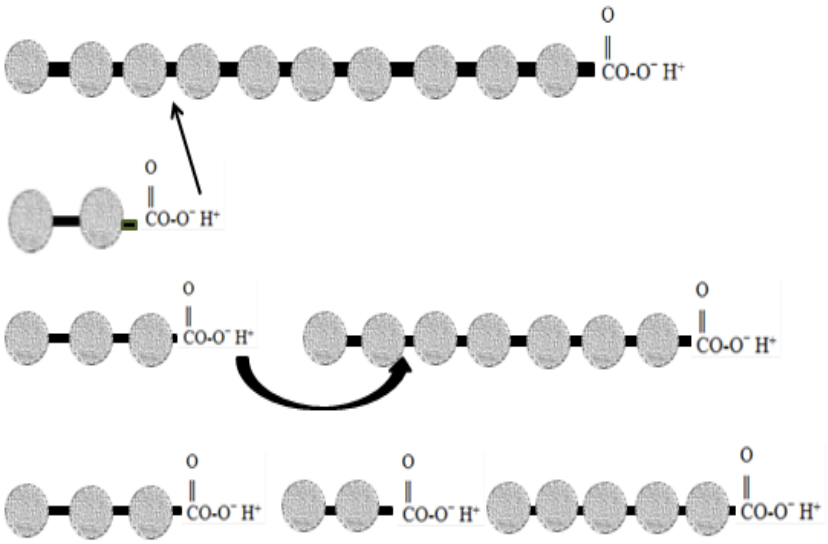

Figure 2.9. Autocatalytic reaction

Since the polyester underwent hydrolytic degradation via random scission, the polymer chains would have equal probability to be hydrolyzed. By using the kinetic relationship, the reaction pattern can be further confirmed. Previously, Yoon *et al*., (1997) proposed a kinetic model for non-autocatalytic reaction (Figure 2.10) during hydrolysis. In the non-autocatalytic reaction, the reactant does not contributes to the hydrolysis reaction. Yoon *et al*. (1997) proposed a kinetic model for non-autocatalytic reaction by taking account the changes in number-average molecular weight (M_n) as shown in Equation 2.1.

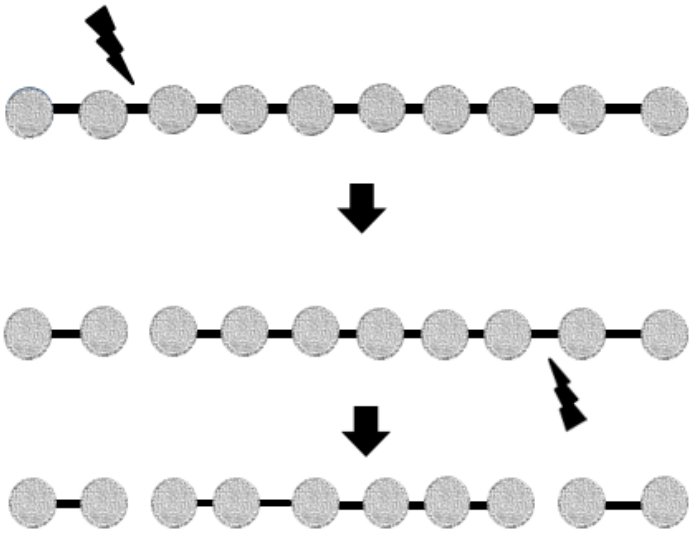

Figure 2.10. Non-autocatalytic reaction

$$\frac{t^{\frac{1}{3}}}{M_w} = \frac{1}{2}(kt)^{\frac{4}{3}} + \left(\frac{1}{M_{n0}}\right)^{\frac{1}{3}}\left(\frac{1}{M_{w0}} - \frac{1}{2M_{n0}}\right) \quad (2.1)$$

Where,

M_n = number average molecular weight value

M_{n0} = initial number average molecular weight value

M_w = weight average molecular weight value

M_{w0} = initial weight average molecular weight value

k = rate constant

t = time

Later, Nishida *et al*., (2000a) described the kinetic relationship of autocatalytic reaction during hydrolysis of polyesters by taking account weight loss of low molecular weight hydrolyzates for both number-average molecular weight (M_n) and weight-average molecular weight (M_w) as shown in Equation 2.2. The linear relationship of the equation predcits the auto-catalytic degradation mechanism of the polyester during hydrolysis reaction.

$$\ln M_n = \ln M_{n0} - kt$$
$$\ln M_w = \ln M_{w0} - kt \qquad (2.2)$$

Where,

M_n = number average molecular weight value

M_{n0} = initial number average molecular weight value

M_w = weight average molecular weight value

M_{w0} = initial weight average molecular weight value

k = rate constant

t = time

2.3.3 Factors affecting degradation mechanism of PHA

The PHA consists of amorphous (loosely packed) and crystalline (closely packed) regions. It is well accepted that the homogeneous hydrolytic degradation of polyesters occurs through random scission at the ester linkages of amorphous regions of polymer matrix where it accompanied with a reduction in M_w with unimodal distribution and relatively narrow polydispersity (Mohd-Adnan *et al*., 2008). On the other hand, heterogenous hydrolytic degradation results in a decrease of M_w with bimodal distribution, increased polydispersity and increased crystallinity. This is mainly due to the amorphous region that acts as a reactive site for hydrolysis to occur as it is more easilly accessible, causing difference in degradation rate at amorphous and crystalline region of the polymer (Qu *et al*., 2006b).

A number of properties of the original polymer, such as glass transition temperature and crystallinity can be significantly altered by the incorporation of the second monomer into the polymer chain. Previously Wang *et al*. (2002) observed that the increasing of 3-hydroxypropionate (3HP) unit from 0 to 48.8 mol% caused the crystallinity of the poly(3-hydroxybutyrate-*co*-3-hydroxypropionate) [P(3HB-*co*-3HP)] to decrease from 68% to below 10%. Moreover, it was also observed that the degradation rate of P(3HB-*co*-3HP) increased with reduction in crystallinity of the copolymers as the 3HP unit increased. In another study conducted by Wang *et al*. (2004) on the biodegadation of PHBHHx, PHB-*co*-12%HHx was found to degrade faster than PHB-*co*-5%HHx and PHB-*co*-20%HHx due to the combined effect of low crystallinity and rough, porous surface.

Moreover, the degradation of polymer was also influenced by its molecular weight. It had been reported in a study conducted by Tokiwa and Suzuki (1978), where the poly(ε-caprolactone) (PCL) diol with smaller molecular weight have been degraded faster during the enzymatic hydrolysis by *Rhizopusdelemar* lipase which indicates that the low molecular weight is favorable for biodegradation. Manavitehrani *et al*. (2016) also supported the fact that the higher molecular weight contributes to the slower degradation due to the bulky polymer chains. The rate of hydrolytic degradation was also found to be dependent on the temperature at which the degradation process takes place; the higher the temperature, the faster the degradation rate (Li and McCarthy, 1999).

2.4 Applications of PHA

2.4.1 Current application of PHA oligomers

As abovementined, PHA oligomers are currently produced using acid-catalyzed methanolysis, acid-base hydrolysis, enzymatic degradation as well as thermal degradation (Sin *et al*., 2011). Previously, it was reported that PHA oligomers exhibits potential applications in industrials, medicals as well as pharmaceuticals (Sin *et al*., 2011). In addition, low molecular weight PHAs can be used for controlled delivery systems in various fields including agro-chemistry, cosmetic industry, and pharmaceutical in the form of nano or microspheres, in household products and in coating systems (Scandola *et al*., 2011). On the other hand, Chen (2010) reported that PHA oligomers can be used as nutrients source for animals while the PHA monomers can be used in the synthesis of biofuels, drugs as well as chiral intermediates. Moreover, one of the *R*-3HB oligomer constituent, the *R*-3HB dimer has potential application as an optically pure building block for the development of useful recycling materials (Kaihara *et al*., 2005). In the agricultural field, the PHB oligomers are used to prepare the specialty graft such as grafting PHB oligomers into chitosan, a plant growth promoter (Yu and Marchessault, 2000). Besides, PHB oligomers also can be used to prepare block copolymers such as development of amphiphilic block copolymers of PHB onto poly(oxyethylene) (Yu and Marchessault, 2000). A number of other applications of PHA monomers and oligomers with selected examples are summarized in Table 2.6.

Table 2.6. Applications of PHA monomer and oligomers

PHA Monomer/ Oligomer	Field	Applications	References
PHA monomers (R-3HB)	Medical	Therapeutic agent for Alzheimers and Parkinson's diseases, osteoporosis and memory improvement	Chen, 2009
PHA oligomers	Healthy food additives	Used as food supplements to obtain ketone bodies	Chen, 2009
PHA monomers (chiral R-forms)	Fine chemical industry	Used as a starting materials in the synthesis of antibiotics and other fine chemicals	Chen, 2009
PHA oligomer (low molecular weight PHB)	Agriculture	Used to prepare biodegradable nanoparticles using amphiphilic triblock copolymer	Alejandra *et al*., 2012
PHA oligomer (R-3HB dimer)	Industrial	Act as optically pure building blocks that used in the synthesis of other useful materials	Kaihara *et al*., 2005
PHA oligomers Oligo-[*R*,*S*]-3-hydroxybutyrates	Medical	Act as a carrier in drug delivery	Piddubnyak *et al*., 2004
PHA copolymer oligomer (P(3HB-*co*-4HB)	Functional polymer	As a specialty polymer such as amphiphilic block copolymers	Rodriguez-Contreras *et al*., 2012

2.4.2 Biomedical applications of PHA

Nowadays, biodegradable polymeric materials are being investigated intensively to be used in biomedical applications. The current biomedical applications of biodegradable polymeric materials are as large implants such as bone screws, bone plates, contraceptive reservoirs as well as small implants that includes staples, sutures, nano- or micro-sized drug delivery systems, plain membranes for guided tissue regeneration and multifilament meshes or porous structures for tissue engineering (Nair and Laurencin, 2007). Due to the versatility of polymeric materials, they are rapidly replacing other material classes, such as metals, alloys and ceramics to be used as biomaterials. In 2003, the sales of polymeric biomaterials exceeded $7 billion, accounting for almost 88% of the total biomaterial market for that year. Moreover, some traditionally used polymers in the past such as silicone was suspected to induce cancer (Shrivastav *et al*., 2013). Therefore, there is a crucial need for the discovery of nontoxic, biodegradable and biocompatible polymers.

Biodegradable plastic which also known as biopolymer, able to replace the currently existing conventional polymers. Recently, many medical applications are being explored for PHA, a type of biodegradable plastic. PHAs have been used to develop devices including nerve repair devices, repair patches, cardiovascular patches, orthopaedic pins, adhesion barriers guided tissue repair/regeneration devices, nerve guides, tendon repair devices, bone-marrow scaffolds, tissue engineered cardiovascular devices, and wound dressings (Shrivastav *et al*., 2013).

Recently, Hazer (2010) reported that PHAs are promising materials for biomedical applications, particularly for tissue engineering and drug delivery due to their properties of natural, renewable, biodegradable and biocompatibility. The hydrolytic degradation product of PHB, 3HB unit is a commonly found metabolite in the blood of human body; therefore it does not cause any adverse effect when degraded in body through enzymatic hydrolysis. Moreover, the 3HB unit itself possesses pharmaceutical properties as their derivatives found to reduce the cell apoptosis (Manavitehrani *et al*., 2016). Shrivastav *et al*. (2013) also reported that PHA-degraded products are nontoxic in nature. The biodegradability attribute coupled with nontoxicity makes PHAs attractive biomaterials for biomedical applications. It was also found that the surface properties of PHA films enhance the cell attachment and proliferation which makes them desirable to be used as a scaffolding material in tissue engineering (Brigham and Sinskey, 2012). Moreover, *in vitro* tests have shown that PHB is biocompatible to various cell lines that consist of osteoblastic, epithelial cell and chondrocytes (Kai *et al*., 2003). This makes PHA a promising material for biomedical applications.

Among the PHA family, PHBHHx has gained immense interest to be used as implant material in comparison to PHB due to their better mechanical properties, biodegradability and biocompatibility with various cell lines (Yang et al., 2002; Qu *et al*., 2006a and 2006b). In tissue engineering applications, it is desirable that the scaffolds to be degraded as soon as possible after the serve the intended purpose of application and absorbed by the body to reduce the side effects (Yang *et al*., 2014). Wang *et al*. (2004) evaluated the biodegradability of PHBHHx with different HHx content against PHB and Ecoflex (marketed biodegradable polymer of BASF company).

It was found that after 18 days of incubation, 40% of PHBHHx, 20% of PHB and only 5% of Ecoflex was degraded from its original weight. PHBHHx films were degraded at faster rate compare to PHB, however, among the different percentage of HHx unit (5%, 12% and 20%), PHB-*co*-12%HHx had the highest degradation rate. It was concluded that the combination of low crystallinity and surface roughness plays an important role in degradation rate (Wang *et al*., 2004).

On the other hand, few studies have reported that when PHB and PHBV implanted *in vivo,* it have induced prolonged acute inflammatory responses, which could be mainly due to the incompatibility between the polymer surface and *in vivo* environments. A number of studies were reported on the effect of PHBHHx implantation towards different cell lines. In a study conducted by Yang *et al*. (2002), PHBHHx films promoted the cell proliferation of mouse fibroblasts L929 cell lines when cultured in high-density where the growth of cell lines were much better than those plated on PHB and polylactic acid (PLA) films. Later, Qu *et al*. (2006b) reported that PHBHHx film were found to be inert *in vivo* after implanted subcutaneously in rabbit as indicated by the thinnest surrounding capsule containing fibers and fibroblast that are free from inflammatory cells. In another study, Qu *et al*. (2006a) reported that PHBHHx films with high HHx unit significantly enhanced the differentiation of smooth muscle cells whereby it could be possibly used in blood vessel tissue engineering. The aforementioned studies prove that the PHBHHx films are highly biocompatible with various cell lines.

2.4.3 Potential biomedical application of PHA oligomers

In general, polyhydroxyalkanoate (PHA) monomer that being polymerized intracellularly exhibits high molecular weight (200 to 3000 kDa) (Sudesh *et al*., 2000) which makes it undesirable for the production of specialty polymers that requires a low, specific range of molecular weight (1-5 kDa) (Chen and Wu, 2005; Rodriquez-Contreras *et al*., 2012; Gumel *et al*., 2013). The molecular weight in the range of 1-5 kDa is useful in biomedical applications such as drug delivery, amphiphilic block copolymer, therapeutic agent and building block. The low molecular weight for this type of application indicates fast degradation. The reported preferable range of weight average molecular weight (M_w) of PHA oligomers is 1,200 to 25, 000 Da (Scandola *et al*., 2011). Chen *et al*. (2009) have reported that oligo[(*R*)-3-hydroxybutyrate]s (OHBs; less than 14 kDa) naturally exists in various organisms and they capable to form complex structure with inorganic polyphosphates, proteins as well as nucleic acids.

In a study of *in vitro* cytotoxicity conducted by Sun *et al*. (2007) for oligo-hydroxyalkanoates (OHAs); oligo[(*R*)-3-hydroxybutyrate], OHB (M_n 2,000), oligo[(*R*)-3-hydroxybutyrate-*co*-4-hydroxybutyrate], (O3HB4HB, M_n 2,100, 6 mol% 4-hydroxybutyrate), oligo[(*R*)-3-hydroxybutyrate-*co*-(*R*)-3-hydroxyhexanoate] (OHBHHx, M_n 2,800, 12 mol%3HHx), and mcl oligo[(*R*)-3-hydroxyalkanoate]s (M_n 2,400, 71.2 mol% 3HD), better biocompatibility and bioabsorbability was observed for the combination of more flexible chain and *R*3HB units. Therefore, the study serves as a guideline for the selection of PHA oligomers as biomaterials for further biomedical applications.

2.5 Concluding remark

Polyhydroxyalkanoate (PHA) oligomers have potential applications in various fields such as in controlled delivery, cosmetics, medicine (nano- or microsperes), as well as in households and coatings. Despite it uses in many fields, PHA oligomers currently not well explored. The study on PHA oligomers mainly limited by the current trend of oligoesters production which is via the utilization of petroleum based polyesters that could deplete by time and the multi-step petrochemical synthesis able to release harmful by-products to the environment. Nevertheless, the currently existing PHA degradation methods, acid-catalyzed methanolysis, acid-base hydrolysis, enzymatic degradation, thermal degradation and hydrothermal degradation have its own shortcomings for the further application, especially to be used in biomedical field. However, PHA oligomers have a good, potential application in biomedical field due to its attributes of fast biodegradability and biocompatibility with various cell lines. Therefore, by introducing an alternative, greener production method of PHA oligomers, it can be further evaluated and well utilized for biomedical applications than ever before.

CHAPTER 3

CONTROLLED DEPOLYMERIZATION OF POLY(3-HYDROXYBUTYRATE-*CO*-3-HYDROXYHEXANOATE) INTO OLIGOESTER AND THE CHARACTERISTICS OF OLIGOESTER PRODUCED

3.1 Introduction

Polyhydroxyalkanoates (PHAs) are microbial polyesters produced by many types of bacteria as an intracellular energy reserve material under substrate limiting conditions and in the presence of excessive carbon sources (Tian *et al*., 2009). The PHAs can be completely biodegraded into oligomers, monomers and then into carbon dioxide and water (Tripathi *et al*, 2012). The first and most common member of PHA, poly((*R*)-3-hydroxybutyrate) (PHB) is polymerized as high molecular weight polymer in the range of 200 to 3,000 kDa with a perfect chiral carbon isotactic structure of (*R*)-configuration only in nature (Sudesh *et al*., 2000) and more than 150 other monomer units have been reported to date (Keshavarz and Roy, 2010; Chen, 2010). Poly((*R*)-3-hydroxybutyrate-*co*-(*R*)-3-hydroxyhexanoate) (PHBHHx) is a copolymer in the PHA family that consists of randomly distributed (*R*)-3-hydroxybutyrate (HB) and (*R*)-3-hydroxyhexanoate (HHx) units (Yang *et al*., 2012). This type of copolymer exhibits improved mechanical properties and processability compared with those of PHB and poly((*R*)-3-hydroxyvalerate) (PHBV) (Wang *et al*., 2004).

The mole fraction of (*R*)-3HHx in PHBHHx varies according to the fermentation condition and estimated to be in the range of 0-31 mol% (Chen *et al*., 2005b). PHBHHx copolymers are currently produced on a large scale and have proven to be biocompatible in clinical studies using mouse fibroblasts cells, and rabbit articular cartilage-derived chondrocytes (Zheng *et al*., 2005), the most important factors for their practical applications. PHBHHx is a highly favorable copolymer of the PHB family due to its biodegradability, flexible mechanical properties and good melt processability. Due to attractive application of PHAs such as bioplastics for packaging, biomaterial for medical applications, biofuels as well as fine chemicals, intense interest has been diverted into PHA production (Tripathi *et al*., 2012). Nevertheless, the PHA oligomers also can be used as building block intermediates for the synthesis of useful materials such as block and graft copolymers (Nguyen *et al*., 2002; Ramier *et al*., 2012), for the repolymerization of corresponding polymer (Kaihara *et al*., 2005) as well as a source of reactive oligoesters (Ramier *et al*., 2012). The preferable molecular weight of PHA oligomer was reported to be in the range of 1, 200 to 25, 000 Da (Scandola *et al*., 2011).

Previously, controlled degradation studies on members of the PHA family have mainly focused on biodegradation (Wang *et al*., 2004), enzymatic degradation (Shimamura and Kasuya, 1994; Doi *et al*, 1995; Sudesh *et al*., 2000; Alejandra *et al*., 2012), thermal degradation (Ariffin *et al*., 2010b; Ramier *et al*., 2012), acid and alkaline hydrolysis (Yu and Marchessault, 2000; Yu *et al*., 2005) as well as hydrothermal degradation (Saeki *et al*., 2005). The resulted oligomers or degradation products are dependent on the degradation mechanisms. Ramier *et al*. (2012) reported that the thermal degradation by microwave irradiation and conventional heating of PHAs at 190 °C, resulted in

oligomers having crotonoyl and carboxyl terminal groups in the same way as PHB thermal degradation (Ariffin *et al*., 2010b). It is well accepted that the thermal degradation of PHB occurs through random chain scission via β-elimination, results in final products with unsaturated crotonate chain end groups, followed by a kinetically favored chain reaction of β-elimination from crotonate chain ends. Unfortunately, this simple thermal degradation process is not desirable as a method of oligoester production for biomedical use as crotonic acid and unsaturated bonds have been suggested to be toxic to the growth of mouse fibroblast cells (Sun *et al*., 2007).

Acid-catalyzed hydrolysis results in linear oligomers with hydroxyl and carboxyl end-groups together with low amount of cyclic structures, on the other hand, alkaline hydrolysis in the presence of alcohols results in oligomers with hydroxyl and ester end-groups (Ramier *et al*., 2012). These thermal, acidic, and basic hydrolytic degradation yields crotonic acid as well as 3HB oligomers with crotonate end groups via β-elimination (Kaihara *et al*., 2005). In the hydrothermal degradation of PHB, homogenous and random degradation occurs via bulk erosion mechanism at high temperature (180-300 °C) and high pressure, which result in the formation of water-soluble monomers and oligomers (Saeki *et al*., 2005). In a study conducted by Doi *et al*. (1995) on enzymatic degradation of PHBHHx films in an aqueous solution of PHB depolymerase derived from *Alcaligenes faecalis,* it was found that the depolymerase was specifically incapable of hydrolyzing the ester bond of HB-HHx sequence. Later, Wang *et al*. (2004) reported that when biodegradation of PHBHHx was carried out in activated

sludge, it showed a good biodegradability due to advantageous combination of low crystallinity and rough surface.

Despite of the existence of various degradation methods, super-heated steam (SHS) hydrolysis was introduced as an alternative method for the hydrolysis of PHBHHx in the present study, because super-heated steam assisted degradation of PHBHHx has not been investigated yet. SHS uses unsaturated steam produced by the addition of heat to saturated steam, which enables the steam's temperature to exceed its boiling point (Bahrin *et al*., 2012). SHS is widely applicable because it is operable at atmospheric pressure, (Nordin *et al*., 2013) allows steam to homogeneously diffuse into PHBHHx, and specifically degrades ester bonds without any dissolving out of hydrolysates into a liquid solvent, which interrupts quantitative analysis of degradation behavior (Mohd-Adnan *et al*., 2008). Thus, the present study was aimed at the unprecedented oligoester production using SHS treatment, where the weight-average molecular weight (M_w) reduction was monitored precisely using size-exclusion chromatography (SEC). Characteristics of the oligoester produced also were discussed in this chapter. In general, the current approach of SHS treatment for PHBHHx oligoester production appears to be a cost effective and greener method for various applications as aforementioned.

3.2 Materials and Methods

3.2.1 Materials

P((*R*)-3HB-*co*-6%-(*R*)-3HHx) (PHBHHx LOT 1406, M_n: 193,000 Da, M_w: 406,000 Da) and P((*R*)-3HB-*co*-11%-(*R*)-3HHx) (PHBHHx LOT 1404, M_n: 171,000 Da, M_w: 370,000

Da) were kindly provided by Kaneka Corporation, Japan. The PHBHHx was purified by a reprecipitation method (Figure 3.1) by dissolving in hot chloroform (2% w/v) as a good solvent and precipitated in cold methanol as a poor solvent prior to vacuum drying at room temperature with a basement of Whatman No.1 filter paper as previously reported (Ariffin *et al*., 2008). Solvents: chloroform (with 0.3-1.0% ethanol stabilizer) and methanol were obtained from Wako Pure Chemical Industries (Wako, Osaka, Japan) and used as received.

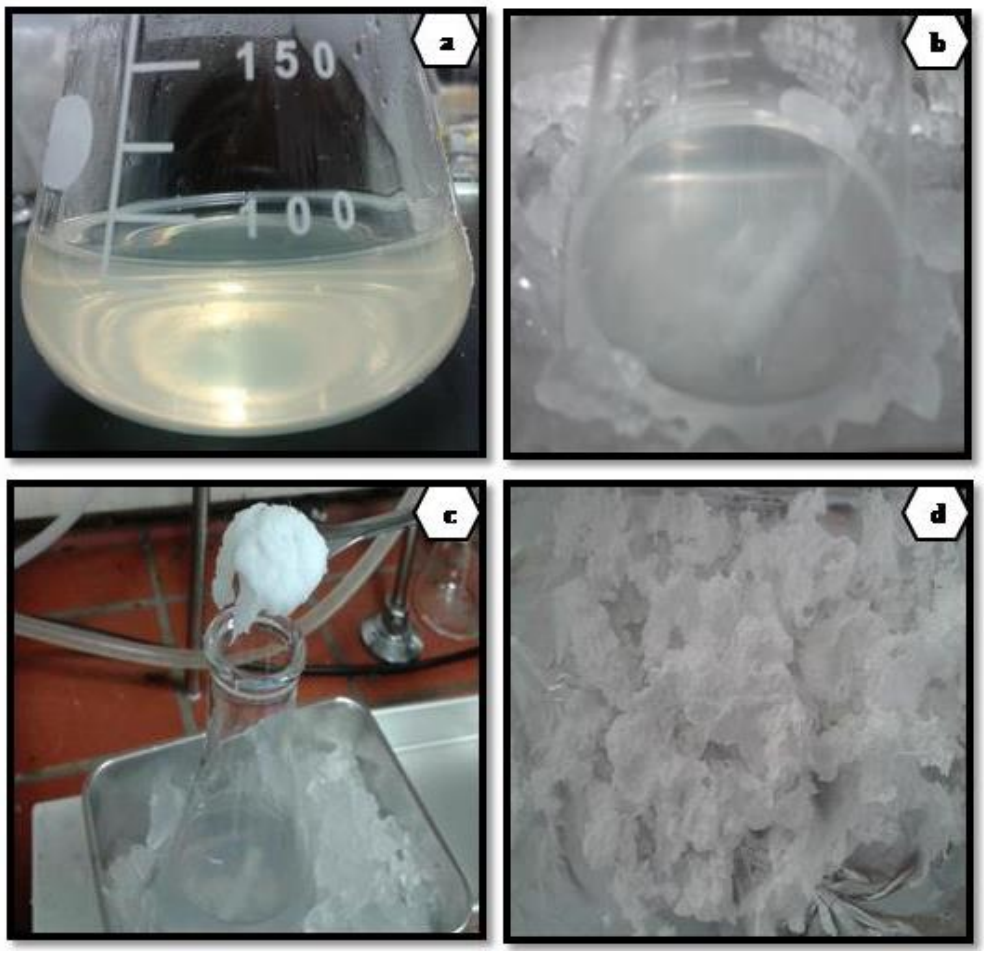

Figure 3.1. Purification process of PHBHHx (a) PHBHHx dissolved in chloroform (b) drop-wise added PHBHHx solution into cold methanol (c) precipitation of dissolved PHBHHx (d) vacuum dried PHBHHx

3.2.2 Preparation of PHBHHx films

The PHBHHx films were prepared using a compressed molding technique with the aid of heat pressure film forming machine IMC-180C (Imoto Machinery, Kyoto, Japan) as shown in Figure 3.2. Before compression, hotplates of the machine were preheated to 145 ℃ for PHBHHx samples, where the temperature was employed based on T_m value of samples. About 5g of sample was weighed and placed in a metal mold (0.5 mm thickness, 10 × 10 cm^2) with a teflon-coated bottom, followed by an up-down close-up with Al plates. The sample sandwiched between Al plates was then placed on the hotplate and pressed at force of 10 MPa for 3 min followed by 40-50 MPa for 5 min to form transparent film. The temperature was maintained throughout the molding process. Upon the hot pressing, Al plates was taken out from the hotplate and cooled for 5 min at room temperature to easily peel off the sample films attached to the mold. Later, the films were cut into sample strips (1 × 4 cm^2, 0.5mm thickness) and stored in airtight bag at 4 ºC prior to be evaluated in superheated steam (SHS) treatment.

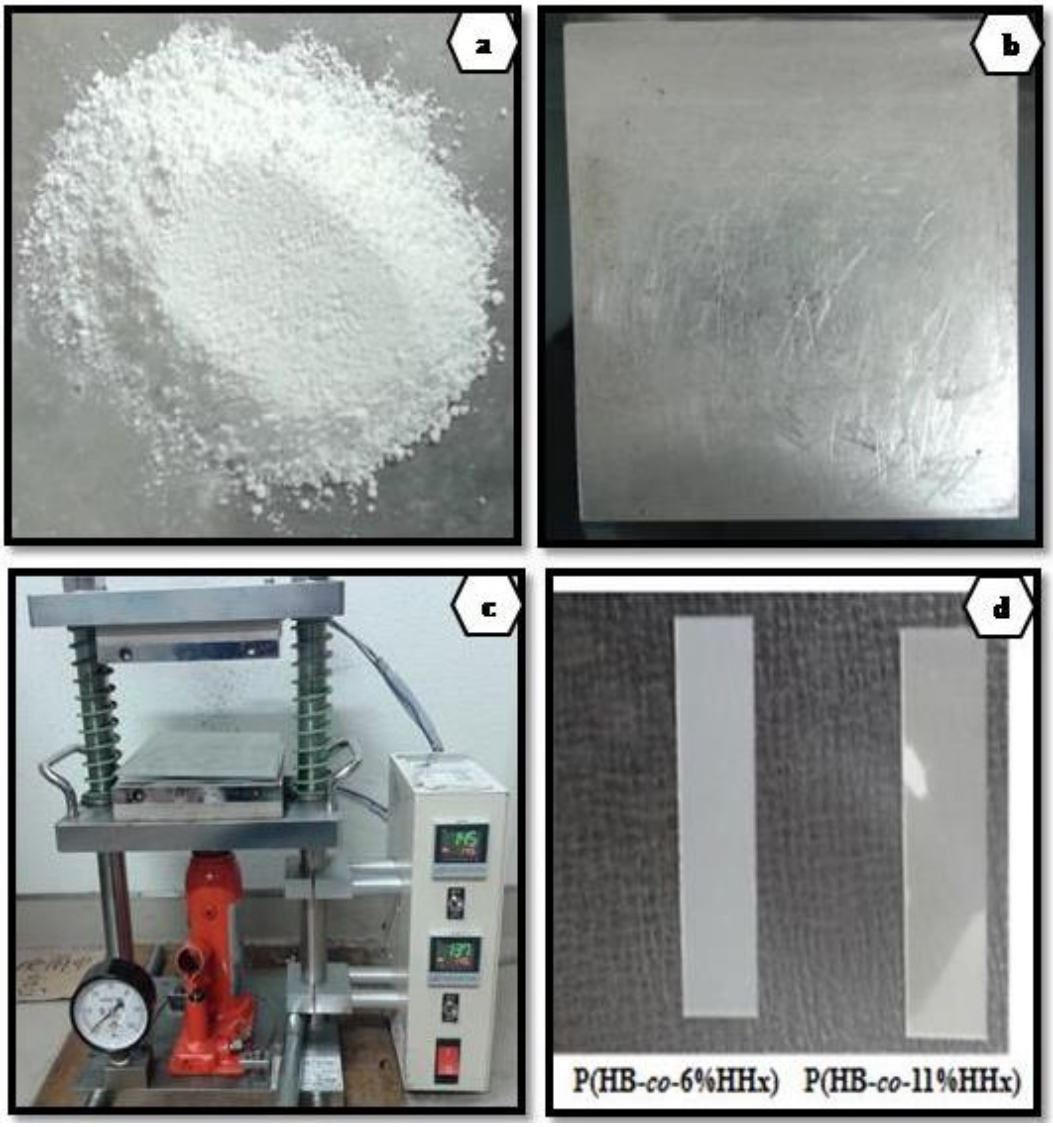

Figure 3.2. Preparation of PHBHHx films (a) PHBHHx sample (b) sandwiched PHBHHx sample between Al plates (c) compressed molding of PHBHHx sample (d) PHBHHx sample strips for SHS treatment

3.2.3 Hydrothermal degradation of PHBHHx films by superheated steam

Hydrothermal degradation of PHBHHx films was done by superheated steam (SHS) in an oven QF-5200C (Naomoto Corporation, Osaka, Japan) as shown in Figure 3.3. Superheated steam system consists of stainless steel chamber and a heating boiler that was operated at the power of 6.3 kW with water evaporation rate of 9.45 kg h^{-1} (Nordin *et al*., 2013). The steam was produced by the heating boiler that attached to the superheated steam system and was then injected to the samples placed in the heating chamber. Heating chamber installed with an electric heater that operates at 8kW, ensures the steam temperature to be under superheated conditions (Nordin *et al*., 2013).

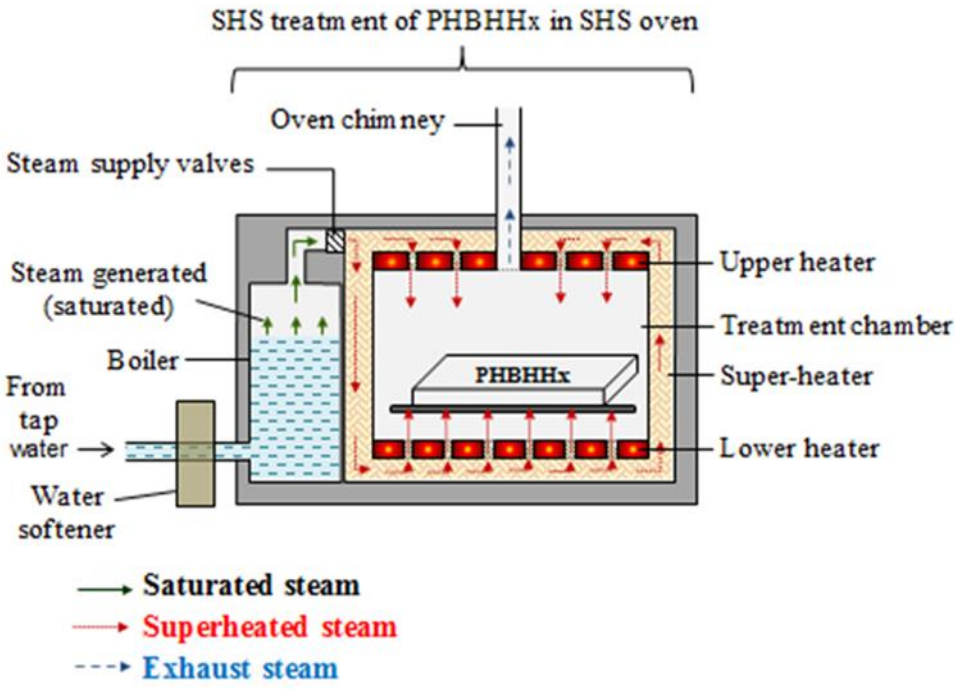

Figure 3.3. Overview of SHS oven

Each sample strip was weighed, put in an Al pan, and followed by arrangement on a stainless steel tray before placed into the SHS oven (Figure 3.4). The sample strips were treated under prescribed conditions as shown in Table 3.1. The SHS treatment temperature was maintained throughout the experiment via online monitoring with Wave Logger Pro software version 3.0. After SHS treatment, the samples strips were kept overnight in a desiccator until constant weights were obtained. The weight and noticeable physical changes of the sample strips were recorded. Subsequently, each sample strip was kept in an airtight bag at 4 °C prior to analysis. The SHS treatment was carried out in duplicate with reasonable reproducibility.

Table 3.1. Superheated steam (SHS) treatment conditions of PHBHHx

Temperature (°C)	Time (min)	Sampling time (min)
130	600	60
150	400	40
170	300	30
190	200	20

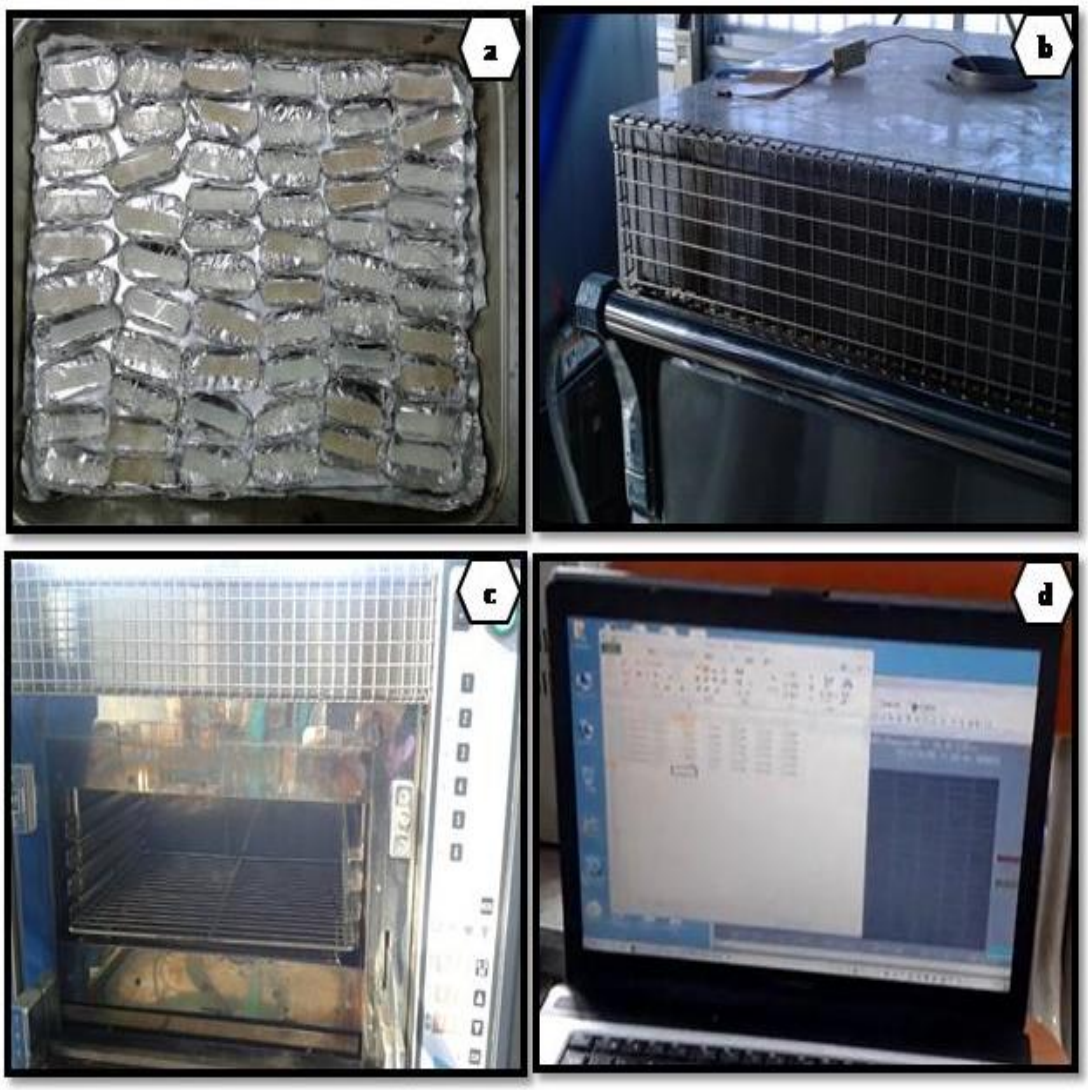

Figure 3.4. Hydrothermal degradation of PHBHHx films by superheated steam (SHS). (a) Al pan with PHBHHx sample strips arrangement in stainless steel tray (b) temperature sensor that attached to the SHS oven (c) heating chamber of SHS oven (d) online temperature monitoring using Wave Logger Pro software version 3.0

3.2.4 Analytical procedures

3.2.4.1 Molecular weight determination

Number and weight-average molecular weights (M_n and M_w) of the PHBHHx samples were analyzed by size exclusion chromatography (SEC) on a TOSOH HLC-8320 Gel Permeation Chromatography (GPC) system with a refractive index (RI) detector at 40 ºC using TOSOH TSK Gel Super HM-M column (linearity range: $1 \times 10^3 - 8 \times 10^6$; molecular weight exclusion limit 4×10^8) and a chloroform eluent (0.6 mL min^{-1}). The calibration curves for SEC analysis were obtained using polystyrene standards with a low polydispersity; M_n of 5.89×10^2, 1.01×10^3, 2.5×10^3, 5.43×10^3, 9.49×10^3, 1.37×10^4, 3.72×10^4, 9.89×10^4, 1.89×10^5, 3.97×10^5, 7.07×10^5 and 1.11×10^6. Approximately 10 mg of PHBHHx was dissolved in 2mL chloroform and stirred overnight at room temperature. The solution was filtered through a membrane filter with 0.45μm pore size to be used for the SEC analysis.

3.2.4.2 Thermogravimetric analysis

Thermogravimetric (TG) measurement was performed on an EXSTAR 6000-TG/DTA 6200 TG (Seiko Instruments Inc, Chiba, Japan) in aluminium pans (5mmØ) to determine the degradation temperature of PHBHHx samples. Blank aluminium pan was used as reference. About 5-9 mg of PHBHHx sample was measured in an aluminium pan to be used as sample pan. The sample pan was then set in TG and heated with heating rate of 10°C min^{-1} in a temperature range of 30-550 °C under a steady flow of nitrogen

(100 mL min^{-1}). The corresponding weight loss (μg) and its derivative DTG (μg min^{-1}) were recorded for the calculation of degradation temperature in an analytical computer system.

3.2.4.3 Differential scanning calorimetry analysis

Thermal properties of PHBHHx samples including glass transition temperature (T_g), melting point (T_m) and crystallization temperature (T_c) as well as the crystallinity (X_c%) were determined by a differential scanning calorimetry (DSC) (EXSTAR 6000-DSC 6220, Seiko Instruments Inc, Chiba, Japan) that has been calibrated with indium standard (T_m = 156.60 ºC, ΔH = 28.59 J g^{-1}) and nitrogen flow (20 mL min^{-1}) was used throughout the study. A sample in a range of 5-12 mg was weighed and encapsulated in an aluminium pan. The P(HB-*co*-6%HHx) and P(HB-*co*-11%HHx) encapsulated pans were heated in temperature ranges of 30-180 ºC and 30-150 ºC, respectively, at a heating rate of 10 ºC min^{-1} in the first scan. Then, the samples were quenched to -100 ºC at a cooling rate of 100 ºC min^{-1} before reheating to 180 ºC and 150 ºC, respectively, at a heating rate of 10 ºC min^{-1} for the second scan. The thermal properties were determined based on data obtained at the second heating scan after removal of thermal history in the first scan. Glass transition temperature (T_g) was determined as a midpoint of change in heat capacity, melting point (T_m) was taken from the highest point of melting peak, and cold crystallization temperature (T_c) was determined based on exothermal peak value of DSC during the second scan. Crystallinity of PHA samples was calculated using Equation 3.1:

$$X_c\,(\%) = \Delta H_m / \Delta H°_{m\,(\mathrm{PHB})} \times 100\% \qquad (3.1)$$

where, ΔH_m is the enthalpy of whole sample and $\Delta H°_{m(\mathrm{PHB})}$ is 146.6 J g^{-1} , which indicates the enthalpy of melting per gram of PHB in 100% crystallinity (Yang *et al*., 2009).

The SHS treated PHBHHx sample strip encapsulated pans was heated from 30 to 200 ºC at a heating rate of 10 ºC•min^{-1} in the first scan to determine the melting point (T_m) and crystallinity (X_c%). The melting point (T_m) was taken from the highest point of melting peak during the first scan and the crystallinity of PHBHHx sample was calculated using Equation 3.1.

3.2.4.4 Wide angle X-ray diffraction analysis

Wide Angle X-ray Diffraction (WAXD) analysis was performed on an X-Ray Diffractometer RINT 2100 (Rigaku Corporation, Tokyo, Japan), operated at 40 kV and 20 mA with Cu Kα (λ = 0.1542 nm) radiation. Every scan was recorded in the range of 2θ = 5-80º under room temperature at a scan speed of 10º min^{-1}. The depth of each crystalline direction of PHBHHx was calculated using Debye-Scherrer equation (Equation 3.2), which involves relationship between peak width in XRD diffraction profiles and the depth of crystalline. The XRD peak was simulated using Gauss function in a PeakFit software version 4.12 to estimate the intensity of the peak area.

$$D = k\lambda/(\beta \bullet \cos\theta) \qquad (3.2)$$

Where, *D* is the depth of a crystalline direction, k is the Scherrer constant (0.9), λ is the X-ray wavelength (0.1542 nm), β is the width of the XRD peak at half-height, and θ is the Bragg diffraction angle.

3.2.4.5 Nuclear magnetic resonance spectroscopy

Proton nuclear magnetic resonance (^{1}H NMR) spectra were recorded on a 500-MHz JEOL JNM-ECP500 FT NMR system to determine the chemical structure of PHBHHx samples. Two dimensional (2D) homonuclear correlation spectroscopy (^{1}H-^{1}H COSY) spectra were recorded on 500-MHz Bruker NMR system to determine the correlation between the coupling protons. Chloroform-*d* ($CDCl_3$) was used to dissolve the samples. The chemical shift was reported as δ values (ppm) relative to internal standards tetramethylsilane (TMS) and $CDCl_3$ unless otherwise noted. Total of 8 and 16 scans was performed for ^{1}H NMR and ^{1}H-^{1}H COSY measurements, respectively. Composition of HB and HHx components was calculated from integration values of detected peaks in ^{1}H NMR spectrum obtained using Ramo1D NMR software version.3.7.28. Cross peaks of the coupling protons were determined using Ramo2D NMR software version.3.7.28.

3.2.4.6 Weight loss analysis

The percentage of weight loss of SHS treated PHBHHx sample strips were calculated using Equation 3.4 in duplicate analysis:

$$\frac{\text{Initial weight} - \text{weight after SHS treatment (g)}}{\text{Initial weight (g)}} \times 100 \qquad (3.4)$$

3.3 Results and discussion

In this study, SHS treatment was performed to introduce an alternative method to produce PHBHHx oligoesters in the range of 1,200–25,000 Da. The effect of SHS treatment (130–190 °C) on the oligoesters produced was evaluated in terms of physical, structural and thermal properties. In addition, the influence of increased percentage of co-monomer unit within the heteropolymer type towards hydrothermal treatment was compared by using different percentage of PHBHHx samples, which are P(HB-*co*-6%HHx) and P(HB-*co*-11%HHx). The aforementioned results are discussed in detail in the following sections.

3.3.1 Characteristics of original PHBHHx

In order to determine the compositions of co-monomer units in the two different batches of PHBHHx, proton resonances of 3-hydroxybutyrate (3HB) and 3-hydroxyhexanoate (3HHx) units on ^{1}H NMR spectra were integrated. The chemical structure of PHBHHx contains [-O-CH(CH_3)-CH_2-CO-] for HB units and [-O-CH(C_3H_7)-CH_2-CO-] for HHx units as shown in Figure 3.5. Based on the integration of proton resonances, the different batches of PHBHHx were found to contain 6 and 11% of HHx units. The GPC results showed that PHBHHx sample with 6% HHx unit exhibited higher M_w and M_n values compare to the PHBHHx sample with 11% HHx unit. However, both PHBHHx samples showed a similar polydispersity index (PDI) values of around 2 which indicates the most probable distribution (MPD). The broader range of molecular weight of PHA is mainly influenced by various strains of microorganism as well as different stage and cultivation conditions such as pH of culture medium and the type and concentration of carbon source used (Sudesh *et al*., 2000).

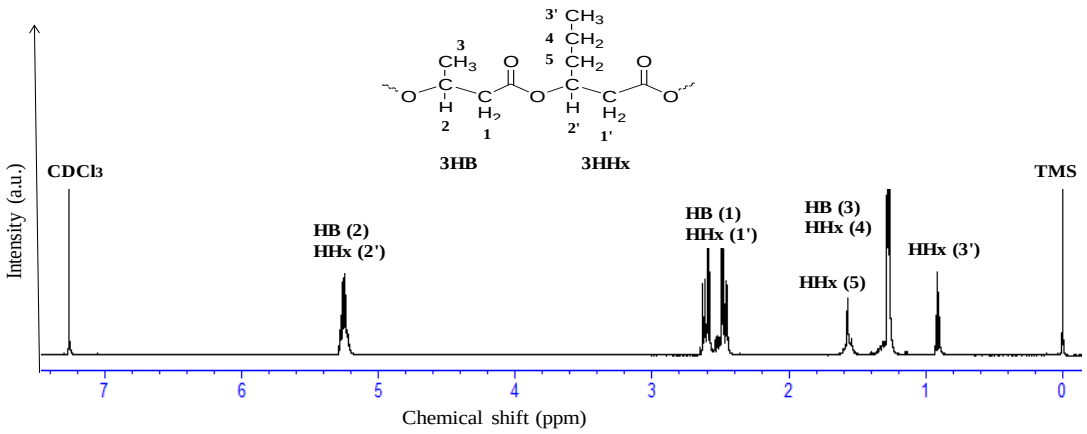

Figure 3.5. Chemical structure of PHBHHx in ^{1}HNMR spectra

The degradation temperatures of P(HB-*co*-6%HHx) and P(HB-*co*-11%HHx) were determined using TG by the measurement of residual weight over the degradation temperature. According to the degradation profile as shown in Figure 3.6, PHBHHx samples showed complete one-step degradation without any leftover of carbonaceous residue, due to its relatively high purity during the industrial production process. The degradation profile also clearly indicates that PHBHHx exhibits a good thermal stability where both P(HB-*co*-6%HHx) and P(HB-*co*-11%HHx) showed a close degradation temperatures, 294 and 291 °C, respectively, which were determined based on 50% weight loss.

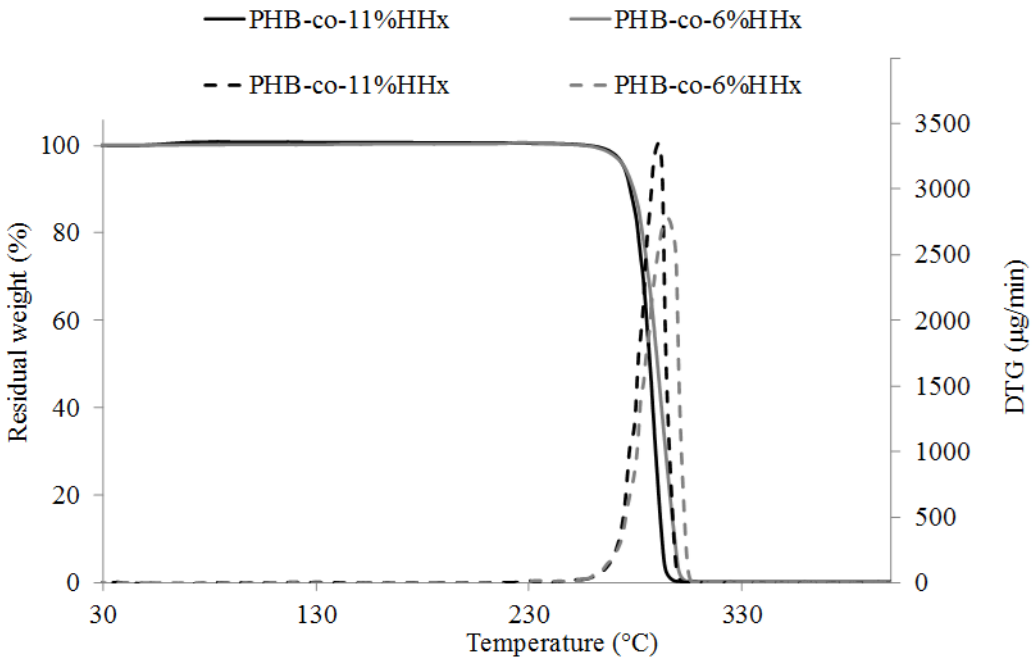

Figure 3.6. Thermogravimetric (TG) and differential thermogravimetric (DTG) profile of PHBHHx samples

Thermal properties measured by calorimetric analysis (DSC) (Figure 3.7) showed that as the percentage of co-monomer unit increased, the thermal properties that include glass transition temperature (T_g), melting point (T_m), enthalpy of fusion (ΔH_m) and the crystallinity (X_c) decreased. In the present study, as the mol (%) of 3HHx unit increased from 6 to 11%, T_m value decreased from 128 and 143 °C to 109 and 124 °C with decrease in ΔH_m from 37 to 20 J g^{-1}, and T_c value decreased from 84 to 68 °C, moreover T_g value also decreased from -1 to -2 °C, respectively. The results obtained are in line with previous studies, where Doi *et al*. (1995) also reported that as the mol (%) of 3HHx unit increased from 0 to 25, T_m, ΔH_m as well as T_g of P(3HB-*co*-3HHx) samples decreased from 177 to 52 °C, 97 to 19 J g^{-1} and 4 to -4 °C, respectively. In general, PHB and its copolymers are not stable above their melting points, which are at 180 °C and in the range of 70-180 °C, respectively, due to the elimination of β-hydrogen of carboxylic esters in the absence of solvent (Nguyen *et al.*, 2002). In addition, T_g and T_m of PHBHHx depended on the content of 3HHx unit in the statistically random copolymer (Chen *et al*., 2005b).

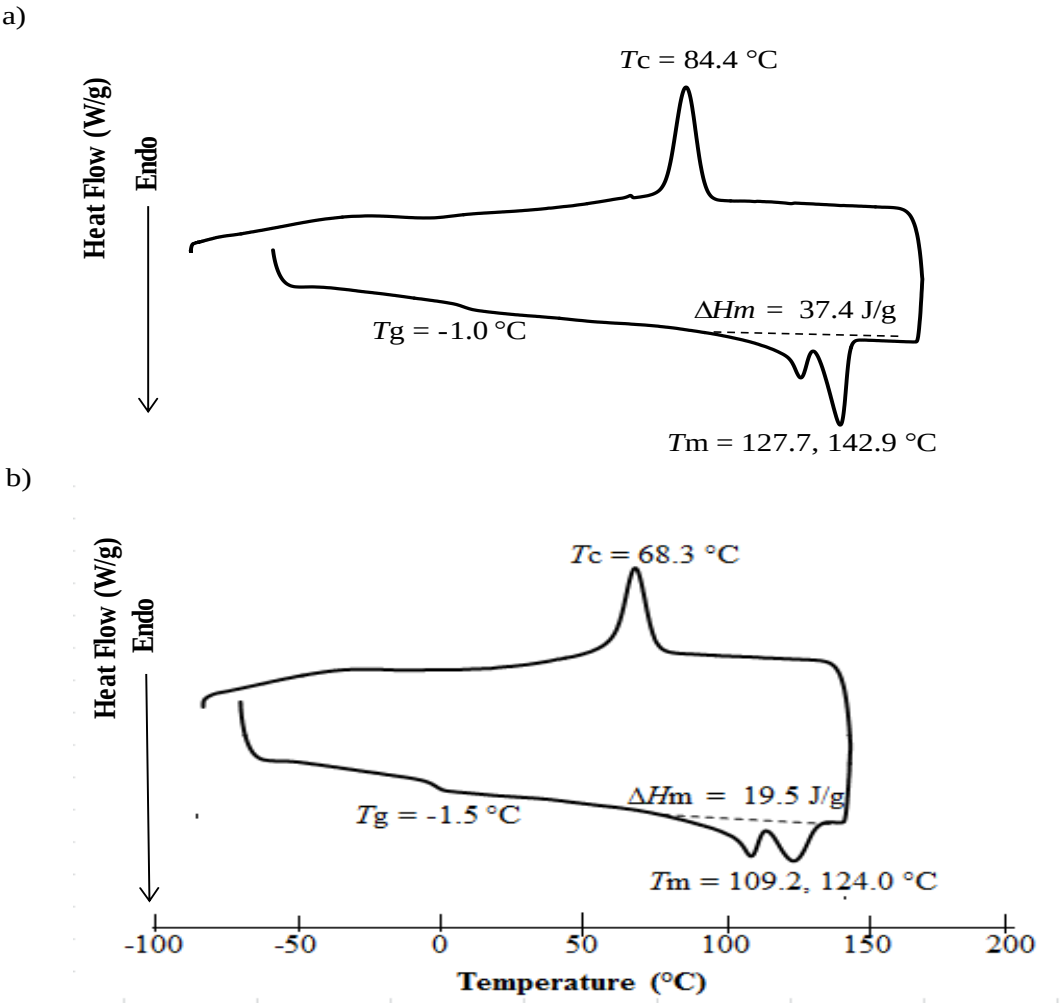

Figure 3.7. DSC thermograms of (a) P(HB-*co*-6%HHx) and (b) P(HB-*co*-11%HHx)

The bacterially produced and isolated PHB exhibits 55-80% crystallinity value in nature, where the PHB within bacteria exists as amorphous and water insoluble inclusions (Sudesh *et al*., 2000). Since the homopolymer type PHB is a highly crystallized material and the homopolymer type PHHx is an amorphous and sticky material, the copolymerization of 3HB and 3HHx results in PHBHHx with improved properties for a broad spectrum of applications (Tripathi *et al*., 2012). Due to this, as the percentage of 3HHx unit increased, the crystallinity decreased. In the present study, crystallinity

values of P(HB-*co*-11%HHx) and P(HB-*co*-6%HHx) were calculated from DSC profiles. The crystallinity of P(HB-*co*-6%HHx) and P(HB-*co*-11%HHx) calculated from calorimetry analysis were 26 and 13% respectively. Similar results were obtained in previous study by Chen *et al*. (2005b) where, the crystallinity of PHBHHx from X-ray diffraction analysis decreased from 60 to 18% as the (*R*)-3HHx content increased from 0 to 25 mol%, which suggested that PHBHHx exhibits wider thermal processability and longer elongation to break than PHB.

Moreover, crystallographic parameters that have been calculated for the strong diffraction peaks with 2θ values corresponding to crystal planes of (020), (110), and (101) are shown in Appendix A1~A2. The *d* spacings of (020), (110), and (101) were slightly increased as the (*R*)-3HHx content increased from 6 to 11%. This result indicates that the presence of (*R*)-3HHx unit slightly influenced the crystallographic parameters that lead to the differences in the *d*-spacing between PHB and its copolymers (Shimamura and Kasuya, 1994; Doi *et al*., 1995). It can be concluded that the propyl side chains of (*R*)-3HHx units expanded the spaces of (020), (110) and (101) planes of the P(3HB) crystal lattice due to steric effects. Thus, it was acceptable that (*R*)-3HHx units were excluded from the crystalline lamella consisting of 3HB sequence (Sudesh *et al*., 2000). Based on the Scherrer equation, the depths of crystalline plane directions: *D* for P(HB-*co*-6%HHx) and P(HB-*co*-11%HHx) were found to decrease with increase in 3HHx unit content. This proves that the 3HHx unit disturbs the crystallization of 3HB unit sequence. The structural and thermal characteristics of the original PHA samples:

P((*R*)-3HB-*co*-6%-(*R*)-3HHx) and P((*R*)-3HB-*co*-11%-(*R*)-3HHx) were summarized in Table 3.2.

Table 3.2. Characterization details of original PHBHHx samples

Characterization details		PHBHHx	
		P(HB-*co*-6%HHx)	**P(HB-*co*-11%HHx)**
Composition (mol%)[a]	HB	94	89
	HHx	6	11
*Molecular weight[b]	M_w (kDa)	406	370
	M_n (kDa)	193	171
	M_w/M_n	2.10	2.16
Degradation temperature[c]	T_{d50} (°C)	290.0	287.0
	T_{max} (°C)	294.0	291.0
Thermal properties[d]	T_g (°C)	-1.0	-1.5
	T_m (°C)	127.7, 142.9	109.2, 124.0
	T_c (°C)	84.4	68.3
	ΔH_m ($J \cdot g^{-1}$)	37.4	19.5
	X_c (%)	25.5	13.3

*Data shown are the average of triplicate analyses
[a]Determined by ^{1}HNMR
[b]Determined by GPC
[c]Determined by TGA. T_{d50} is temperature at 50% weight loss and T_{max} is maximum temperature of DTG peak
[d]Measured by DSC

3.3.2 Characteristics of degradation products of SHS treatment

3.3.2.1 Physical changes of SHS treated samples

The PHBHHx sample strips (1 x 4 cm^2, 0.5 mm thickness) were used in the SHS hydrothermal treatment at 130, 150, 170 and 190 °C. Before the SHS treatment, P(HB-*co*-11%HHx) was found to be more soft and flexible compare to P(HB-*co*-6%HHx). In general, the PHBHHx samples were present in the molten state at all the temperatures used for SHS treatment. The melting behavior in the SHS treatment is closely associated with T_m values of PHBHHx samples, P(HB-*co*-6%HHx) and P(HB-*co*-11%HHx) with melting points of 127.7 / 142.9 °C and 109.2 / 124.0 °C, respectively. At the molten state, PHBHHx sample strips changed to shiny gel-like strips from original solid state. However, upon overnight cooling and drying in desiccator, the melted gel-like films returned back to its original solid state. This is mainly due to recrystallization of 3HB sequence preceded during cooling that aids the rearrangement into its original morphology (Sin *et al*., 2011). The physical changes occurred on the PHBHHx sample strips at the beginning and end of SHS treatment are summarized in Table 3.3.

Table 3.3. Physical changes of PHBHHx sample strips after SHS treatment

SHS treatment condition		P(HB-*co*-6%HHx)	P(HB-*co*-11%HHx)
(°C)	(min)		
130	60		
	600	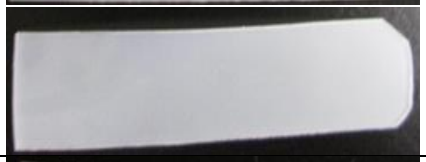	
150	40		
	400		
170	30		
	300		
190	20	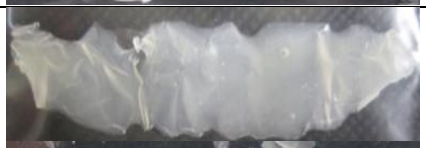	
	200		

As aforementioned, the SHS treatment was conducted above the melting temperatures of PHBHHx. Even though PHBHHx samples apparently melted at all the treatment temperatures used, the exact melting time varied for each sample with different co-monomer unit contents. Generally, at the higher temperatures of SHS treatment (170 and 190 °C), the onset of melting and formation of hollow structures were faster than lower temperatures of SHS treatment (130 and 150 °C) for both PHBHHx samples. During the SHS treatment at 130 °C, P(HB-*co*-6%HHx) slightly melt at 300 minutes onwards, with no formation of bubbles within the film strips. However, P(HB-*co*-11%HHx) melt at 60 minutes onwards, where the bubbles and few hollow structures forms at treatment time of 120 minutes onwards. During the SHS treatment at 150 °C, both P(HB-*co*-6%HHx) and P(HB-*co*-11%HHx) melt at 40 minutes onwards, where the bubbles and few hollow structures forms at treatment time of 80 and 40 minutes onwards, respectively. During the SHS treatment at 170 and 190 °C, both PHBHHx samples melt and forms bubbles and few hollow structures simultaneously as early as 40 and 30 minutes of treatment time, respectively. As an additional observation, the PHBHHx samples become brittle at 170 and 190 °C, particularly at 150 and 40 minutes of treatment time, respectively.

Beyond the melting temperature, water molecules from superheated steam specificically break the weak intermolecular forces that are responsible to hold the polymer chains together (Sin *et al*., 2011). This resulted in the shiny gel-like, film strips upon melting. However, at lower temperatures (130 and 150 °C), the sample strips retained its original shape and size before being distorted at higher temperatures (170 and 190 °C) due to remaining microcrystalline consisting of 3HB sequence. The formation of bubbles and

hollow structures during the hydrothermal treatment may be due to volatile products such as crotonic acid and water. The hydrolysis of polyesters proceeds according to the auto-catalytic random chain scission, where the hydrolysis is catalyzed by carboxylic acid end groups of their own hydrolytic products that are being retained within the films (Nishida *et al*., 2000a; Gajjar and King, 2014). The formation of acidic hydrolysis products enhances water permeability, which thus increases the rate of degradation via the self-catalyzed hydrolysis resulting in accumulation of hydrolysis products including volatile products. The accumulated volatile products may form bubbles and hollow structures (Gopferich, 1996; Gajjar and King, 2014).

Changes in brittle materials were confirmed when the SHS treated film strips were transferred from the Al pan to be stored for further analysis. As the film strips becomes brittle with increase in treatment time and temperature, it was seen to be easily cracked or even breaks into pieces during the transferring. As reported in many previous studies, the hydrolysis reaction of PHBHHx would be preferentially occurring at amorphous phase rather than crystalline phase (Shimamura and Kasuya, 1994; Doi *et al*., 1995; Yang *et al*., 2009). Therefore, during the hydrothermal treatment by SHS, amorphous regions of the polymer would be degraded first, followed by the degradation of crystalline region. The degraded chain-ends have higher mobility than amorphous chains, resulting in enhancement of the recrystallization on original crystalline phases. As a result, the increase in crystallinity occurs and the mechanical properties of amorphous regions are weakened, resulting in the overall brittleness of the polymer.

3.3.2.2 Determination of weight loss

The weight loss measurement is often regarded as a baseline indication for the amount of water-soluble oligomers formed during the hydrolysis that was released to the surrounding from the mother films (Tsuji, 2002; Lyu and Untereker, 2009). The weight loss of the PHB normally occurs right after the random scission of the polymer chains that leads to the further degradation (Yu and Marchessault, 2000). In the present study, hydrothermal treatment of PHBHHx films by SHS resulted in their weight loss mainly due to the formation of volatile, low molecular weight compounds that were small enough to diffuse out of the films during the SHS treatment. The detailed percentage of weight loss of SHS treated PHBHHx film strips are shown in Appendix A3 ~ A6. In overall, percentages of weight loss (%) of all the samples: P(HB-*co*-6%HHx) and P(HB-*co*-11%HHx) were found to be directly proportional to the treatment temperature and treatment time. As the treatment temperature and treatment time increased, the weight loss percentage of the films also increased proportionally. The differences in the weight loss behavior were illustrated in Figure 3.8.

As shown in Figure 3.8, P(HB-*co*-6%HHx) exhibited higher weight loss compared to P(HB-*co*-11%HHx). This trend was observed at all the treatment temperatures used. At the end of SHS treatment at 130 °C (600 min), weight loss percentages of both P(HB-*co*-6%HHx) and P(HB-*co*-11%HHx) were only 0.3% and even at the highest treatment conditions (190 °C, 200 min) merely increased up to 3.1 and 2.6% respectively . The increase of weight loss percentage was accompanied by higher treatment temperature

because the reactive compounds vibrate vigorously at higher temperature to overcome the activation energy (Wang *et al*., 2012) which accordingly led to the accelerated hydrolytic degradation of the PHBHHx films. The minutely recorded weight loss data showed that, P(HB-*co*-6%HHx) exhibited higher weight loss than P(HB-*co*-11%HHx) for all the treatment temperatures used. This is due to the presence of more HB sequence on P(HB-*co*-6%HHx) which is thermally unstable, nearly and above the T_m (Morikawa and Marchessault, 1981; Nguyen *et al.*, 2002). Thus, it is concluded that during the hydrothermal treatment by SHS, the more degradation products were produced from the HB fractions of PHBHHx. It is also interesting to note that, the percentage of weight loss of PHBHHx samples at highest SHS treatment condition of 190/200 (°C/min) were ten times higher than at lower SHS treatment condition of 130/600 (°C/min) as shown in Appendix A3~A6. These noticeable changes could indicate the occurrence of different degradation mechanisms at lower and higher SHS treatment conditions. It is proposed that the simple hydrolytic degradation at lower temperature gradually mimics the thermal degradation at higher temperature. The detailed degradation mechanism will be discussed in Chapter 4.

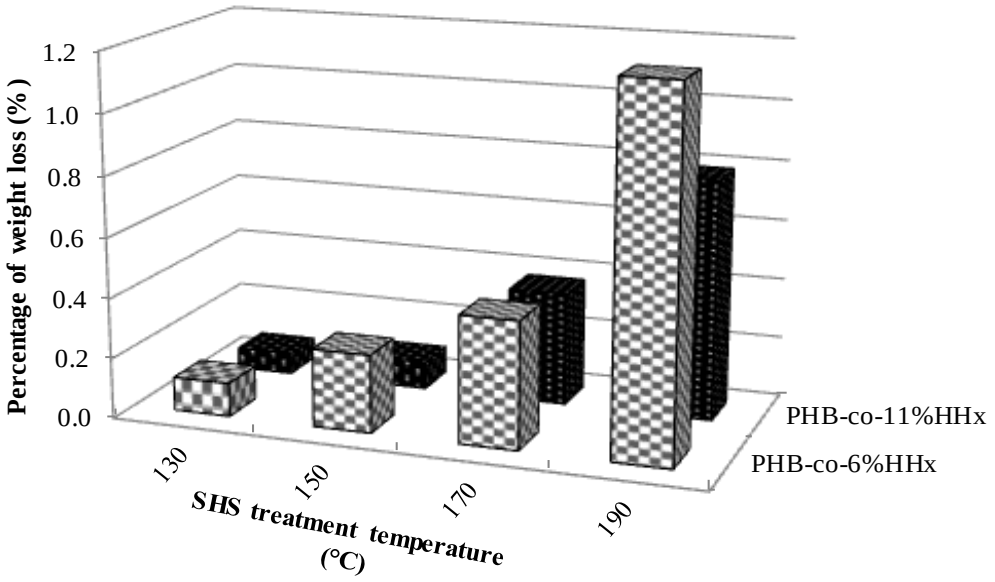

Figure 3.8. Percentage of weight loss for different type of PHBHHx film strips after SHS treatment at prescribed temperatures at treatment time of 120 minutes. The data represent average values of duplicate measurements.

3.3.2.3 Molecular weight reduction

In the present study, PHBHHx oligoesters were prepared by controlled degradation of hydrothermal treatment with the aid of SHS. In general, during hydrolytic degradation, the molecular weight reduction occurs before substantial changes in mechanical or morphological properties (Nishida *et al*., 2000a). Thus, changes in molecular weight during the passive degradation such as hydrolysis are considered to be the most important parameter in the evaluation of polymer degradation velocity (Gopferich, 1996; Gomes and Reis, 2004). The time-dependent changes in M_w of PHBHHx during the hydrothermal degradation by SHS treatment in a temperature range of 130 to 190 °C are

shown in Appendix A7~A10. The M_w of PHBHHx at the end of SHS treatment for the temperature range of 130 to 190 °C is summarized in Table 3.4.

As shown in Appendix A7~A10 and Table 3.4, PHBHHx samples showed a decrease in M_w proportional to the increases in treatment time and treatment temperature. On the additional note, the higher the treatment temperature used, the higher the molecular weight reduction. In the present study, M_w was taken into account to precisely measure the molecular weight reduction to make the influence of weight loss to be negligible. This is in line with speculation of Yoon *et al*. (1997), which conceptualized that high molecular weight polymers are sensitive to the changes in weight-average molecular weight and the changes in number-average molecular weight are more reliable to low molecular weight polymers.

It is obvious that P(HB-*co*-6%HHx) showed higher molecular weight reduction in comparison to P(HB-*co*-11%HHx). The M_w of P(HB-*co*-6%HHx) was greatly reduced from initial high molecular weight of 305 to 139 (55%), 73 (79%), 14 (96%) and 4 (98%) kDa at the end of each SHS treatment temperatures of 130, 150, 170, and 190 °C, respectively. Similarly, P(HB-*co*-11%HHx) with initial molecular weight of 352 was also reduced to 180 (49%), 107 (70%), 21 (94%) and 5 (98%) kDa at the end of prescribed SHS treatment temperatures. These results prove that PHBHHx degradation was greatly favored by the increases in SHS treatment temperature and treatment time. Moreover, among the copolymers, the degradation of P(HB-*co*-6%HHx) was easier than P(HB-*co*-11%HHx). The slower degradation of P(HB-*co*-11%HHx) is considered

mainly due to the steric effects of the bulky side chains groups that hinder the attack of water molecules (Gopferinch, 1996).

In addition, the present results indicate that the crystallinity of the sample does not directly contribute to the degradation behavior of the PHBHHx samples. In previous study, Doi *et al*. (1995) reported that the rate of enzymatic degradation of homopolymer PHB and copolymer type of P(3HB-*co*-3HH) with 0-15mol%3HHx and P(3HB-*co*-3HP) with 0-20 mol%3HP increased with decrease in crystallinity due to the rapid erosion at amorphous phase. However, in the present study, P(HB-*co*-6%HHx) has higher crystallinity than P(HB-*co*-11%HHx), which have crystalline value of 25.5 and 13.3% respectively from DSC measurement. Thus, it is determined that the steric hindrance of side chain groups plays greater role in the degradation behavior of hydrothermal treatment by SHS. Apart from above discussion, the higher degradation behavior in P(HB-*co*-6%HHx) could be also due to the properties of surface morphology in terms of porosity as reported by Wang *et al*. (2004). The P(HB-*co*-6%HHx) could have a more porous surface than P(HB-*co*-11%HHx). This surface morphology may trigger the hydrolytic degradation by SHS. The porous surface has a wide surface area, and allowed water molecules to attack and diffuse into the polymer matrix, eventually lead to the hydrolysis (Wang *et al*., 2004).

Moreover, the polydispersity index (PDI) value decreased and approached 2 as the treatment temperature increased. The variation in PDI value was mainly due to the random chain scission of the polymers. PHBHHx that possessed lower crystallinity led to the formation of oligomers with polydispersity of around 2 due to limitation of lower

molecular weight distribution. On the other hand, oligomers with high polydispersity could be resulted due to substantial heterogeneity during the hydrothermal treatment. Generally, the faster degradation of smaller chains will approach to smaller PDI value. The PDI value would approach 2 if the larger polymer chain with more bonds, more susceptible to react with water molecules, tends to degrade faster than the smaller chains. Therefore, the smaller chains degrade slower and polymer chains would exist in similar size.

It was reported that beyond the critical point, drastic change in M_n and sudden weight loss occurred due to autocatalytic random hydrolysis of polyesters (Nishida *et al*., 2000a). The critical point denoted as a value where the deviation of molecular weight begins to occur from the linear plot of ln M_w against time (Mohd-Adnan *et al*. 2008). Changes in the SEC profiles of SHS-treated PHBHHx at the temperatures of 130 and 190 ℃ are illustrated in Figures 3.9 and 3.10 respectively, whereas the SEC profiles at 150 and 170 ℃ are illustrated in Appendix A11 and A12, respectively. The SEC profile shifted to a lower molecular weight region but maintained a unimodal distribution profile, similar to the most probable distribution, up to a critical point without any formation of specific low-molecular weight peaks arising from the chains in the crystalline residues. This indicates that the hydrolysis reaction of PHBHHx above their melting point (T_m) proceeds effectively and randomly (Saeki *et al*., 2005).

Table 3.4. Molecular weight of SHS treated PHBHHx samples

PHBHHx samples	Treatment temperature (°C/min)	*M*w (kDa)	*M*n (kDa)	PDI
PHB-*co*-6%HHx	Untreated	305	112	2.72
	130/600	139	57	2.44
	150/400	73	31	2.35
	170/300	14	8	1.75
	190/200	4	2	2.00
PHB-*co*-11%HHx	Untreated	352	126	2.79
	130/600	180	77	2.33
	150/400	107	45	2.38
	170/300	21	10	2.10
	190/200	5	2	2.00

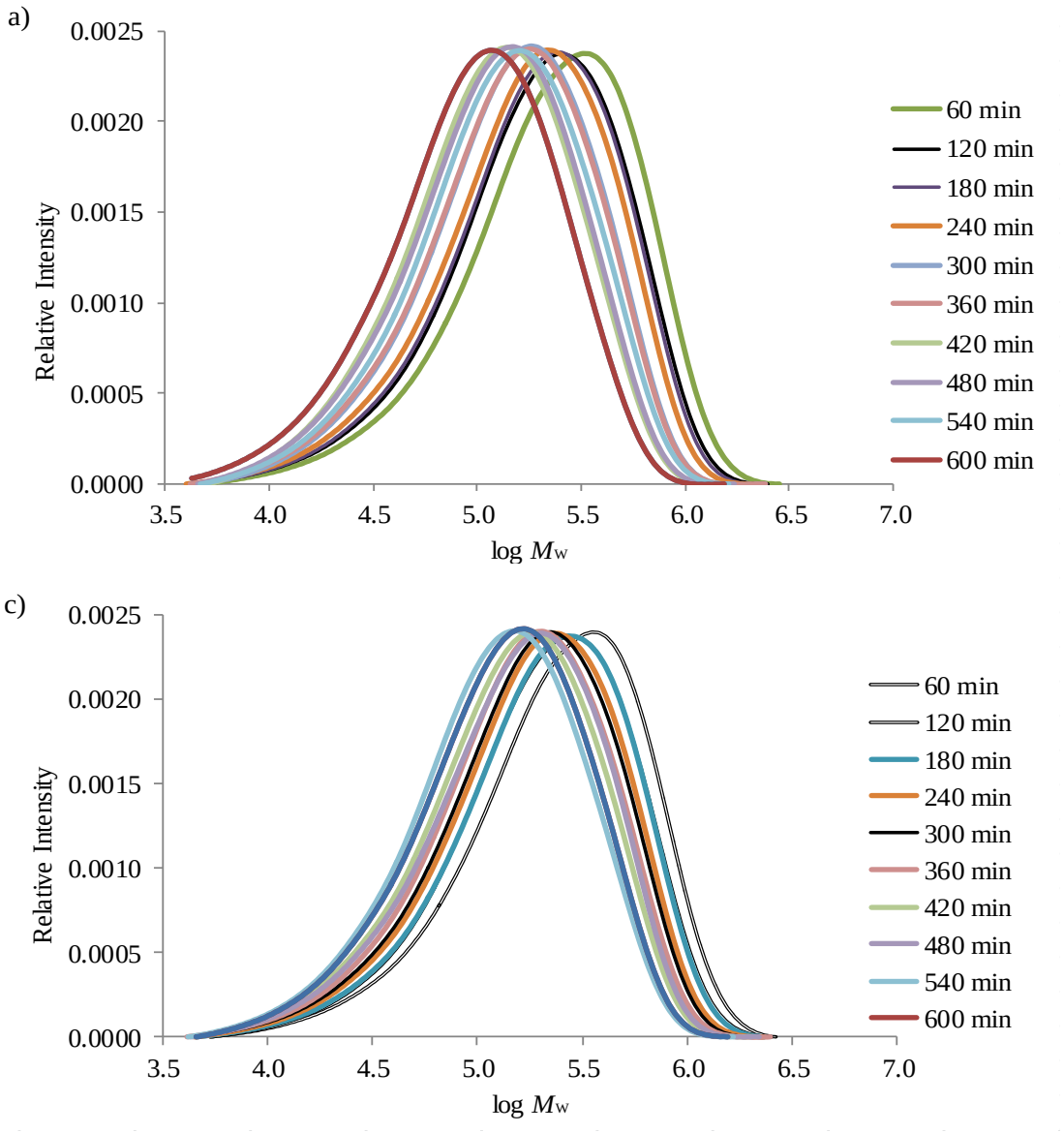

Figure 3.9. Time-dependent changes in SEC profile of (a) P(HB-*co*-6%HHx) (b) P(HB-*co*-11%HHx) during SHS treatment at 130 °C

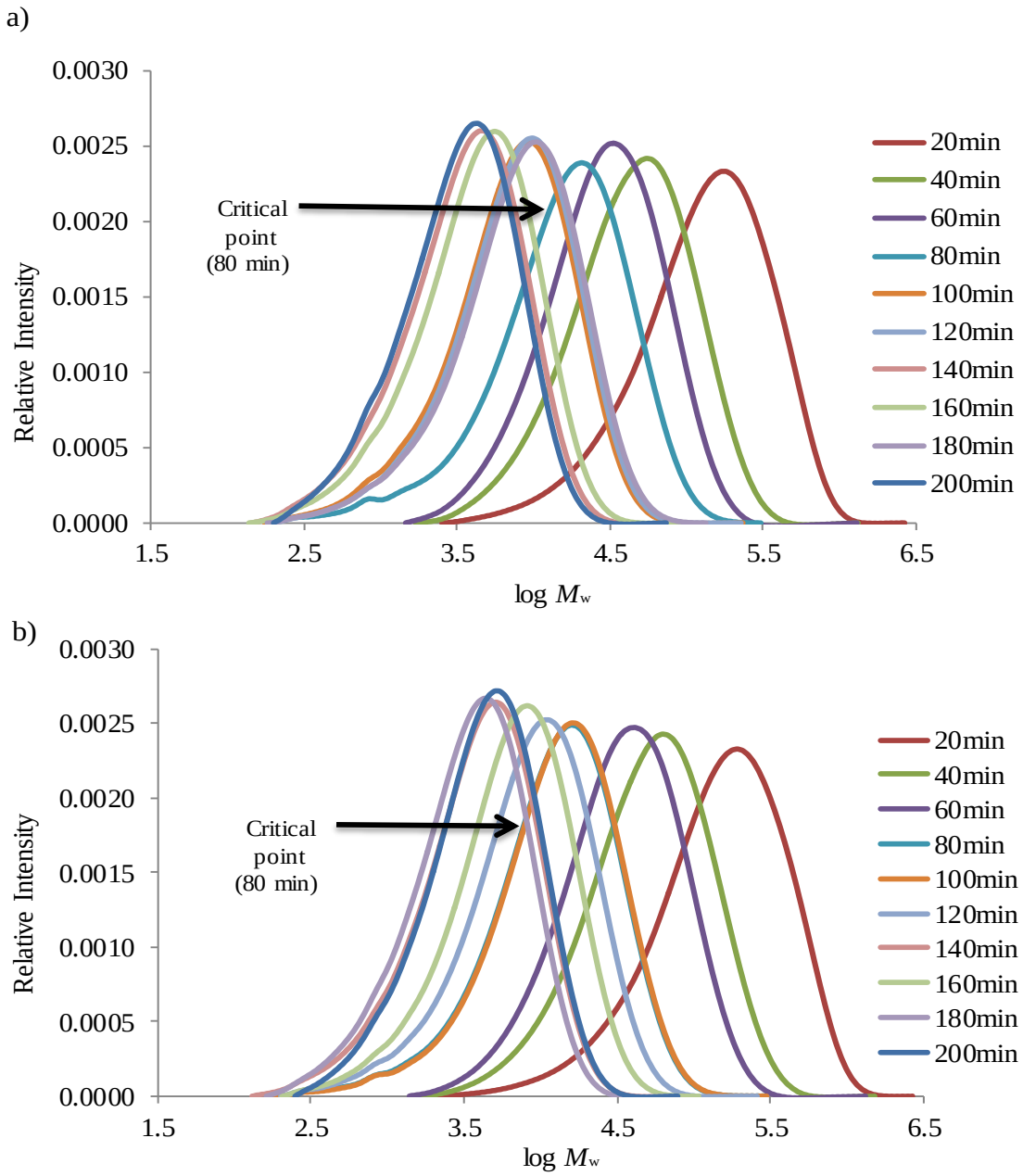

Figure 3.10. Time-dependent changes in SEC profile of (a) P(HB-*co*-6%HHx) (b) P(HB-*co*-11%HHx) during SHS treatment at 190 °C

The most probable distribution also indicates that hydrothermal degradation due to SHS treatment proceeded in a homogeneous and random degradation manner via bulk erosion mechanism (Tsuji and Miyauchi, 2001 and Mohd-Adnan *et al*. 2008). Beyond the critical point, as shown in Appendix A12 and Figure 3.10, the SEC profile gradually changed to a multimodal distribution, indicating that degradation became heterogeneous. However, this result was different from those of previously reported results, where the hydrolysis was performed at high temperatures (180–300 °C) and high pressures (Saeki *et al*., 2005). The observed behavior was similar to the manner accompanying the isolation of crystalline phases during poly(L-lactic acid) hydrolysis (Mohd-Adnan *et al*., 2008). At 170 and 190 °C, in spite of the molten state, critical point where the SEC profile begin to deviate from the single modal-shape was clearly observed at M_w: 29 000 (180 min) and 23 500 Da (80 min), respectively, for P(HB-*co*-6%HHx) and at M_w: 45 000 (180 min) and 18 500 Da (80 min), respectively, for P(HB-*co*-11%HHx). Thus, these suggest that either the dominant and homogeneous bulk erosion mechanism reached the limit.

3.3.2.4 Thermal properties

The thermal properties of SHS treated PHBHHx samples and untreated PHBHHx samples as controls were determined using thermogravimetric (TG) and differential scanning calorimetry (DSC) measurements. The degradation temperature of the P(HB-*co*-6%HHx) and P(HB-*co*-11%HHx) were determined using TG by taking temperature at percentage of 50% weight loss for T_{d50} and at the highest DTG peak for T_{max} as shown in Table 3.5. The degradation profiles of the PHBHHx are shown in Appendix A13 - A14. The results of the highest DTG peak showed that the SHS treated samples slightly had a lower thermal stability than the untreated samples. Moreover, as the treatment temperature increased, the thermal stability of PHBHHx samples decreased. Based on the DTG profile, degradation temperature ranges of PHBHHx samples were determined as 220–320 °C and 210–310 °C at SHS treatment temperatures of 130 and 190 °C, respectively. Thus, the treatment at higher temperatures could have resulted to the decrease in the thermal stability as well as the drastic molecular weight reduction and weight loss of the PHBHHx samples.

The DSC thermograms of SHS treated PHBHHx samples are shown in Figure 3.11 and the summary of thermal properties (T_m, ΔH_m and X_c) that have been determined in the first scan of calorimetric analysis are tabulated in the Table 3.6. PHBHHx samples with two T_m peaks originally, showed triple T_m peaks after SHS treatment at higher temperatures (170 and 190 °C). Previously, Chen *et al*. (2005b) reported that, the formation of multiple peaks resulted from the compositional heterogeneity, formation of

multiple crystalline lamellas, or the recrystallization from the melt state during the heating process of DSC. According to Chen *et al.* (2005b), the lower T_m peak may be due to the melting of crystals formed at the heating process of DSC measurement and the higher T_m peaks resulted from the melting of recrystallized crystals during the cooling process after SHS treatment. As shown in the Figure 3.11 and Table 3.6, the T_m peaks of all the SHS treated PHBHHx samples tended to shift to the lower temperature range at higher treatment temperature. The decreasing melting temperature is closely associated to the reduction in M_w of the PHBHHx samples. The oligomers with lower M_w resulted in its lower $T_{m.}$ This is mainly due to the higher concentration of chain-ends groups in the low molecular weight PHBHHx that lead to the dislocations in the lamellar thickening which eventually interrupt the crystallization (Liu *et al*., 2012).

Table 3.5. Thermal stability of SHS treated PHBHHx samples

PHBHHx sample	SHS treatment condition (°C/min)	Degradation temperature	
		T_{d50} (°C)	T_{max} (°C)
PHB-*co*-6%HHx	Untreated	290.0	293.0
	130/600	290.0	292.0
	190/200	290.0	291.0
PHB-*co*-11%HHx	Untreated	289.0	292.0
	130/600	288.0	291.0
	190/200	288.0	290.0

[a]Determined by TG at 50% weight loss for T_{d50} and at the highest DTG peak for T_{max}

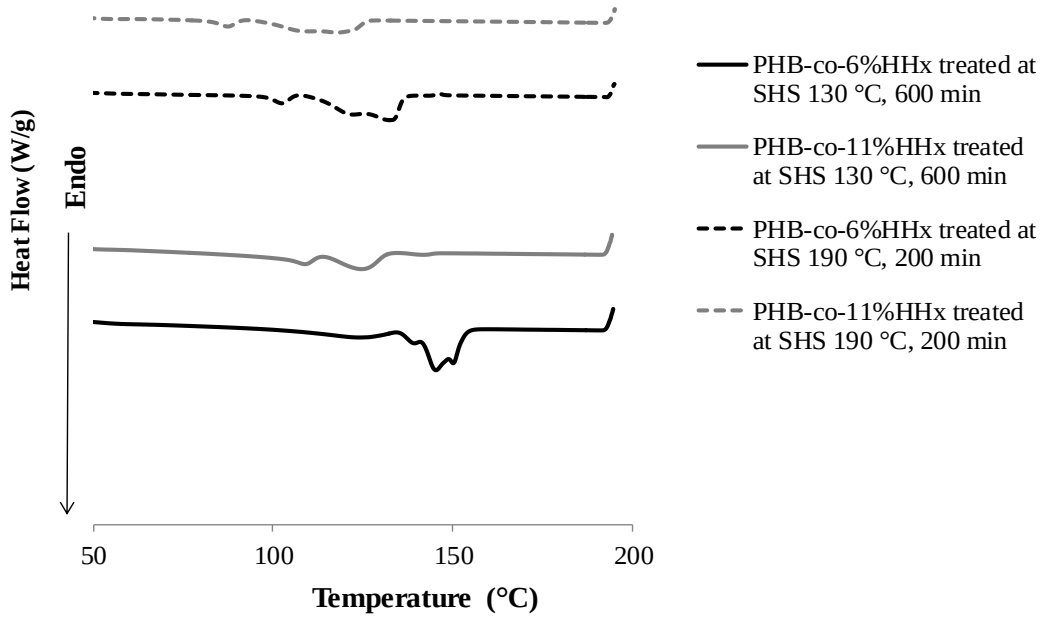

Figure 3.11. DSC thermograms of PHBHHx samples after SHS treatments at 130 and 190 °C for 600 and 200 min, respectively

Moreover, as shown in Table 3.6, ΔH_m and X_c values were found to increase at the end of treatment time for all the temperatures used. In general, due to the faster erosion at amorphous region compared to the crystalline region, the overall crystallinity increased (Gopferinch, 1996; Gomes and Reis, 2004). Moreover, the crystalline structure is normally destructed beyond certain threshold level (Sin *et al*., 2011). The SHS treatment was carried out at higher temperatures than melting points and the overall ΔH_m and X_c values showed complex behaviors at the end of treatment time, due to mixed effects of retaining molecular weight and mobility of molecules for re-crystallization. The crystallinity of P(HB-*co*-6%HHx) was in a range of 53.9% (130 °C, 600 min) to 42.1% (150 °C, 400 min). On the other hand, P(HB-*co*-11%HHx) showed the crystallinity, in a range of 34.9% (130 °C, 600 min) to 28.3% (170 °C, 300 min). This could be mainly due

to the higher percentage of HHx unit in its backbone structure than P(HB-*co*-6%HHx). Thus, the HHx units hinder the crystallization as well as the hydrothermal degradation and weight loss as abovementioned.

Table 3.6. Thermal properties of SHS treated PHBHHx samples based on DSC thermograms for treatment temperature range of 130–190 °C

PHA sample	SHS treatment		T_m (°C)	ΔH_m (J/g)	X_c (%)
	Temperature (°C)	Time (min)			
PHB-*co*-6%HHx	130	60	120.1, 145.3	66.6	45.4
		600	124.0, 145.4	79.0	53.9
	150	40	127.6, 143.0	60.5	41.3
		400	131.7, 144.7	61.7	42.1
	170	30	121.7, 142.1	59.2	40.4
		300	123.8, 138.7	64.4	43.9
	190	20	121.6, 142.7	58.1	39.6
		200	102.2, 122.8, 132.1	62.1	42.4
PHB-*co*-11%HHx	130	60	121.6, 137.2	41.8	28.5
		600	108.8, 124.8, 142.1	51.2	34.9
	150	40	100.0, 121.9	42.5	29.0
		400	109.5, 128.3	45.4	31.0
	170	30	100,7, 122.9	40.9	27.9
		300	95.2, 125.1, 144.1	41.5	28.3
	190	20	99.0,122.8	43.8	29.9
		200	87.3, 108.8, 117.6	46.3	31.6

3.3.2.5 Chemical compositions and chain-end structures of SHS treated PHBHHx

The changes in chemical compositions of co-monomer units of PHBHHx samples after the SHS treatment were calculated from peak signal integration values on ^{1}H NMR spectra as previously described in section 3.3.1. Based on Figure 3.4, strong proton integration signal at 1.26 ppm belonged to the methyl group of HB unit, and another methyl group belonged to the HHx unit appeared at 0.91 ppm , which were integrated in order to determine the percentage of HHx unit of PHBHHx samples. The detailed calculation method is shown in Appendix A15 and summary of HB and HHx fractions of SHS treated PHBHHx samples are summarized in Table 3.7. Based on the obtained results, there was no significant changes in the compositions of the SHS treated samples for all the temperatures used, percentages of co-monomer unit was remained in similar level as of the untreated samples. This could be due to the homogenous random chain scission of the ester bonds at the polymer backbone that occurs without affecting the methyl and propyl side chains of HB and HHx units, respectively. Thus, the percentages of the co-monomer units of the PHBHHx samples were macroscopically remained during the SHS hydrothermal treatment.

In addition, ^{1}H NMR spectra were also used to determine the chain-end structures of oligomers prepared via SHS hydrolysis by detecting the additional peaks attributed to newly formed chemical structures. In the present study, the homonuclear correlated spectroscopy (^{1}H-^{1}H COSY) technique was used to identify the chain end structures based on the cross peak analysis as shown in Figure 3.12 for P(HB-*co*-6%HHx) and

Appendix A16 for P(HB-*co*-11%HHx). The ^{1}HNMR spectra of PHBHHx samples are shown in Figure 3.13 and 3.14.

Table 3.7. Changes in co-monomer units of SHS treated PHBHHx samples

PHBHHx sample	SHS treatment		Composition (%)	
	Temperature (°C)	Time (min)	HHx unit	HB unit
P(HB-*co*-6%HHx)	Untreated	0	6.0	94.0
	130	60	6.0	94.0
		600	6.0	94.0
	150	40	6.0	94.0
		400	6.0	94.0
	170	30	6.0	94.0
		300	6.0	94.0
	190	20	6.0	94.0
		200	6.0	94.0
P(HB-*co*-11%HHx)	Untreated	0	11.0	89.0
	130	60	11.0	89.0
		600	11.0	89.0
	150	40	11.0	89.0
		400	11.0	89.0
	170	30	11.0	89.0
		300	11.0	89.0
	190	20	11.0	89.0
		200	11.0	89.0

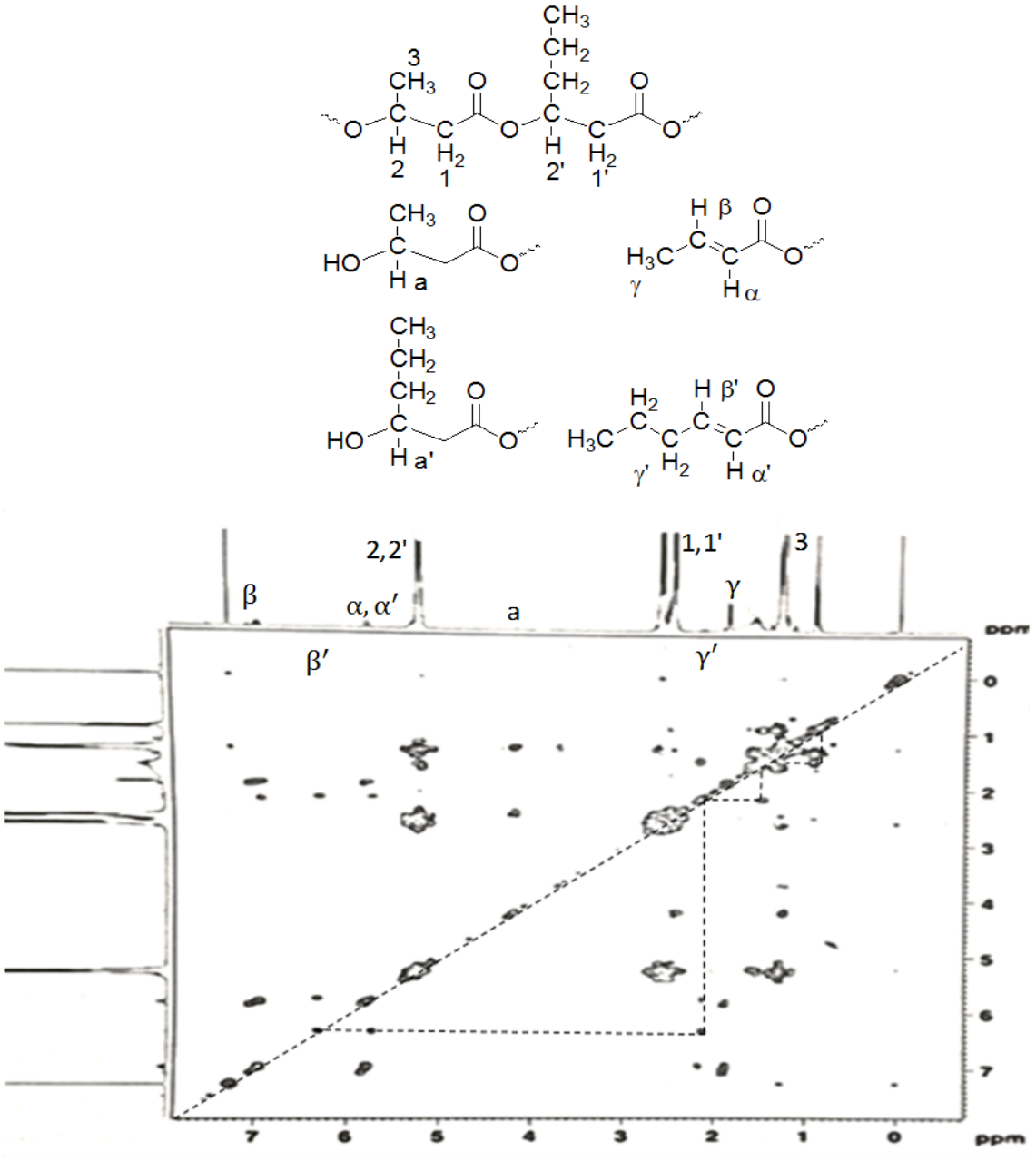

Figure 3.12. ^{1}H–^{1}H COSY of PHB-*co*-6%HHx hydrolyzates at the end of SHS treatment of 190 °C

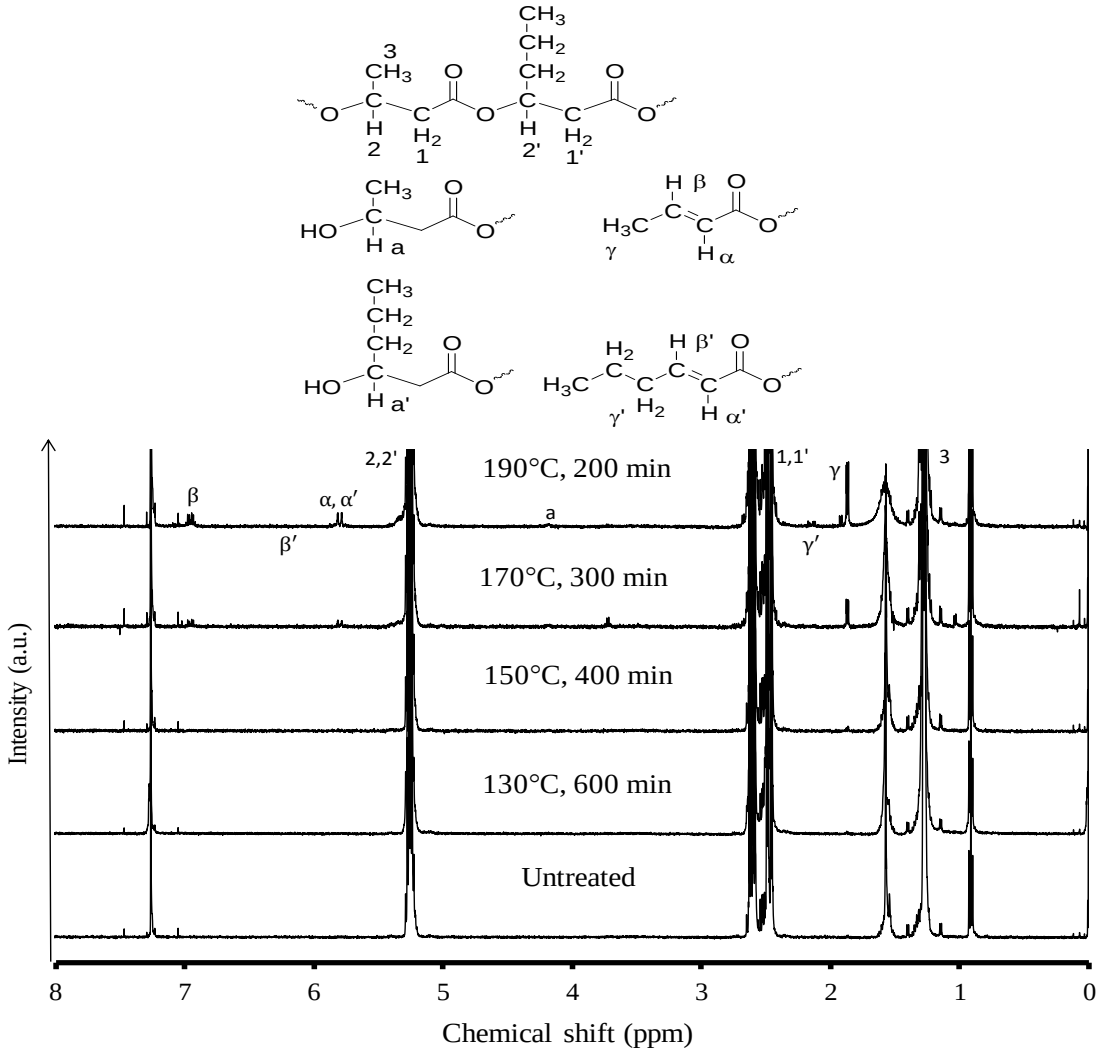

Figure 3.13. ^{1}H NMR spectra of SHS treated P(HB-*co*-6%HHx) samples to confirm chain-end structures

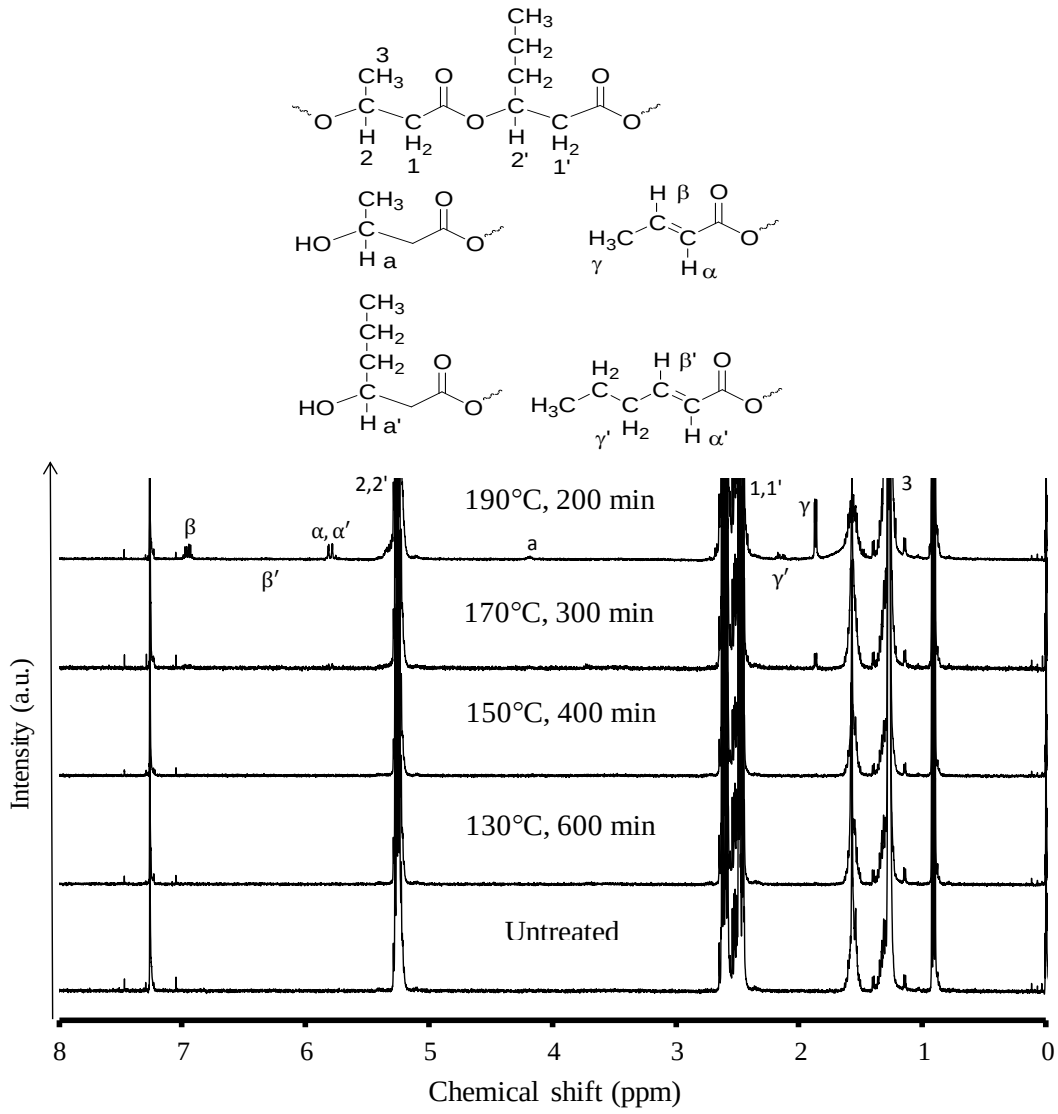

Figure 3.14. ^{1}H NMR spectra of SHS treated P(HB-*co*-11%HHx) samples to confirm chain-end structures

After the SHS treatment, obtained oligomers mainly had hydroxyl and alkenyl (crotonoyl and 2-hexenoyl) chain-end structures based on the employed treatment temperatures. Resonance peaks of protons in a 2-hexenoyl chain end group were detected at 0.91 ($C\underline{H}_3$-CH_2-CH_2-), 1.40 (CH_3-$C\underline{H}_2$-CH_2-), 2.16 (CH_3-CH_2-$C\underline{H}_2$-), 5.85 (C_3H_7-CH=C$\underline{H}$-), and 6.30 (C_3H_7-C$\underline{H}$=CH-). On the other hand, resonance peaks of protons in the crotonoyl chain end group were detected at 1.87 ($C\underline{H}_3$-), 5.85 (-CH=C$\underline{H}$-), and 6.95 (CH_3-C$\underline{H}$=CH-) ppm (Yu and Marchessault, 2000). Resonance peak of methine proton in the hydroxyl chain-end group (HO-C$\underline{H}$(CH_3)-) of HB unit was determined at 4.19 ppm (Yu and Marchessault, 2000). However, the signal for methine proton HO-C$\underline{H}$(C_3H_7)- of HHx unit was not detected clearly.

In Figure 3.13 and 3.14, the characterized peaks of corresponding chain-end structures are shown. The signals at 6.95 (CH_3-C$\underline{H}$=CH-), 6.30 (C_3H_7-C$\underline{H}$=CH-), and 4.19 (HO-C$\underline{H}$(CH_3)-) ppm were integrated to determine percentages of crotonoyl, 2-hexenoyl and 3-hydroxy butanoyl groups (Figure 3.15), respectively, according to the chracterization of Yu and Marchessault (2000). The percentage of hydroxyl and unsaturated chain-end groups of PHBHHx were calculated based on the molar fractions of hydroxyl end (HO-C$\underline{H}$(CH_3)-) as well as unsaturated end (CH_3-C$\underline{H}$=CH- or C_3H_7-C$\underline{H}$=CH-) to the total ends of PHBHHx: (HO-C$\underline{H}$(CH_3)-, CH_3-C$\underline{H}$=CH- and C_3H_7-C$\underline{H}$=CH-), by comparing the intensities of proton integration values of the end groups at their corresponding chemical shifts. Quantitative analytical data of the resulting chain-end groups were listed in Table 3.8.

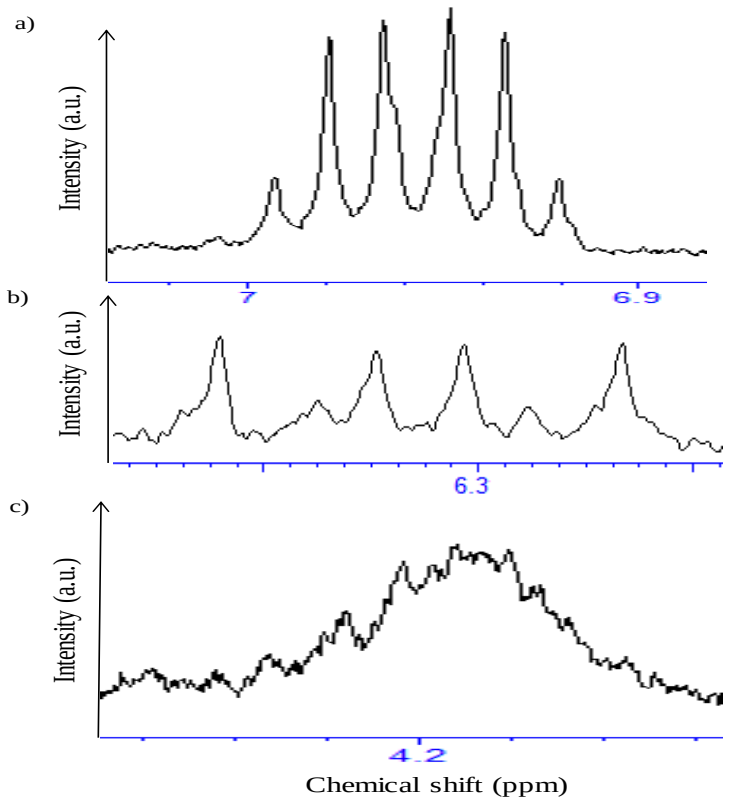

Figure 3.15. Chain-end signals of methine proton of PHBHHx on ^{1}H NMR (a) crotonoyl (b) 2-hexenoyl (c) 3-hydroxy butanoyl groups

Table 3.8. Quantitative analytical results of chain-end structures of PHBHHxs samples after SHS treatment

Sample	Treatment condition		Percentage (%) of chain-end groups		
	Temperature (°C)	Time (min)	3-hydroxy butanoyl (HB unit)	Crotonoyl (HB unit)	2-hexenoyl (HHx unit)
P(HB-*co*-6%HHx)	130	600	100.0	n.d*	n.d
	150	400	68.1	31.9	n.d
	170	300	31.1	68.9	n.d
	190	200	19.2	76.5	4.3
P(HB-*co*-11%HHx)	130	600	100.0	n.d	n.d
	150	400	100.0	n.d	n.d
	170	300	37.9	62.1	n.d
	190	200	18.3	74.5	7.2

* Undetected

All the samples had a hydroxyl chain-end group only and there was no formation of an alkenyl group after SHS treatment at 130 °C. This indicates that the ester hydrolysis proceeded selectively. After SHS treatment at 150 °C, P(HB-*co*-6%HHx) showed the formation of crotonoyl chain-end groups under higher magnification, but there was no signal representing 2-hexenoyl group. As the treatment temperature raised to 170 °C, P(HB-*co*-11%HHx) also showed the formation of crotonoyl group. Interestingly, the production ratio of crotonoyl group was superior to hydroxyl group, but there was no detectable 2-hexenoyl group. After SHS treatment at 190 °C, PHBHHx samples formed 2-hexenoyl chain-end groups.

The above results indicate that HHx unit suppresses the hydrolysis and thermal degradation of HB*HHx sequence with the formation of 2-hydroxy-hexanoyl and 2-hexenoyl groups, respectively. The crotonoyl chain-end group from HB unit in the polymer chain rapidly increased at higher temperatures to take the place of the main chain-end structure from the hydroxyl group. The rapid formation of crotonoyl chain end group suggests a shift to thermal degradation from thermal hydrolysis as a main reaction. In many previous studies, the crotonoyl chain ends were formed mainly due to the dehydration of hydroxyl chain-end as observed in alkaline hydrolysis or via β-elimination as observed in thermal degradation of PHB. The second preference, β-elimination reaction mainly occurs during the heating of PHB and in a molten state (Yu *et al*., 2005). Thus, as the treatment temperatures increased to 170 °C, PHBHHx samples were completely melted and crotonoyl chain ends could readily formed. The formation of crotonoyl chain ends also suggests the occurrence of β-elimination reaction at the

higher temperatures mimicking the thermal degradation due to the characteristics of SHS, which is a kind of dry steam that is commercially used in the drying process. As the treatment temperature was raised to 190 °C, the same trend was observed and the percentage of crotonoyl chain-ends got even higher as shown in Table 3.8. This could be due to the auto-acceleration effect of the unsaturated, crotonoyl chain end groups that accelerates the bond cleavage by β-elimination reaction of neighboring ester linkage (Ariffin *et al*., 2008; Ariffin *et al*., 2010b; Nyugen *et al*., 2002). The contribution of these chain ends in the hydrothermal degradation mechanism of PHBHHx will be discussed in the next chapter.

3.4 Conclusion

In a nutshell, the present study introduced SHS hydrothermal treatment as an alternative, eco-friendly degradation method to precisely degrade the high molecular weight PHBHHx polymers into low molecular weight oligomers to make it favorable for biomedical applications such as drug delivery and medical sutures. The molecular weight reduction was clearly observed for P(HB-*co*-6%HHx) and P(HB-*co*-11%HHx) for all the SHS treatment temperatures of 130, 150, 170, and 190 °C in the order of P(HB-*co*-6%HHx) > P(HB-*co*-11%HHx). The present study also revealed that the SHS hydrolysis of PHBHHx preferentially occurs at amorphous phase via bulk erosion and beyond the critical point, heterogeneous degradation was observed. PHBHHx oligomers obtained at highest treatment temperature, 190 °C had molecular weight in the range of 4-5 kDa and mainly consists of hydroxyl, crotonoyl and 2-hexenoyl chain-ends. The superior production of crotonoyl group compare to hydroxyl and 2-hexenoyl groups in PHBHHx samples with the increase in treatment temperature indicates a possible shift to a thermal degradation from thermal hydrolysis as a main reaction. The expected SHS hydrolysis mechanism of PHBHHx samples will be discussed further in Chapter 4.

CHAPTER 4

EVALUATION OF KINETICS AND DEGRADATION BEHAVIOR DURING THE HYDROTHERMAL DEGRADATION OF POLY(3-HYDROXYBUTYRATE-*CO*-3-HYDROXYHEXANOATE)

4.1 Introduction

Poly((*R*)-3-hydroxybutyrate-*co*-(*R*)-3-hydroxyhexanoate) (PHBHHx) is a type of copolymer in PHA family that consists of randomly distributed (*R*)-3-hyroxybutyrate (HB) and (*R*)-3-hydroxyhexanoate (HHx) units (Yang *et al*., 2012). PHBHHx with the estimated mole fraction of HHx in the range of 0-31 mol% (Chen *et al*., 2005b) has better mechanical properties and can be more easily processed compared to PHB and poly((*R*)-3-hydroxyvalerate) (PHBV) (Wang *et al*., 2004). Because PHBHHx has potential applications in various fields, the degradation properties of PHBHHx must be determined, especially those related to thermal degradation and hydrolysis, which causes substantial changes in the mechanical properties after melt processing. Thus, it is important to clarify the degradation properties of PHBHHx to oligoesters. As discussed in Chapter 3, SHS hydrolysis was introduced in the present study as an alternative method to currently existing PHA degradation methods. The resulted PHBHHx oligomers from SHS hydrolysis had a hydroxyl, crotonoyl and 2-hexenoyl chain-ends. Since the chemical structures of the resulting oligomers and degradation products are likely dependent on the degradation mechanisms, it is important to determine SHS hydrolysis mechanism of PHBHHx. The well understood degradation kinetics also

necessary to control functional and disappearance time as well as degradation products and release rates, in the making of PHBHHx based biomedical devices.

Previously, studies on the hydrolysis of PHBHHx have shown that hydrolysis occurs preferentially at the amorphous phase, rather than the crystalline phase (Shimamura *et al*., 1994; Doi *et al*., 1995; Yang *et al*., 2009). However, effects of HHx unit in the HB unit sequence on the hydrothermal degradation of PHBHHx have not yet been determined. To evaluate the effects of HHx unit on the hydrothermal degradation, super-heated steam (SHS) hydrolysis was introduced for the hydrolysis of PHBHHx. In the present study, the effects of HHx units on the hydrothermal degradation of PHBHHx with 6% HHx and 11% HHx were investigated, with a focus on changes in the diad sequence distribution after SHS hydrolysis. The diad sequence distribution for PHBHHx has been determined in previous studies (Shimamura *et al*., 1994; Doi *et al*., 1995). However, to date changes in diad sequence distribution during degradation, that is, the effects of HHx on the sequence during hydrolysis remain unknown. Moreover, as discussed in Chapter 3, the oligomers resulted from the SHS treatment had higher percentage of crotonoyl chain end which could be due to the β-elimination reaction.

Therefore, in this chapter, in order to clarify the relationship between the chain scission behaviors and the chain-end structures during the hydrothermal degradation and to determine the effects of HHx unit in HB sequence, P(HB-*co*-6%HHx) and P(HB-*co*-11%HHx) were selected as they showed contrary degradation behaviors in preliminary experiments despite having nearby contents of the HHx unit. To clarify the changes in

the first-order structure and degradation behavior of PHBHHx during SHS hydrolysis, precise structural analyses, including size-exclusion chromatography (SEC), proton (^{1}H) and carbon (^{13}C) nuclear magnetic resonance (NMR) spectroscopies, differential scanning calorimetry (DSC) and thermogravimetry (TG) were employed in the present study. Thermal degradation in TG was conducted in order to clarify the SHS hydrolysis mechanism that resulted in the crotonyl-chain ends. The obtained results and the expected SHS hydrolysis mechanism of PHBHHx were discussed in the present chapter.

4.2 Materials and Methods

4.2.1 Materials

The materials used in the present study were previously described in section 3.2.1 of Chapter 3.

4.2.2 Preparation of PHBHHx film samples

The PHBHHx films were prepared using a compressed molding technique with the aid of heat pressure film forming machine IMC-180C (Imoto Machinery, Kyoto, Japan) as previously described in section 3.2.2 of Chapter 3.

4.2.3 Hydrothermal degradation of PHBHHx films by superheated steam

Hydrothermal degradation of PHBHHx films was done by SHS in an oven QF-5200C (Naomoto Corporation, Osaka, Japan) as previously described in section 3.2.3 of Chapter 3.

4.2.4 Analytical procedures

4.2.4.1 Size exclusion chromatography

The analysis of molecular weight changes was determined with SEC as previously described in section 3.2.4.1 of Chapter 3. The obtained molecular weight data was used calculate the kinetic parameters based on Nishida's method (Nishida *et al*., 2000a).

4.2.4.2 Thermogravimetric analysis

Thermogravimetric (TG) measurement was performed on a Seiko Instruments Inc. EXSTAR 6200 TG system in an aluminium pan (5mmØ) to determine the degradation temperature of the SHS treated PHBHHx sample strips as previously described in section 3.2.4.2 of Chapter 3**.**

In order to determine kinetic parameters during thermal degradation, PHBHHx samples (5-6 mg) were measured in aluminum pans. The sample pan was set and heated at prescribed multiple heating rates (ϕ) of 1, 3, 5, 7 and 9 °C min^{-1} in a temperature range

of 30-550 °C in a steady flow of nitrogen (100 mL min^{-1}). The corresponding weight loss (μg) and its derivative DTG values were recorded for the calculation of apparent activation energy E_a value in an analytical computer system. The E_a value was calculated using Doyle's equation and compared with Reich's equation.

4.2.4.3 Nuclear magnetic resonance spectroscopy

The analytical procedures of proton (^1H) NMR were as previously described in section 3.2.4.5 of Chapter 3. Carbon (^{13}C) NMR spectra were recorded on a 125-MHz JEOL JNM-ECP500 FT NMR system. Chloroform-*d* ($CDCl_3$) was used to dissolve the sample. The chemical shift was reported as δ values (ppm) relative to internal standards tetramethylsilane (TMS) and $CDCl_3$ unless otherwise noted. Total of 1004 scans were performed for ^{13}C NMR measurements. The diad sequence distributions of HB*HB, HB*HHx, HHx*HB, and HHx*HHx were determined from corresponding signals on a ^{13}C NMR spectrum (Shimamura *et al*., 1994). In order to estimate the peak area, each resonance peak was simulated using the Lorentzian function in PeakFit Software version 4.12.

4.2.4.4 Differential scanning calorimetry analysis

Thermal properties of SHS treated PHBHHx sample strips including melting point (T_m) and crystallinity (X_c%) were determined on a differential scanning calorimeter (DSC)

(Seiko Instruments Inc, EXSTAR 6000-DSC 6220) as previously described in section 3.2.4.3 of Chapter 3.

4.3 Results and discussion

In the present Chapter, PHBHHx samples: P(HB-*co*-6%-HHx) and P(HB-*co*-11%-HHx), were used to investigate the effects of HHx unit on the hydrothermal degradation of HB unit sequence. The structural, physical and thermal properties of the PHBHHx samples before and after the SHS treatment were discussed in detail in Chapter 3. In the present chapter, the relationship between the chain scission behaviors and the chain-end structures during the hydrothermal degradation and as well as the effects of HHx unit in HB unit sequence was clarified in terms of the changes in diad sequence distribution after the SHS hydrolysis.

4.3.1 Hydrothermal degradation rate of PHBHHx

In the previous chapter, the SHS hydrolysis behaviors of P(HB-*co*-6%-HHx) and P(HB-*co*-11%-HHx) which were treated at 130, 150, 170 and 190 °C, were reported with changes in SEC profiles. The SEC profiles shifted to a lower molecular weight region maintaining a unimodal distribution profile close to the most probable distribution (MPD), up to a critical point. The MPD indicated that the hydrothermal degradation under SHS treatments proceeded in a homogeneous random degradation manner *via* the bulk-erosion mechanism (Tsuji and Miyauchi, 2001; Mohd-Adnan *et al*., 2008). In

general, it was reported that the hydrolysis of polymer bonds obeys second order reaction kinetics, where the rate of reaction is proportional to the hydrolytic products, which is the chain-ends (Lyu and Untereker, 2009). Hydrolysis kinetics are also usually analyzed by the changes in molecular weight versus time, where in the case of second order reaction, $1/M_n$ versus time must have a linear or proportional relationship (Lyu and Untereker, 2009). As previously mentioned in Chapter 3, M_w was adopted for more reliable calculation of kinetic parameters in the present study to neglect the influence of weight loss, where just 1% of weight loss in lower molecular weight fractions resulted in 15% increase in M_n, contrastively, only 0.95% increases in M_w (Nishida *et al*., 2000a; Mohd-Adnan *et al*., 2008). In order to estimate the rate constant: *k* value accurately, only the data obtained during homogenous hydrolysis which is before the critical point were taken into consideration as shown in Figure 4.1. The *k* value was calculated based on slope of the plot ln M_w versus time which was calculated using Equation 4.1 for auto-catalytic random degradation kinetics.

$$\ln M_w = \ln M_{w0} - kt \qquad (4.1)$$

where, M_{w0} and *k* are initial weight-average molecular weight and rate constant of reaction, respectively (Mohd-Adnan *et al*., 2008).

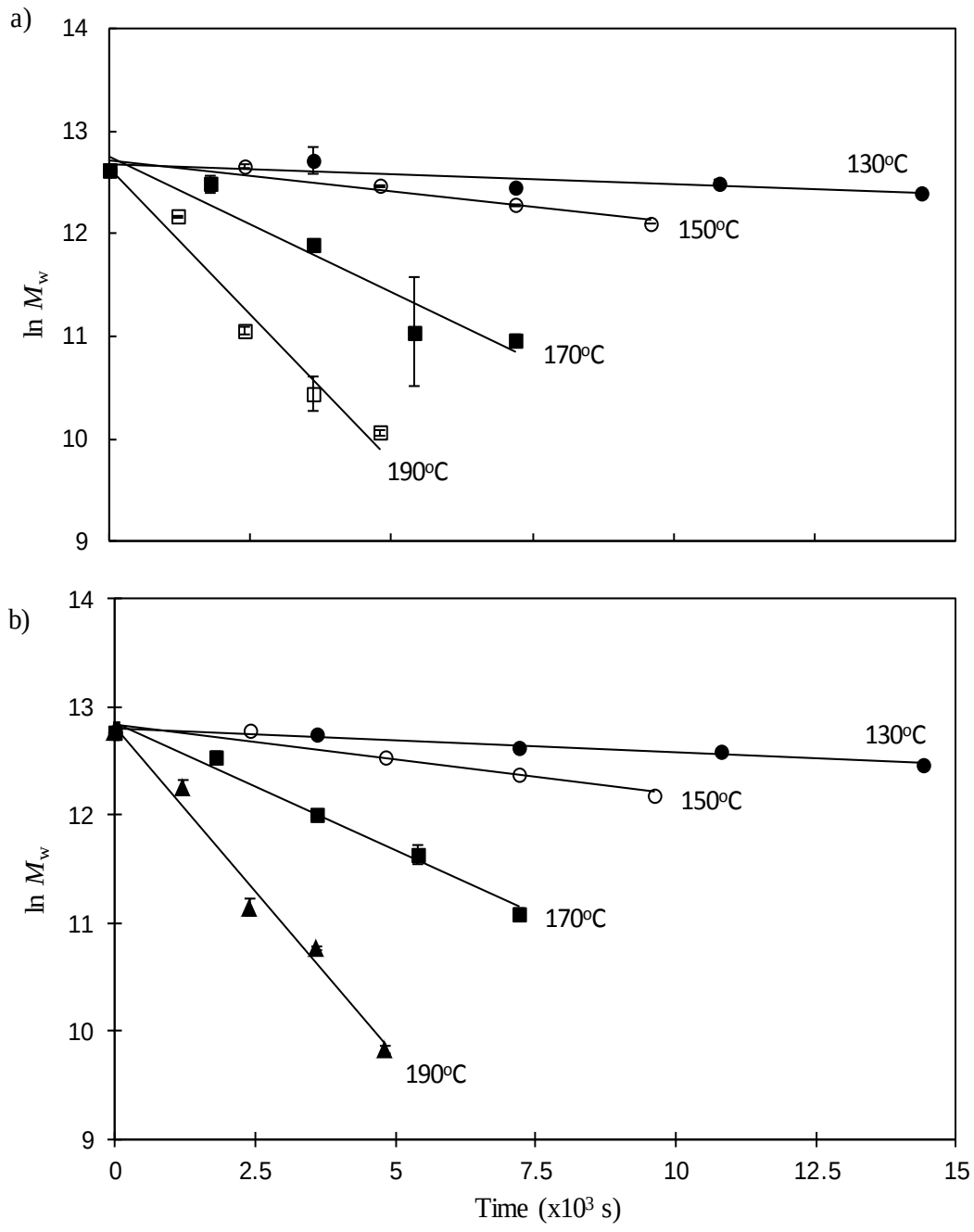

Figure 4.1. Relationships between ln M_w and reaction time of (a) P(HB-*co*-6%-HHx) and (b) P(HB-*co*-11%-HHx) during SHS treatment

The logarithmic plots of ln M_w versus time of both P(HB-*co*-6%-HHx) and P(HB-*co*-11%-HHx) showed a linear relationship, therefore it is obvious that the PHBHHx hydrolysis proceeded in a manner of auto-catalytic random degradation and follows the first-order kinetics (Nishida *et al*., 2000a). Reaction rate constant value *k* was calculated according to Nishida's method (Mohd-Adnan *et al*., 2008) as listed in Table 4.1 and the regression coefficient, R^2 values were displayed in Appendix B1. The resulted rate constant *k* values for P(HB-*co*-6%HHx) and P(HB-*co*-11%HHx) were found to be in the ranges of 19.3 x 10^{-6} (130 °C) – 571.4 x 10^{-6} s^{-1} (190 °C) and 21.2 x 10^{-6} (130 °C) – 614.2 x 10^{-6} s^{-1} (190 °C), respectively. The Arrhenius plots were obtained using ln *k* and 1/T for PHBHHx samples as shown in Figure 4.2 with good R^2 values of more than 0.990 (Appendix B1).

Table 4.1. Reaction rate constant *k* value for SHS hydrolysis of PHBHHx samples

Temperature (°C)	Rate constant[a]: k_{M_w} (s^{-1})	
	P(HB-*co*-6%HHx)	P(HB-*co*-11%HHx)
130	0.019	0.021
150	0.059	0.065
170	0.265	0.237
190	0.571	0.614

[a]Based on the changes in M_w

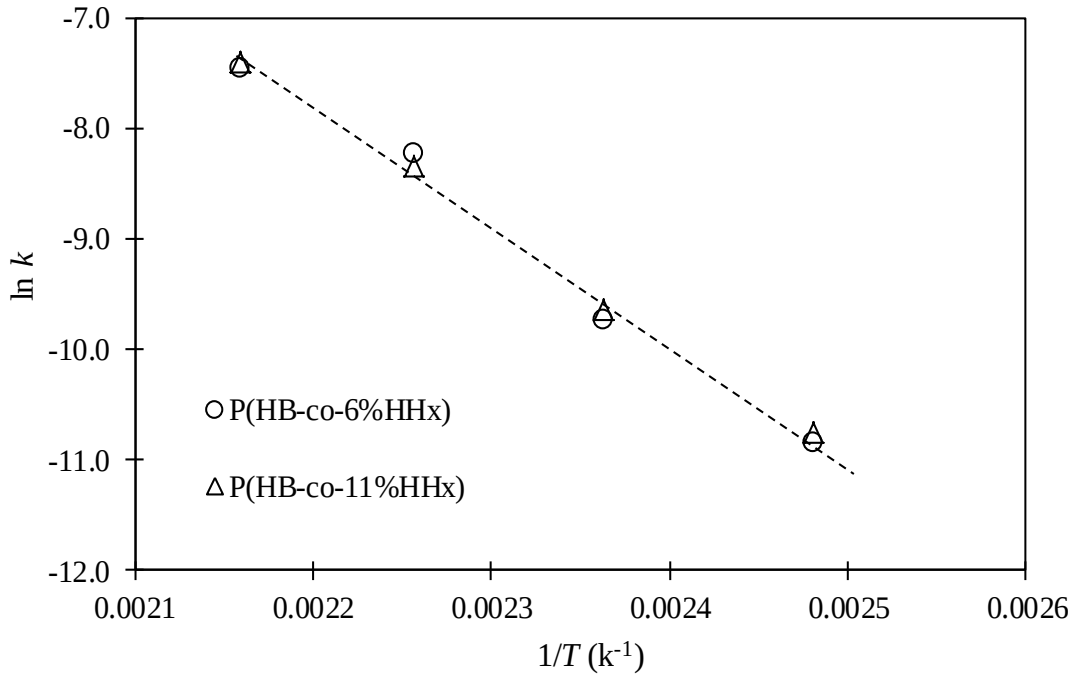

Figure 4.2. Arrhenius plots for the SHS degradation of PHBHHx for the temperature range of 130–190 °C

According to Figure 4.2, a strong linear relationship was obtained for both P(HB-*co*-6%HHx) and P(HB-*co*-11%HHx) samples and the activation energy, E_a value was determined from the Arrhenius plots based on Equation 4.2:

$$k = A \exp(-E/RT)$$

By inserting ln,

$$\ln k = \ln A - (E/RT) \qquad (4.2)$$

where, k is the rate constant, A is the frequency factor (s^{-1}), E is the activation energy (kJ mol^{-1}), T is absolute temperature in Kelvin and R is the universal gas constant (8.314 J mol^{-1}) (Yu *et al*, 2005). The values of A and E was determined from the plot of ln k versus $1/T$ of Figure 4.2.

The activation energy values (E_a) of P(HB-*co*-6%HHx) and P(HB-*co*-11%HHx) during SHS hydrolysis for the temperature range of 130–190 °C were 88.4 and 90.6 $kJmol^{-1}$, respectively. The values were close to each other, showing that the reaction occurred dominantly on HB*HB sequences (will be discussed in next section).

4.3.2 Behavior of PHBHHx degradation

4.3.2.1 Preferences on chain scission of diad sequences of PHBHHx

In order to elucidate the effects of HHx units on the SHS degradation of PHBHHx, changes in molecular structure, focusing on the diad sequence distribution were calculated on the basis of integration values of the carbonyl resonance peaks in the ^{13}C NMR spectra for the following diad sequences (Figure 4.3): HB*HB, HB*HHx, and HHx*HB at 169.100, 169.253, and 169.284 ppm, respectively for the typical samples degraded at employed temperatures (Figure 4.4).

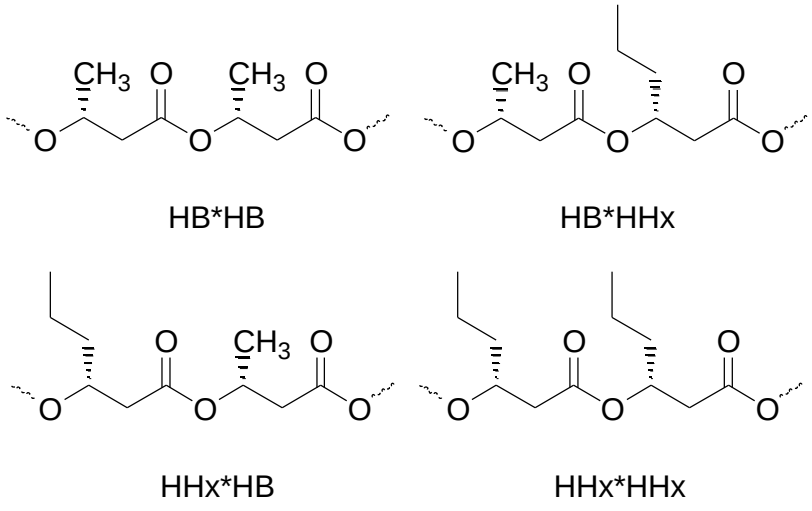

Figure 4.3. Diad sequences of PHBHHx

Each resonance peak was simulated using the Lorentzian function to estimate the peak area, resulting in a list that shown in Table 4.2. The calculated diad sequence distribution values of original P(HB-*co*-6%-HHx) and P(HB-*co*-11%-HHx) were compared with values calculated with Bernoulian statistics, which are applicable to a statistically random copolymerization. In the Bernoulian model, mole fraction F_{i*j} of diad sequence i*j can be expressed as $F_{i*j} = F_iF_j$. The mole fractions F_i and F_j have units of *i* and *j*, respectively. The calculated diad fractions: $F_{HB*HB,}$ $F_{HB*HHx,}$ F_{HHx*HB} and $F_{HHx*HHx}$ of original P(HB-*co*-6%-HHx) were 88.36, 5.64, 5.64, and 0.36% respectively, which was in good agreement with the observed values: 88.6, 5.8, 5.6, and ~0% for F_{HB*HB}, F_{HB*HHx}, F_{HHx*HB}, and $F_{HHx*HHx}$, respectively. In the case of P(HB-*co*-11%-HHx), the calculated diad fractions: $F_{HB*HB,}$ $F_{HB*HHx,}$ F_{HHx*HB} and $F_{HHx*HHx}$ of original P(HB-*co*-11%-HHx) was 79.21, 9.79, 9.79, and 1.21% respectively, which were also in good agreement with the observed values: 77.8, 11.4, 10.8, and ~0% for F_{HB*HB}, F_{HB*HHx}, F_{HHx*HB}, and $F_{HHx*HHx}$, respectively. A possible peak assignable to diad sequence fraction $F_{HHx*HHx}$ was difficult to detect on ^{13}C NMR spectrum for both PHBHHx samples due to the very small portion of HHx*HHx unit sequence. Thus, it was confirmed that the sequence distribution of HB and HHx units in P(HB-*co*-6%-HHx) and P(HB-*co*-11%-HHx) was statistically random (Shimamura *et al*., 1994).

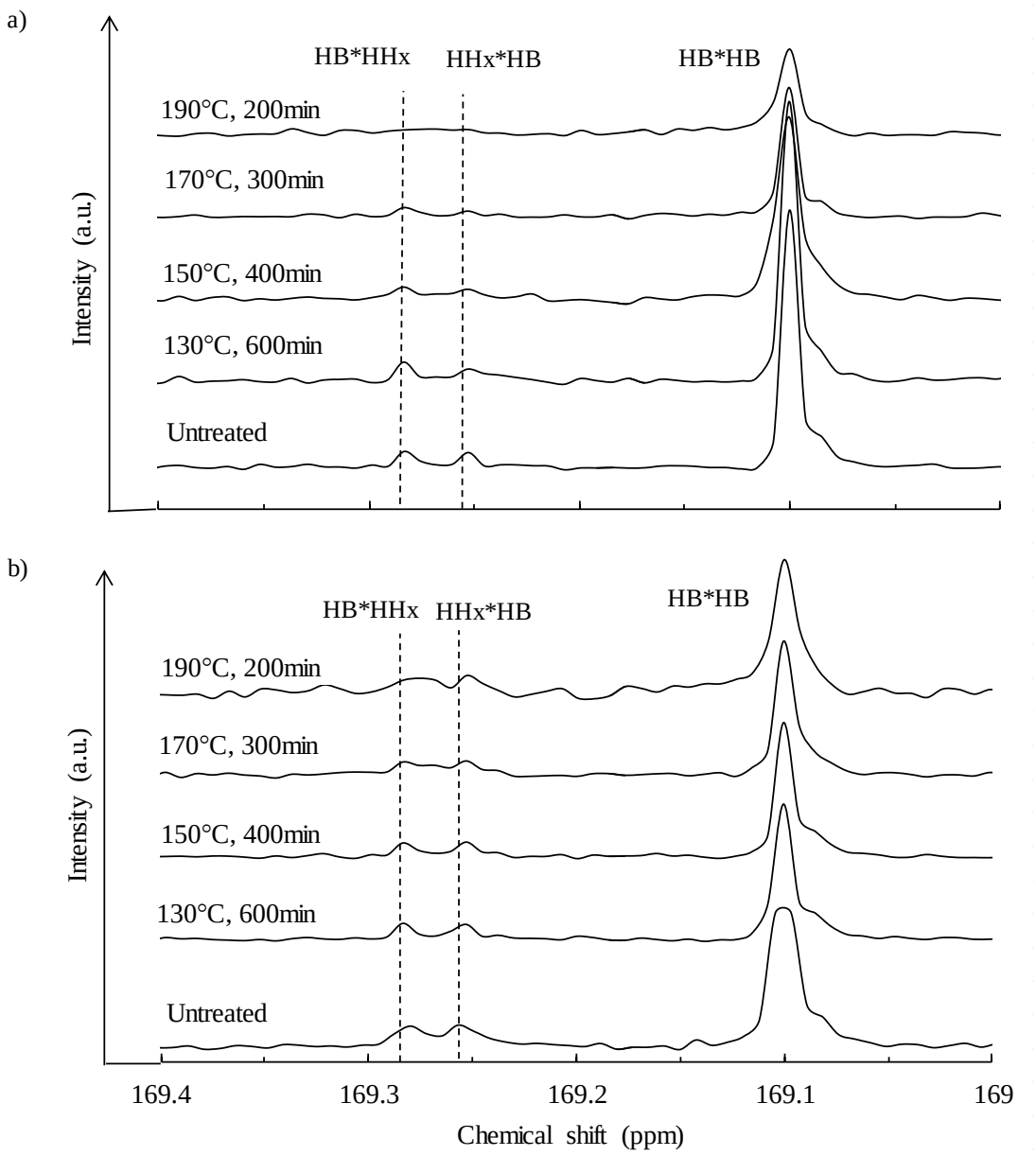

Figure 4.4. Carbonyl resonances of diad sequences on ^{13}C NMR spectra of (a) P(HB-*co*-6%-HHx) and (b) P(HB-*co*-11%-HHx) after SHS treatment under different conditions

From the results listed in Table 4.2, both PHBHHx samples showed a gradual increase in relative peak intensity of the diad sequence: HB*HB and conversely a gradual decrease in relative peak intensity of HHx*HB diad sequence. Although, untreated P(HB-*co*-6%-HHx) showed similar intensity values of 5.8% and 5.6% for HB*HHx and HHx*HB sequences, respectively, after the SHS treatment at 170 ℃ for 300 min, the relative intensity of HHx*HB decreased to 3.9%, whereas the value of HB*HHx increased to 6.9%. After SHS treatment at 190 ℃ for 200 min, the spectrum broadened because of the extreme decrease in molecular weight as shown in Appendix A8. In the case of P(HB-*co*-11%-HHx), it also showed similar intensity values of 10.8% and 11.4% for HB*HHx and HHx*HB sequences, respectively. After the SHS treatment at 170 ℃ for 300 min, the relative intensity of HHx*HB decreased to 9.2%, whereas the value of HB*HHx also decreased to 9.7%. At the end of SHS treatment at 190 ℃ for 200 min, the spectrum of P(HB-*co*-11%-HHx) also broadened similar to P(HB-*co*-6%-HHx) due the extreme decrease in molecular weight (Appendix A10) and the peak intensity of HB*HHx and HHx*HB sequences remained similar.

The gradual increase and decrease in relative peak intensity of the diad sequence: HB*HB and HHx*HB of PHBHHx must simply reflect the preferential hydrolysis of ester bonds in flexible chain sequences, in which HHx units locate selectively. Interestingly, a contrastive degradation behavior of HB*HHx sequence was found between P(HB-*co*-6%-HHx) and P(HB-*co*-11%-HHx), where it gradually increasing and decreasing, respectively, with increase in temperature during the SHS treatment (Appendix B3). These specific chain scission behaviors are considered to be due to the

combined results of the suppressive effects of hydrophobicity and steric hindrance of propyl group in the HHx unit as well as the promotive effects of lower crystallinity and the easier diffusion of steam into the wider and more flexible amorphous region of P(HB-*co*-11%-HHx) due to concentration of HHx units compared with that of P(HB-*co*-6%-HHx). This combination of influences may resulted in no selectivity on the SHS degradation between HHx*HB and HB*HHx sequences as shown in Appendix B3 and Table 4.2.

Table 4.2. Changes in diad sequence distribution of SHS treated PHBHHx

SHS treatment		Diad sequence composition (%)					
Temperature	Time	P(HB-*co*-6%-HHx)			P(HB-*co*-11%-HHx)		
(°C)	(min)	F_{HB*HB} [a]	F_{HB*HHx} [a]	F_{HHx*HB} [a]	F_{HB*HB} [a]	F_{HB*HHx} [a]	F_{HHx*HB} [a]
Untreated	-	88.6	5.8	5.6	77.8	10.8	11.4
130	600	88.7	5.9	5.4	79.3	10.2	10.5
150	400	88.6	6.2	5.2	80.0	9.8	10.2
170	300	89.2	6.9	3.9	81.1	9.7	9.2
190	200	89.3	7.1	3.6	81.7	9.1	9.2

[a] Mole fraction based on peak area of corresponding carbonyl resonance on ^{13}C NMR spectrum.

4.3.2.2 Thermal degradation behavior of PHBHHx

In order to clarify the formation of crotonoyl chain-end during SHS treatment and the to determine the effects of HHx unit on hydrothermal degradation of PHBHHx, the thermal degradation behavior of both PHBHHx samples was investigated by dynamic pyrolysis in a TGA at a heating rate, 10 °C min^{-1} in a temperature range of 30-550 °C in N_2 flow. The difference of half weight loss temperature (T_{d50}) and melting temperature ($T_{m)}$ values was used to determine the influence of HHx unit on HB sequence towards the

thermal stability. In Table 4.3, T_{d50} values of untreated and SHS-treated samples are listed. The order of T_{d50} was P(HB-*co*-6%-HHx) > P(HB-*co*-11%-HHx), while the order of difference between T_{d50} and T_m: T_{d50}-T_m was found to be P(HB-*co*-11%-HHx) > P(HB-*co*-6%-HHx). These results indicate that HHx units functionally contribute to the thermal stability of the HB unit sequence, probably due to various mechanisms hindering the thermal degradation pathway of PHB. Similar trend of results were obtained by Liu *et al*. (2012), where PHBV-diol which had a lower molecular weight and lower T_m than the original PHBV, had a higher T_{max}-T_m, at most by 57.9 °C compared to the T_{max}-T_m of original PHBV.

Table 4.3. Thermal degradation properties of PHBHHx samples

Samples	SHS treatment condition (°C/min)	Degradation temperature.[a] T_{d50} (°C)	T_{d50} - T_m (°C)
PHB-*co*-6%-HHx	Untreated	290.0	146.9 ~ 162.1
	130 / 600	290.0	-
	190 / 200	290.0	-
PHB-*co*-11%-HHx	Untreated	289.0	165.4 ~ 180.2
	130 / 600	288.0	-
	190 / 200	288.0	-

[a] Measured with TG at a heating rate of 10 °C min^{-1} in N_2 flow (100 mL·min^{-1}).

To clarify the effects of HHx units on the thermal degradation, the thermal degradation kinetic parameter: E_a values of PHBHHx samples were analyzed with TG at multiple heating rates (ϕ) of 1, 3, 5, 7 and 9 °C (K) min^{-1} in N_2 flow (100 mL min^{-1}). The TG curves of PHBHHx samples at multiple heating rates from 1–9 Kmin^{-1} were shown in Figure 4.5, where each TG curve displayed a smooth and one-step decomposition from the initial to completion of treatment temperature, and also shifted to higher temperature

ranges with the increase in the heating rate. The DTG curves of the PHBHHx samples are shown in Figure 4.6, where single DTG peaks were detected. Similar to TG curves, DTG curves also shifted to higher temperature ranges with the increase in the heating rate. This could possibly indicate the occurrence of single-step reaction.

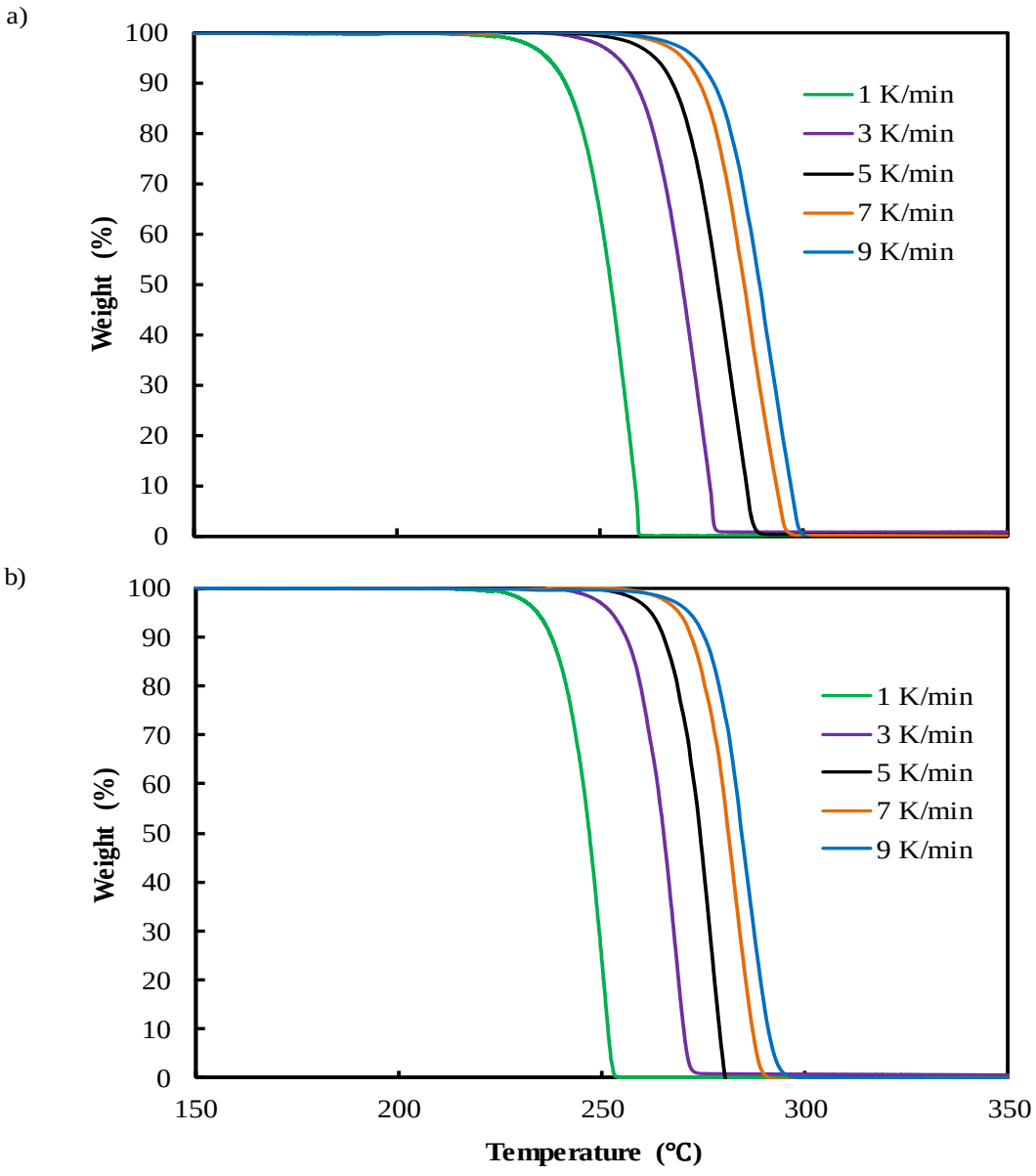

Figure 4.5. Thermogravimetric (TG) curves of (a) P(HB-*co*-6%-HHx) and (b) P(HB-*co*-11%-HHx) at multiple heating rates (1, 3, 5, 7, and 9 K min^{-1}) in N_2 flow (100 mL min^{-1})

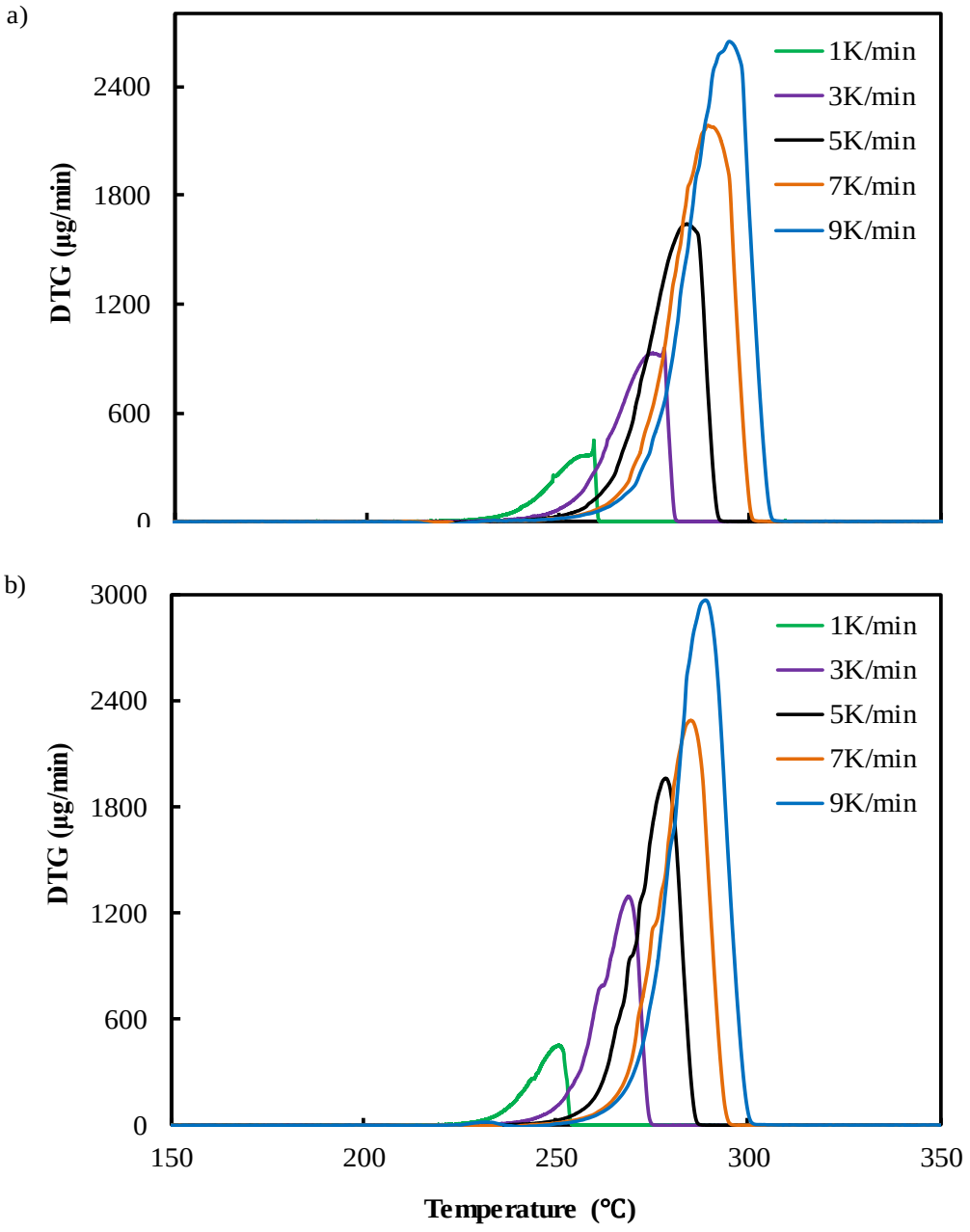

Figure 4.6. Differential thermogravimetric (DTG) curves of (a) P(HB-*co*-6%-HHx) and (b) P(HB-*co*-11%-HHx) at multiple heating rates (1, 3, 5, 7, and 9 K/min) in N_2 flow (100 mL·min^{-1})

In the present study, modified Doyle's method was used to determine the activation energy (E_a) and compared with Reich's method, which was successfully utilized by Nishida *et al*. (2000b) for the evaluation of kinetic parameters during pyrolysis of poly(1,4-diaxan-2-one) {poly(p-dioxanone), PPDO} in TGA at the temperature range of 30-350 °C. It was reported that, if the pyrolysis of PHBHHx samples occurs via a single degradation process with the fixed apparent parameters: activation energy (E_a) and pre-exponential factor (*A)* during the employed temperature range, the TG curves can be superposed among them via abscissa shifting using Equation 4.3:

$$1/T_1 = 1/T_2 + (R/bE_a)(\log \phi_2 - \log \phi_1) \qquad (4.3)$$

where, *T*, *R* and ϕ are absolute temperature in Kelvin (273.14), universal gas constant (8.314 J $mol^{-1}K^{-1}$) and heating rate (K min^{-1}), respectively. The *b* value is a constant of Doyle's approximation that obeys Equation 4.4:

$$\log p(y) \cong -a - bE_a/RT \qquad (4.4)$$

Where $y = E_a/RT$. If the value of $y > 20$ in the function of $p(y)$, the *a* and *b* constants values are 2.315 and 0.4567, respectively (Nishida *et al*., 2000b; Liu *et al*., 2012)

The superpositions of TG curves of PHBHHx are shown in Figure 4.7 with Equation 4.3 displayed on x-axis. The superposed TG curves displayed a single curve, meaning that the TG curves of PHBHHx pyrolysis were able to be analyzed apparently as a single degradation process with the fixed apparent parameters (E_a and *A*) (Nishida *et al*., 2000b; Liu *et al*., 2012). In order to determine the pyrolysis activation energy, the logarithms of heating rate (log ϕ) versus reciprocal absolute temperature (1/*T)* were plotted (Figure 4.8) as shown in Equation 4.3. Based on Equation 4.3, the plot of log ϕ versus 1/*T* for

the given fractional weight: w must produce a linear plot, where the activation energy: E_a of thermal degradation can be obtained from the slope of the plot and the pre-exponential factor, A can be obtained from the intersection at y-axis.

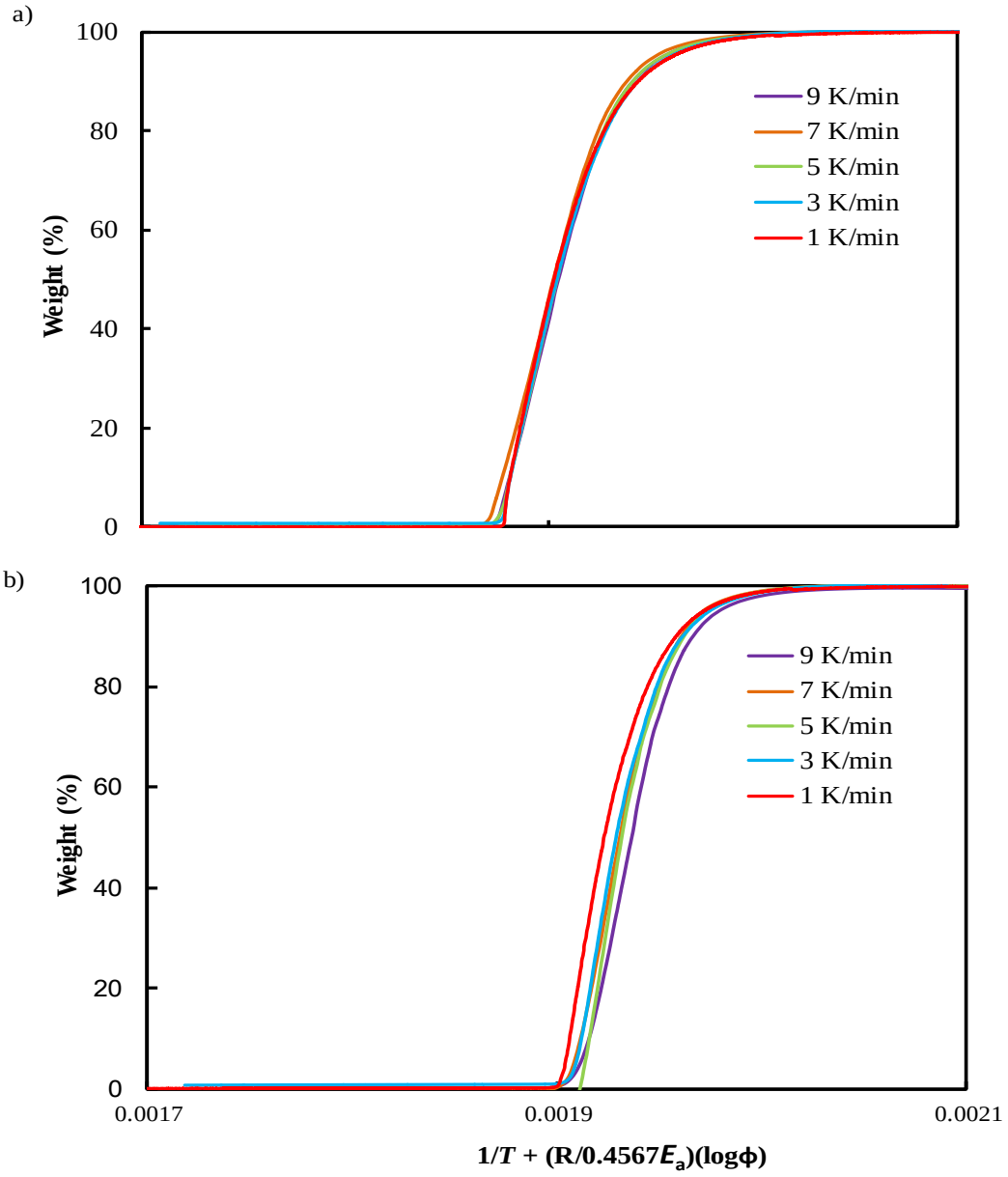

Figure 4.7. Superposition of thermogravimetric (TG) curves of (a) P(HB-*co*-6%-HHx) and (b) P(HB-*co*-11%-HHx) at multiple heating rates

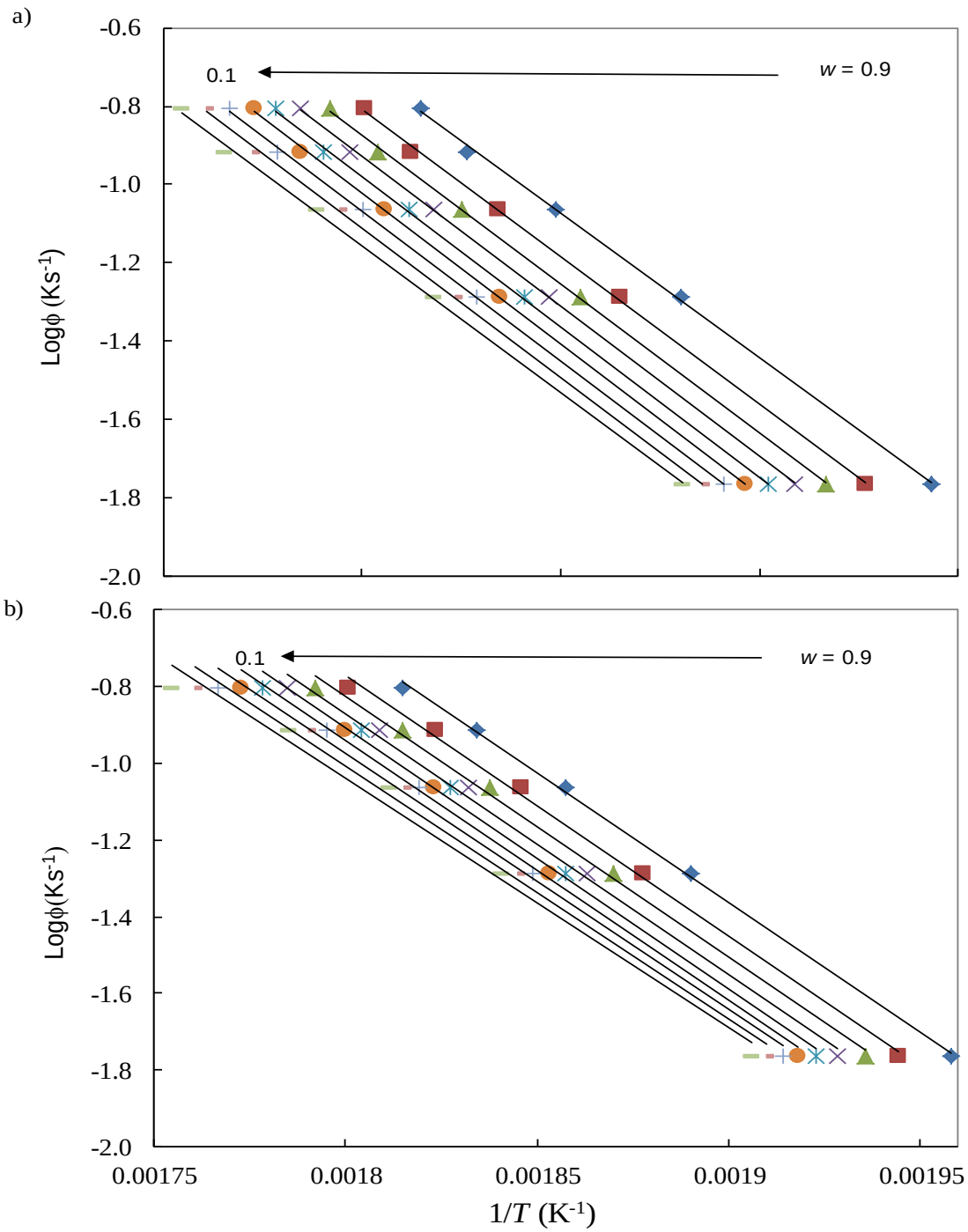

Figure 4.8. Plots of heating rate (log ϕ) versus 1/*T* for fractional weight, *w* of (a) P(HB-*co*-6%-HHx) and (b) P(HB-*co*-11%-HHx) decompositions

As shown in Figure 4.8, the plots of log ϕ versus 1/*T* for the given *w,* showed good linear relationships for both PHBHHx samples. Based on slopes of the plots, the tentative E_a values were calculated using tentative *b* value: 0.4567 as shown in Table 4.4 and 4.5 for P(HB-*co*-6%-HHx) and P(HB-*co*-11%-HHx), respectively. The average tentative E_a values of 138.1±1.9 and 122.4±1.8 kJ mol^{-1} were obtained for P(HB-*co*-6%-HHx) and P(HB-*co*-11%-HHx), respectively. Based on the average E_a value of 138.1± 1.9 kJ mol^{-1} obtained for P(HB-*co*-6%-HHx), the function *y* was calculated to be approximately 28–40 for the corresponding temperature range of 150–295 °C. On the other hand, for P(HB-*co*-11%-HHx) with average E_a value of 122.4 kJ·mol^{-1}, the function *y* was calculated to be approximately 25–35 for the corresponding temperature range of 150–295 °C as well.

Based on the specified range of function *y,* values of constants *a* and *b* were recalculated for more accurate estimation shown in Appendix B4. The recalculated values of constants *a* and *b* were 2.2305 and 0.4593 for P(HB-*co*-6%HHx) as well as 2.128 and 0.4626 for P(HB-*co*-11%HHx), respectively. These recalculated values were used to re-determine the apparent E_a values of PHBHHx (Table 4.4 and Table 4.5). The average E_a value of P(HB-*co*-6%-HHx) and P(HB-*co*-11%-HHx) were evaluated to be in the range of 137.9±1.9 and 120.8±1.8 kJ·mol^{-1}, respectively, where the values were only slightly lower than the tentative E_a values. Moreover, E_a value was also calculated from slope of Equation 4.5 (Reich, 1964) for the same fractional weight: *w* of PHBHHx samples for comparison.

$$E_a = R\,\{\ln(T_1^2/\phi_1) - \ln(T_2^2/\phi_2)\}\,/(1/T_1 - 1/T_2) \qquad (4.5)$$

Linear relationship were obtained for the plot of $\ln(T^2/\phi)$ versus $1/T$ for fractional weight: w (Figure 4.9) and the E_a values calculated from slopes was listed in Table 4.4 and Table 4.5.

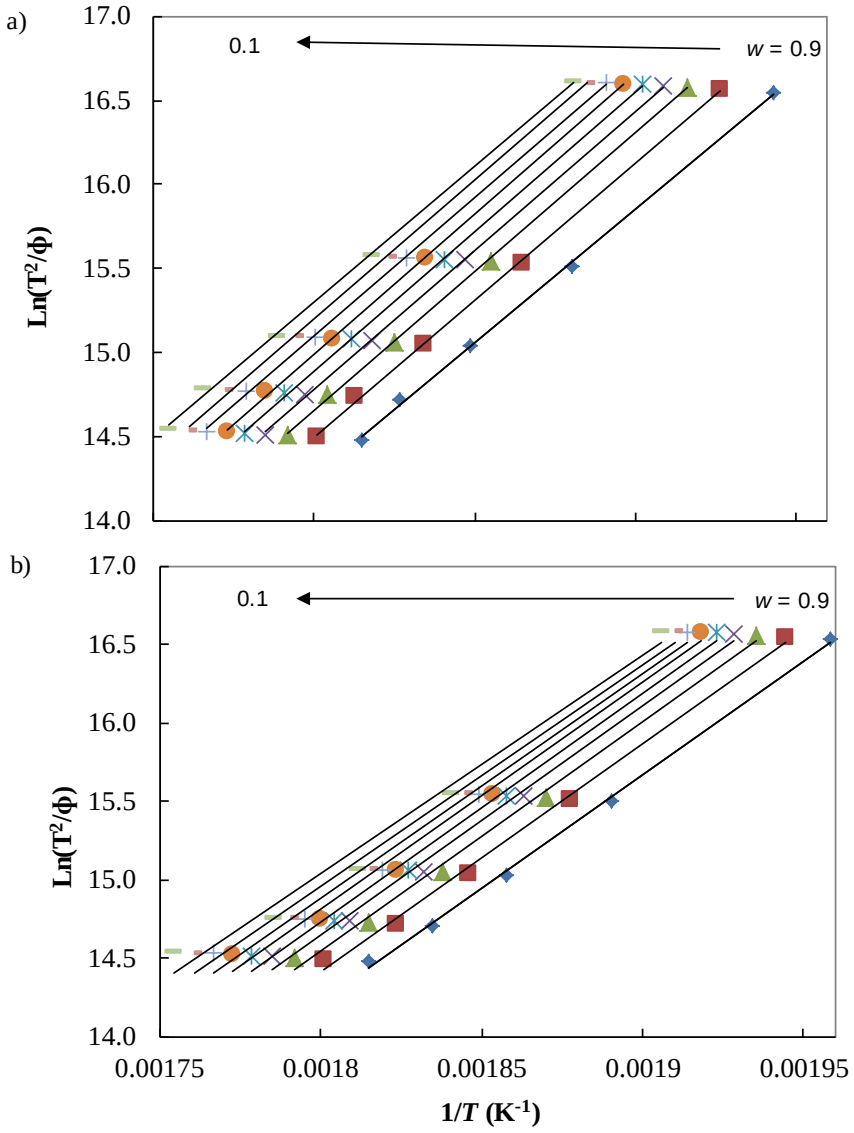

Figure 4.9. Plots of $\ln(T^2/\phi)$ versus $1/T$ for fractional weight, w of (a) P(HB-*co*-6%-HHx) and (b) P(HB-*co*-11%-HHx) decompositions

Table 4.4. Activation energy, E_a of P(HB-*co*-6%HHx) decomposition in N_2

	Doyle's Equation			Reich's Equation	
w	E_a (kJ/mol)		$R^{2\,a)}$	E_a (kJ/mol)	R^2
	a = 2.315 b = 0.4567	a = 2.2305 b = 0.4593			
0.9	134.0	133.5	0.9991	132.0	0.9990
0.8	136.9	136.4	0.9993	135.0	0.9992
0.7	138.7	138.3	0.9995	136.9	0.9995
0.6	139.6	139.2	0.9996	137.8	0.9996
0.5	139.9	139.6	0.9996	138.1	0.9995
0.4	140.0	139.7	0.9996	138.1	0.9995
0.3	139.3	139.0	0.9996	137.3	0.9995
0.2	138.6	138.4	0.9994	136.6	0.9993
0.1	136.5	136.6	0.9991	134.4	0.9990
Mean	138.1	137.9	0.9994	136.3	0.9993
σ_n [b)]	1.9	1.9		1.9	

[a)] regression coefficient; [b)] standard deviation.

Table 4.5. Activation energy, E_a of P(HB-*co*-11%HHx) decomposition in N_2

	Doyle's Equation			Reich's Equation	
w	E_a (kJ/mol)		$R^{2\,a)}$	E_a (kJ/mol)	R^2
	a = 2.315 b = 0.4567	a = 2.128 b = 0.4626			
0.9	122.9	121.3	0.9988	120.4	0.9986
0.8	123.9	122.3	0.9969	121.4	0.9964
0.7	123.6	122.0	0.9961	121.1	0.9955
0.6	123.9	122.3	0.9949	121.4	0.9940
0.5	123.8	122.2	0.9932	121.2	0.9920
0.4	123.1	121.5	0.9916	120.4	0.9901
0.3	121.6	120.1	0.9891	118.9	0.9872
0.2	120.3	118.7	0.9871	117.4	0.9848
0.1	118.4	116.9	0.9850	115.4	0.9823
Mean	122.4	120.8	0.9925	119.7	0.9912
σ_n [b)]	1.8	1.8		2.0	

[a)] regression coefficient; [b)] standard deviation.

The average E_a values of P(HB-*co*-6%-HHx) and P(HB-*co*-11%-HHx) was calculated to be in the range of 136.3±1.9 and 119.7±2.0 kJ mol^{-1}, respectively, which were very close 137.9±1.9 and 120.8±1.8 kJ·mol^{-1} calculated by modified Doyle's method for P(HB-*co*-6%-HHx) and P(HB-*co*-11%-HHx), respectively. Despite the similar ester cleavage reactions, E_a values obtained during SHS hydrolysis, which were 88.4 and 90.6 kJ mol^{-1} for P(HB-*co*-6%HHx) and P(HB-*co*-11%HHx), respectively, it showed a significant differences with the E_a values during the thermal degradation. These results are very interesting, because the effect of HHx unit varies depending on the HHx unit content not only on thermal degradation, but also on hydrolysis. Similar results were observed by Cai and Qiu (2009) for the isothermal crystallization of P(3HB-*co*-3HHx) using differential scanning calorimetry (DSC), whereby when the percentage of 3HHx unit increased from 7, 10 and 18%, the activation energy reduced to 1.3, 1.1 and 0.6 kJ·mol^{-1}. In general, the activation energy for degradation indicates the energy barrier that controls the chemical bond ruptures, therefore the higher the activation energy, it more difficult for the polymer to be thermally degraded (Liu *et al*., 2012).

The fact that the HHx unit acts as a suppressing factor on the thermal degradation is clear from the T_{d50} and T_{d50}-T_m values. However, the increase in the flexibility of polymer sequence has a tendency to promote the thermal chain cleavage as shown in the case of P(HB-*co*-11%-HHx). As a result, the differences in E_a values between P(HB-*co*-6%-HHx) and P(HB-*co*-11%-HHx) for the thermal and hydrothermal degradation may appear where the E_a was significantly reduced in the presence of flexible chains of PHBHHx. This discussion may support the changes noted in diad sequence distribution of SHS treated P(HB-*co*-11%-HHx), where the increase in flexibility of polymer chain

causes a vigorous vibration of the chain making the chemical differences between HB*HHx and HHx*HB sequences unimportant.

4.3.2.3 Expected mechanism of PHBHHx hydrothermal degradation

In many previous studies, it was reported that short-chain length (scl)-PHA such as PHB undergoes β-elimination as a dominant reaction mechanism during the thermal degradation. For an example, Ariffin *et al*. (2008) have reported that the kinetically favored 0th-order weight loss process was assumed to be an unzipping β-elimination reaction occurring at ester groups neighboring the crotonate end groups. The scl-PHA with only 4 carbons at the backbone structure and with a methyl side chain (1 carbon) forms a stable 6-membered ring ester intermediate during the thermal degradation where the β-hydrogen transfer occurs at the ester linkage (Sin *et al*., 2010). However, in the case of PHBHHx, the bulky, propyl side chain with 3 carbons could hinder the formation of the stable 6-membered ring ester intermediate. Therefore, instead of β-elimination, there is a possibility for the occurrence of hydrolysis of ester linkages, especially at the lower temperatures.

The expected mechanisms of PHBHHx thermal hydrolysis are illustrated in Figure 4.10. As shown in Figure 4.10, HHx unit basically suppress the hydrolysis of HB-HHx sequence at lower temperatures due to the steric hindrance and hydrophobicity caused by the propyl group as side chain. At higher temperatures, dehydration of hydroxyl chain end groups may occur to form crotonoyl chain-ends (Yu *et al*., 2005). Thus, during the

hydrothermal degradation of PHBHHx, the hydrolysis reaction occurs at the lower temperatures (130 and 150 °C), gradually preferred β-elimination at the higher temperatures (170 and 190 °C), resulting in the higher concentration of crotonoyl chain-ends as discussed in Chapter 3.

On the other hand, when the β-elimination reaction occurs on the HHx unit at higher temperatures, the +*I* (inductive) and +*R* (resonance) effects of the resulted 2-hexenoyl group at chain-end suppress the β-elimination reaction with neighboring HB unit, compared to the crotonoyl group. This is because, poor inductive effect (+*I*) and electron-donating effect (+*R*) of crotonoyl group make the β-elimination reaction easier. Therefore, the HHx unit basically acts as a suppression point in the unzipping β-elimination reaction mechanism of the HB unit sequence as shown by the results of increased T_{d50}-T_m, with the increased percentage of HHx unit in the PHBHHx samples.

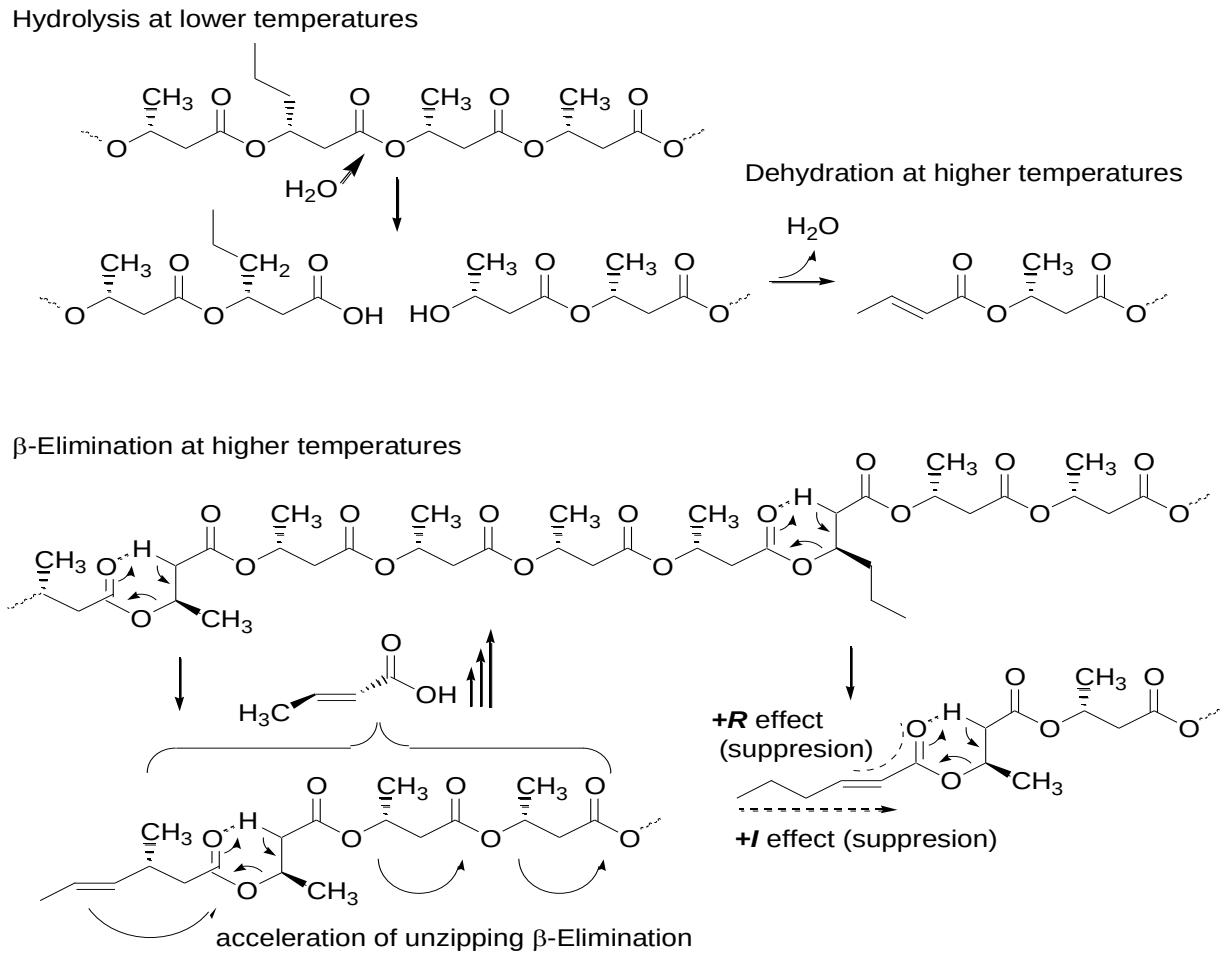

Figure 4.10. Effects of HHx units in hydrolysis and thermal degradation of PHBHHx

4.4 Conclusion

In order to clarify effects of HHx unit in HB unit sequence during hydrothermal degradation, PHBHHx samples with different content of HHx unit: P(HB-*co*-6%-HHx) and P(HB-*co*-11%-HHx) were treated by SHS at 130-190 °C. Interestingly, despite having the nearby HHx unit contents, contradictory scission behavior of HB*HHx sequence were obtained. Basically, HHx unit suppressed the hydrolysis of HB-HHx linkage due to its hydrophobicity and steric hindrance of propyl group in HHx unit. The rapid formation of crotonoyl chain-end group at higher temperatures suggests a shift to thermal degradation from thermal hydrolysis as a main reaction. Thermal degradation using TG resulted in apparent E_a values: 138±1.9 and 121±1.8 kJ·mol^{-1} for P(HB-*co*-6%-HHx), P(HB-*co*-11%-HHx), respectively.

The effect of HHx unit on thermal degradation of PHBHHx varied depending on the HHx unit content. The HHx unit basically acts as suppressing factor of the thermal degradation from T_{d50}-T_m values; however, the increase in flexibility of polymer sequence promoted the thermal chain cleavage. As a result, the differences in E_a values between P(HB-*co*-6%-HHx) and P(HB-*co*-11%-HHx) were evident. The complex hydrothermal degradation behaviors were considered to be due to the combined results of the suppression effects by hydrophobicity and steric hindrance of propyl group in HHx unit as well as the promotive effects of lower crystallinity and easier steam diffusion into more flexible amorphous region of PHBHHx. As a combined outcome, P(HB-*co*-11%-HHx) might act as a superior factor for the differences on the thermal

hydrolysis between HHx*HB and HB*HHx sequences to be overlooked, compare to P(HB-*co*-6%-HHx).

CHAPTER 5

IN VITRO CYTOTOXICITY STUDY OF SUPERHEATED STEAM HYDROLYZED POLY(3-HYDROXYBUTYRATE-*CO*-3-HYDROXYHEXANOATE) OLIGOESTERS AND THE CHARACTERISTICS OF POLY(3-HYDROXYBUTYRATE-*CO*-3-HYDROXYHEXANOATE) OLIGOESTER/POLY(L-LACTIC ACID) BLEND FOR BIOMATERIAL APPLICATIONS

5.1 Introduction

Polyhydroxyalkanoates (PHAs) are bacterial polymer produced as an intracellular polymeric material through microbial fermentation under unbalanced nutrient conditions. Poly(3-hydroxybutyrate) (PHB), is the most common representative of PHA family exhibits a strong configuration of stereo regularity due to isotactic arrangements of pendant groups in its carbon backbone as a result of biologically catalyzed polymerization (Lim and Kim, 2016) that leads to its brittleness. Besides its brittleness, the narrow window processing ability, which directly contributes to its higher production cost, makes it insufficient to replace the commercial plastics for packaging purposes (Zhao *et al*., 2003). However, since PHB naturally possess biodegradability and has been proven to be biocompatible in many studies, it has a potential to serve as a biomaterial in biomedical and tissue engineering applications such as in wound dressings, bone regeneration and drug deliveries (Chen and Wu, 2005; Sun *et al*., 2007).

Poly((*R*)-3-hydroxybutyrate-*co*-(*R*)-3-hydroxyhexanoate) (PHBHHx) is a third generation of PHA that consists of randomly distributed (*R*)-3-hyroxybutyrate (HB) and (*R*)-3-hydroxyhexanoate (HHx) units, which has improved mechanical properties and processability compared to PHB and poly((*R*)-3-hydroxyvalerate) (PHBV) (Wang *et al*., 2004). PHBHHx copolymers are currently produced on a large scale and have been proven to be biocompatible in clinical studies using mouse fibroblasts cells, and rabbit articular cartilage-derived chondrocytes (Zheng *et al*., 2005), the most important factors for their practical tissue engineering applications besides their other favorable properties such as affinity towards various mammalian cells including smooth muscle cells, fibroblasts, chondrocytes, oeteoblasts and bone marrow cells, *in-vitro* biodegradability as well as flexible mechanical properties (Qu *et al*., 2006a; Yang *et al*., 2014).

Recent biocompatibility studies of PHAs have shown an immense degree of biocompatible and biodegradable properties, where the rate of biodegradation depends on the content of 3-hydroxyhexanoate (HHx) unit in PHBHHx (Yang *et al*., 2009). On the other hand, *in vivo* studies of PHB and PHBV implants are found to induce prolonged acute inflammatory responses (Zhao *et al*., 2003; Qu *et al*., 2006b). Despite the contribution of several factors to these phenomena, polymer surface considered to be one of the most important factors due to its direct interaction to *in vivo* or *in vitro* environments. Poor polymer surface properties such as low surface free energy, smoothness and inert chemical compositions lead to reduced cell adhesions (Yang *et al*., 2014). Thus, many studies focus on the surface modifications such as alteration of chemical group functionality, topography, surface charge and surface wettability which include its hydrophilic and hydrophobic properties (Yang *et al*., 2002; Yang *et al*.,

2009). Often, the aforementioned surface modifications achieved through combination of chemical or physical means such as plasma treatment, electric discharge, surface grafting, surface hydrolysis, chemical reaction, metal vapor deposition, ultraviolet treatment as well as flame treatment (Yang *et al*., 2002; Chen and Wu, 2005; Yang *et al*., 2009, Yang *et al*., 2014) to serve the intended applications. Moreover, the degradation products of PHAs also influence the biocompatibility to some extent as previously reported for degradation product of low molecular weight PHB, 3-hydroxybutyrate (3HB) (Sun *et al*., 2007) which naturally present in human blood as a common metabolite (Qu *et al*., 2006b). Provided PHB and its corresponding oligomers and monomers are non-toxic to cells (Chen and Wu, 2005). The derivatives of 3HB unit, which was found to increase the blood ketone bodies in mammals, reduce the cell line L929 death in high density cultures as well as shield against disease due to its therapeutic properties (Sun *et al*., 2007).

Due to the combined advantages of surface properties and the degradation products towards the biocompatibility, herein the present study proposed to produce biocompatible oligoesters that may serve as a biomaterial. In this research, superheated steam (SHS) treatment was introduced for minor surface modification of the polymer that simultaneously reduces the molar mass of the polymer towards the production of oligoesters. Previously, *in vitro* cytotoxicity effect was evaluated for oligo-hydroxyalkanoates (OHAs) with only saturated bonds in their chemical structure, where the lower concentration of OHAs (20mg l^{-1}) was found to not significantly affect cell viability of mouse fibroblast cell line L929 (Sun *et al*., 2007). However, at higher temperature, SHS treatment produces hydroxyl and alkenyl/unsaturated (crotonoyl and

2-hexenoyl) chain ends where their *in-vitro* cytotoxicity effect remains unknown. Thus, the present study was aimed to evaluate the biocompatibility of SHS hydrolyzed PHBHHx oligoesters with low and high content of unsaturated chain ends using mouse fibroblast cell line NIH 3T3, where the untreated PHBHHx samples were used as control. The results of cell viability percentage were discussed in this chapter.

In general, the biocompatible PHBHHx appears to be a cell-friendly biomaterial for various biomedical applications as aforementioned. In order to propose a potential biomedical application for PHBHHx oligoester produced in the present study, especially to serve as a resorbable surgical sutures, it was blended with poly(L-lactic acid) (PLLA). PLLA represents another family of biodegradable polyester that was also extensively studied for biomedical purposes due to its biodegradability (Zhao *et al*., 2012). To serve as surgical sutures, the intended polymeric material must exhibit exceptional tensile strength in order to effectively close the wound (Brigham and Sinskey, 2012). PHBHHx was naturally found to exhibit lower tensile strength with relatively higher percentage of elongation to break, contrastively PLLA exhibits high mechanical strength and good fabricability (Zhao *et al*., 2012). Therefore, by blending these two biodegradable polymers, the overall mechanical properties of the blend can be improved. PHBHHx oligomers with good biocompatibility, fast degradability and improved mechanical properties would be a desirable polymeric material to serve as a resorbable surgical sutures for rapid-healing wounds, also this type of material can be made available for the production of other type of materials such as medical patch or artificial vascular grafts (He *et al*., 2014).

5.2 Materials and Methods

5.2.1 Materials

Untreated (control) PHBHHx films (P(HB-*co*-6%HHx), M_w: 305 kDa; P(HB-*co*-11%HHx), M_w: 352 kDa) and superheated steam (150 and 190 °C) treated PHBHHx films with low percentage of unsaturated chain-ends (P(HB-*co*-6%HHx), M_w: 73 kDa; P(HB-*co*-11%HHx), M_w: 107 kDa) as well as with higher percentage of unsaturated chain-ends (P(HB-*co*-6%HHx), M_w: 4 kDa; P(HB-*co*-11%HHx), M_w: 5 kDa) were used for *in vitro* cytotoxicity evaluation. Poly(L-lactic acid) (PLLA) (U'z S-09, Toyota Eco Plastic, Japan), M_w of 106 kDa and M_n of 66 kDa (Furukawa and Nishida, 2016) was used as received for the preparation of PHBHHx/PLLA blend film, in which PHBHHx treated at 170 °C (P(HB-*co*-6%HHx), M_w: 14 kDa; P(HB-*co*-11%HHx), M_w: 21 kDa) was used to prepare the blend. Chemicals and solvents: Thiazoyl blue tretrazolium bromide (MTT) (Bio Basic Canada Inc), sodium bicarbonate (Sigma-Aldrich), potassium chloride (Fisher scientific), potassium dihydrogen phosphate, anhydrous (*Chem*AR), sodium phosphate, dibasic, anhydrous (1st BASE), sodium chloride (*Chem*AR), D(+)-glucose, anhydrous (ChemPur), trypLE^{TM} Express (Gibco Life Technologies, USA), Dulbecco's modified eagle medium (Gibco Life Technologies, USA), Fetal bovine serum (HyClone^{TM}, South America), Hepes (Sigma-Aldrich), dimethyl sulfoxide (DMSO) (Fisher, USA) and Penicillin-Streptomycin solution (Gibco Life Technologies, USA) were used as received.

5.2.2 *In-vitro* cytotoxicity evaluation of SHS treated PHBHHx films

5.2.2.1 Cell culture of mouse fibroblast cell line NIH 3T3

The National Institute of Health (NIH) 3T3 cell line obtained from American Type Culture Collection (ATCC), USA was kindly provided by Dr. Nik Mohd Afizan Nik Abd. Rahman (Faculty of Biotechnology and Biomolecular Sciences, Universiti Putra Malaysia). The cell line was maintained in Dulbecco's modified eagle medium (DMEM) supplemented with 10% fetal bovine serum (FBS) and 1% penicillin-streptomycin (Appendix C1). The cells were grown in a humidified incubator supplemented with 5% CO_2 at 37 °C and cell morphological examinations of the culture flasks were performed daily under inverted light microscope (NIKON, Japan). After the cells were completely grown by covering the entire 75 cm^2 culture flask (90% confluence), old media was discarded and the cells were washed with sterile phosphate buffer saline (PBS, pH 7.4) (Appendix C1) thrice, detached from the culture flasks using trypleE^{TM} Express (animal origin free) solution and were passaged as single cells in DMEM culture medium. The detached cells were collected in a falcon tube, added with 10 mL of fresh DMEM medium to inactivate the action of trypleE^{TM} and were centrifuged at 3000 rpm for 5 minutes to obtain the cell pellet. After centrifugation, supernatant was discarded, and 10mL of fresh DMEM medium was added and the falcon tube was vortexed to obtain homogenous solution. The viable cells in the solution were counted by Trypan blue using hemocytometer.

5.2.2.2 Cell viability and seeding of NIH 3T3

The viable cells were count using Trypan blue cell count method in order to determine the seeding density of the NIH 3T3 cells. Approximately, 10µl of cell solution was added with 10µl of 0.4% Trypan blue stain in a clean surface. Then, the cell suspension was immediately transferred to the edge of the hemocytometer chamber with a cover slip. The non-stained, shiny cells within four corners of grid were counted as viable cells under the inverted light microscope (NIKON, Japan). Based on the viable cell count obtained, serial dilution was performed to standardize the cell seeding density for each independent experiment. Five-hundred microliter of NIH 3T3 cells at a concentration of 6.25×10^4 cells/mL was seeded into each well of 24-well tissue culture plate for 24hr (Figure 5.1). The following day, after initial morphological examination of NIH 3T3 cells under inverted light microscope, the untreated and SHS treated PHBHHx films (P(HB-*co*-6%HHx) and P(HB-*co*-11%HHx)) with different weight contents (0.5, 1.0, 2.0, 4.0 and 8.0 mg) as shown in Figure 5.2-5.4 were prepared for cytotoxicity evaluation and the cells in DMEM medium with the absence of PHBHHx films were served as control. Prior to inoculation, the films were sterilized under ultraviolet radiation for 10 minutes. After the PHBHHx films inoculation, the tissue culture plate were incubated for 24 and 48 hr at 37 °C under 5% CO_2. The cell growth was observed by phase-contrast microscopy (NIKON, Japan) and digital images were taken after 24 and 48 hr inoculation.

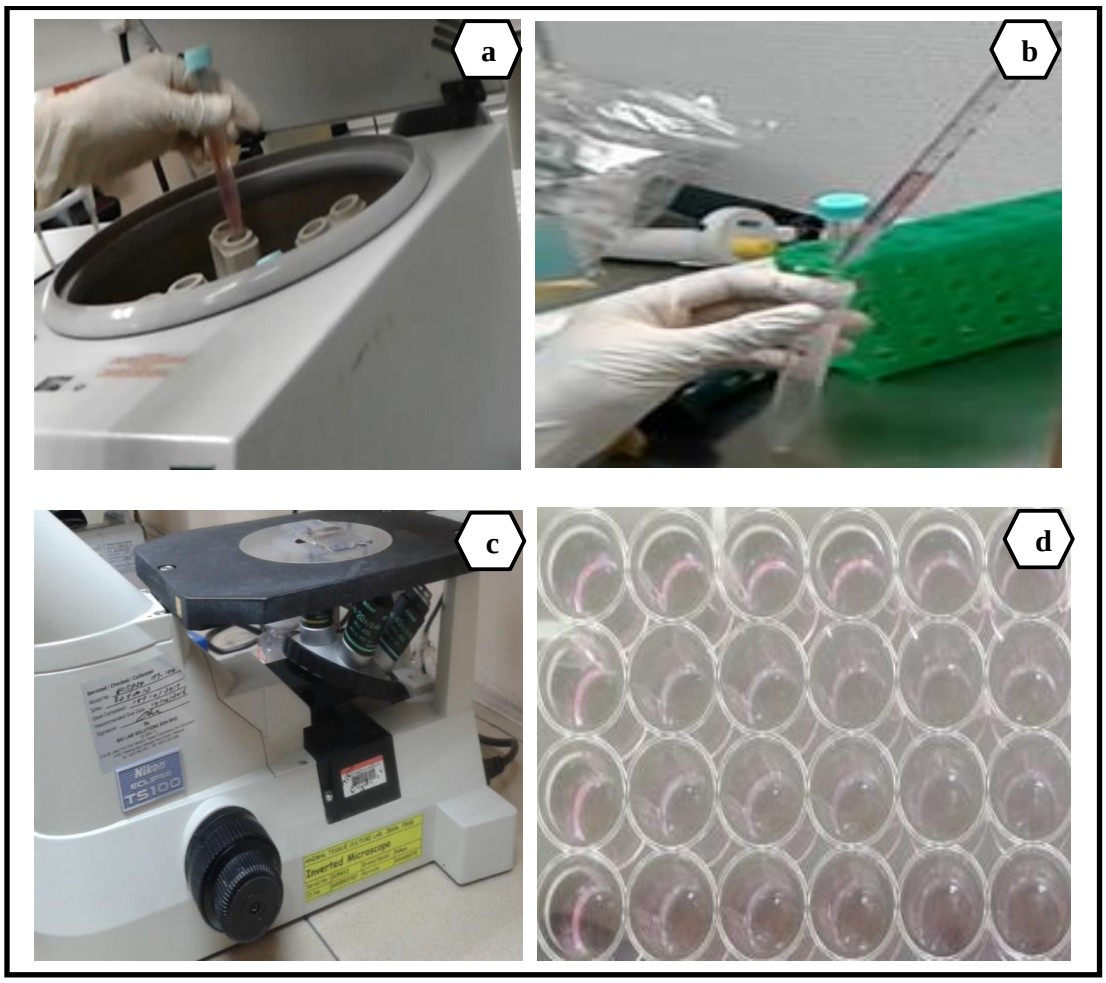

Figure 5.1. Cell culture preparation and cell seeding of NIH 3T3. (a) centrifugation of detached cells from culture flasks (b) stock cell culture preparation by the addition of fresh medium to cell pellet (c) cell viability count using hemocytometer (d) inoculation of serial diluted cell solution into 24-well tissue culture plate

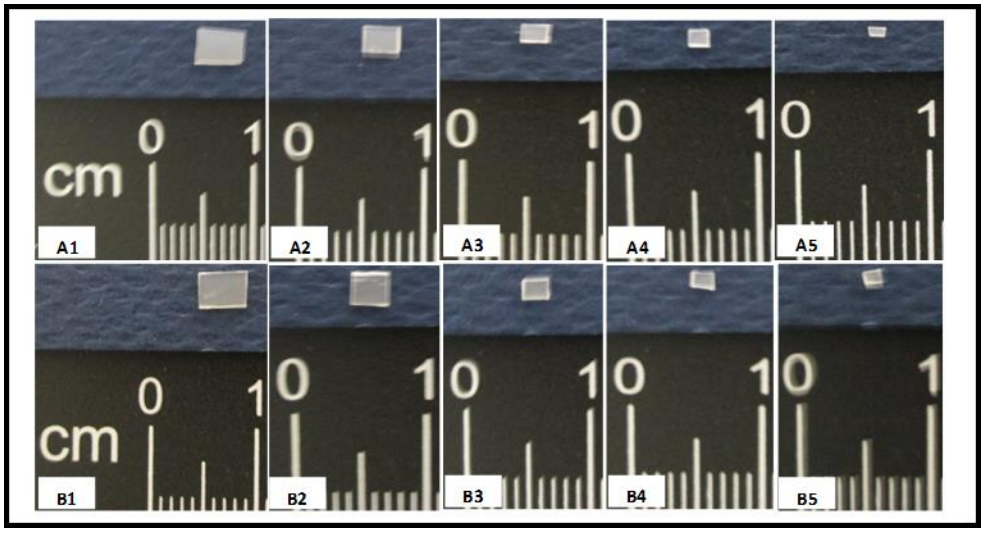

Figure 5.2. Untreated PHBHHx films with different weight contents (mg) arranged in a descending order. A1-A5 are untreated P(HB-*co*-6%HHx) and B1-B5 are untreated P(HB-*co*-11%HHx)

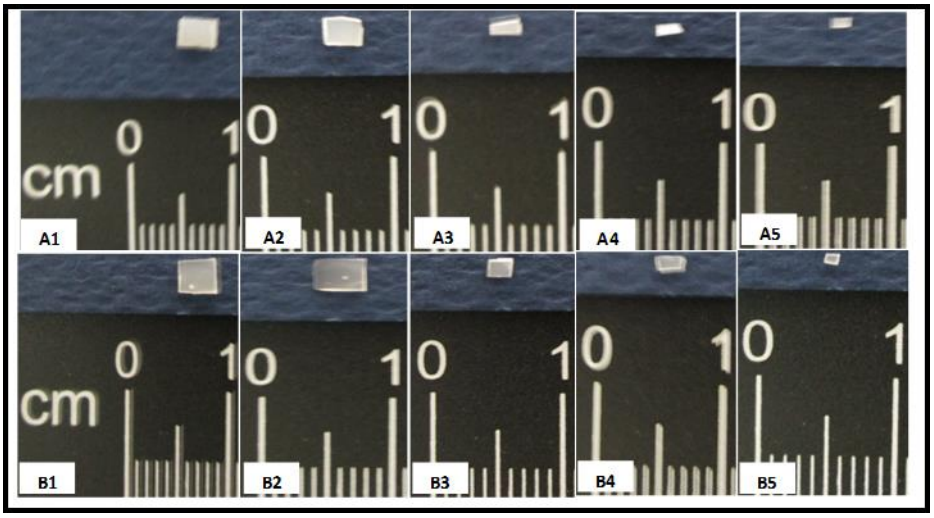

Figure 5.3. SHS treated PHBHHx films at 150 °C with different weight contents (mg) arranged in a descending order. A1-A5 are SHS treated P(HB-*co*-6%HHx) at 150 °C and B1-B5 are SHS treated P(HB-*co*-11%HHx)) at 150 °C

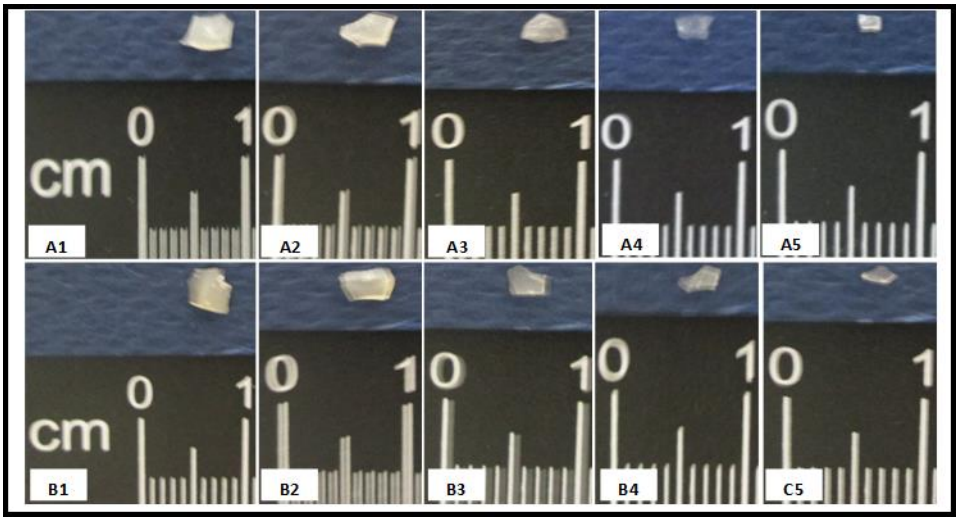

Figure 5.4. SHS treated PHBHHx films at 190 °C with different weight contents (mg) arranged in a descending order. A1-A5 are SHS treated P(HB-*co*-6%HHx) at 190 °C and B1-B5 are SHS treated P(HB-*co*-11%HHx) at 190 °C

5.2.2.3 *In vitro* cytotoxicity assay on NIH 3T3 cells

The mouse fibroblast NIH 3T3 cell line was exposed to different weight contents of PHBHHx films in the culture medium up to 24 and 48 hr to determine the percentage of cell viability. After 24 and 48hr incubation, the PHBHHx films were removed and a total of 50µL of 3-(4,5-dimethylthiazol-2-yl)-diphenyl-tetrazolium bromide **(**MTT) solution (5mg/mL in PBS) was added into each well and was further incubated for 3hr at 37 °C under 5% CO_2 for formazan formation. Later, 200µL of solutions were removed from the wells and 200µL of DMSO were added to dissolve the formazan crystals. Then, the absorbance readings of the plate were quantified at a wavelength of 550nm using ELISA microplate reader (Biotech Instruments, USA). The percentage of cell viability

was calculated based on the absorbance readings which directly indicate the cell viability by following formula (Rezvanian *et al*., 2016):

$$\text{Cell viability (\%)} = \frac{A_{film}}{A_{control}} \times 100 \qquad (5.1)$$

Where, A_{film} = absorbance at 550nm of the cells with PHA film and $A_{control}$ = absorbance at 550nm of the control which was the cells in medium incubated with the absence of PHA film. Each experiment was conducted in triplicate.

5.2.3 Preparation of PLLA/SHS treated PHBHHx blends

SHS treated PHBHHx/PLLA blends were prepared by melt mixing with the ratio (PHBHHx/PLLA) of 20/80 using the twin-screw extruder (IMC-1979, Imoto Machinery Co., Japan) at 180 °C for 10 min, at the rotation speed of 50 rpm. The resulted melt-compounded blends were cut into smaller pieces. Composite films were prepared using compressed molding technique with the aid of heat pressure film forming machine IMC-180C (Imoto Machinery, Kyoto, Japan) at 180 °C under pressure of 50 MPa for 10 min and cooled to room temperature. The thickness of the transparent film formed was about 0.2 mm.

5.2.4 Analytical procedures

5.2.4.1 Differential scanning calorimetry

The melting behavior and the miscibility of the neat PLLA and PHBHHx/PLLA (20/80) blend film was determined using differential scanning calorimetry (DSC Q20, Research Instruments). The samples were heated in the temperature range of 30–200 °C at a heating rate of 10 °C•min^{-1} under nitrogen atmosphere. The melting point (T_m) was taken from the highest point of melting peak.

5.2.4.2 Wide angle X-ray diffraction analysis

Wide Angle X-ray Diffraction (WAXD) analysis was performed on an X-Ray Diffractometer RINT 2100 (Rigaku Corporation, Tokyo, Japan), operated at 40 kV and 20 mA with Cu Kα (λ = 0.1542 nm) radiation. Every scan was recorded in the range of 2θ = 5-50° under room temperature at a scan speed of 10°•min^{-1}. Crystallinity value: X_c (%) was determined by calculating the ratio of crystalline area to total area of profile in diffractogram, where the scattering profile of the amorphous area was taken into account (Equation 5.2).

$$X_c\,(\%) = \frac{\text{Area of crystaline phase peaks}}{\text{Total area of all peaks}} \times 100 \qquad (5.2)$$

5.2.4.3 Mechanical properties

The mechanical properties of the rectangular shape films (40 x 5 x 0.2 mm) were performed on tensile analyzer (IMC-18E0, Imoto Machinery Co., Japan). The mechanical properties of the films were determined by stretching the films at a cross-head speed of 5mm min^{-1} up to their breaking point at 25 °C. The analysis was done in triplicate.

5.2.4.4 Contact angle measurement

The hydrophilic properties of the samples were measured by water contact angle equipment (Biolin Scientific, Finland) packaged with OneAttension software using a sessile drop method. A drop of 3.0μL of distilled water was gently dropped onto the surface of the PHBHHx film and its contact angle (θ) was mean of values recorded for the first 10 seconds. The analysis was repeated thrice at random locations of the film surface.

5.2.5 Data analysis

The experimental data were expressed as the mean ± standard deviation. The analysis was performed with one-way analysis of variance (ANOVA) and the group means were compared by Duncan's multiple range test using SPSS software version 16. Values of $p < 0.05$ were considered as statistically significant.

5.3 Results and discussion

In the present chapter, the *in vitro* cytotoxicity of SHS treated PHBHHx films with low and high percentage of unsaturated chain ends were evaluated using mouse fibroblast NIH 3T3 cell line. The percentage of cell viability was determined for 24 and 48 hr. In addition, to propose a possible application, especially to be used as resorbable medical sutures, the resulted PHBHHx oligoesters was blend with PLLA to improve the mechanical properties of the blend, which is an important criteria of surgical sutures. The aforementioned results are discussed in detail in the following sections.

5.3.1 MTT cell viability of NIH 3T3 cells

As abovementioned, untreated and SHS (150 and 190 °C) treated PHBHHx films with low and high percentage of unsaturated chain-ends were used for *in vitro* cytotoxicity evaluation based on characterization details in Chapter 3. A desirable biomaterial should be biocompatible and should not cause any adverse effect to the surrounding tissues. Thus, the *in vitro* cytotoxicity assay (MTT assay) was performed to predict the biocompatibility of the SHS treated PHBHHx samples with their corresponding percentage of chain ends for the *in vivo* applications. In many previous cell viability studies, the PHBHHx films were found to be biocompatible, non-toxic and even tremendously increased the cell viability and cell proliferation rate of the tested cell lines. For an example, Yang *et al*. (2002) reported that growth of mouse fibroblast cell line L929 on PHBHHx film was 216 and 11 times better than on PHB and PLA films,

respectively. They also have concluded that as the percentage of PHBHHx content increased in the blend with PHB, the number of cell growth on the polymer surface also greatly increased. Later, Sun *et al*., 2007 examined the cell viability of the medium chain length oligo(3-hydroxyalkanoates) particles using mouse fibroblast cell line L929 and found that the concentration range of 2-200 mg L^{-1} did not significantly affect the growth of the cell lines and the cytotoxicity effect of OHAs decreased with increasing side chain content of OHAs such as PHBHHx. Despite the proven data of PHBHHx biocompatibility, Sun *et al*. (2007) reported that the presence of unsaturated bonds in the chemical structure of the polymer surface might be toxic for the growth of the cells. However, there were no proven data to date to support the claim. As discussed in Chapter 3, the SHS treated PHBHHx samples had unsaturated chain ends. Therefore, to ensure the biocompatibility of the resulted chain-ends, cell viability assay was conducted in the present chapter.

DMEM media was used as a medium to culture the mouse fibroblast NIH 3T3 cells as it was proven to increase media stability and cell performance by reducing the toxic ammonia build up (Zulkifli *et al*., 2014). After 24 and 48 hr, the methylthiazol tetrazolium (MTT) assay was performed in order to quantitatively evaluate the cell viability. In general, the MTT assay involves conversion of tetrazolium bromide salt, 3-(4,5-dimethylthiazol-2-yl)-2,5 diphenyl tetrazolium bromide (MTT) into an insoluble formazan crystals, which is a purple colored compound in the mitochondria of living cells that later can be quantified by spectrophotometric analysis (Yang *et al*. 2002). Figure 5.5 illustrates the mitochondrial conversion of tetrazolium dye (yellow colored) into formazan during the cell viability assessment. As shown in Figure 5.5, after the

addition of tetrazolium dye (MTT), all the wells with NIH 3T3 cell line that were incubated with PHBHHx samples for 24 and 48 hr, able to form the formazan crystals which was later quantitatively analyzed using spectrophotometer at OD550 nm. This qualitatively indicates that the presence of the untreated and SHS treated PHBHHx samples did not caused any cytotoxicity to the NIH 3T3 cell lines. The percentage of cell viability of NIH 3T3 cells with untreated and SHS treated PHBHHx films with different weights were shown in Figure 5.6–Figure 5.7.

Figure 5.5. The mitochondrial conversion of tetrazolium dye into formazan during the cell viability assessment

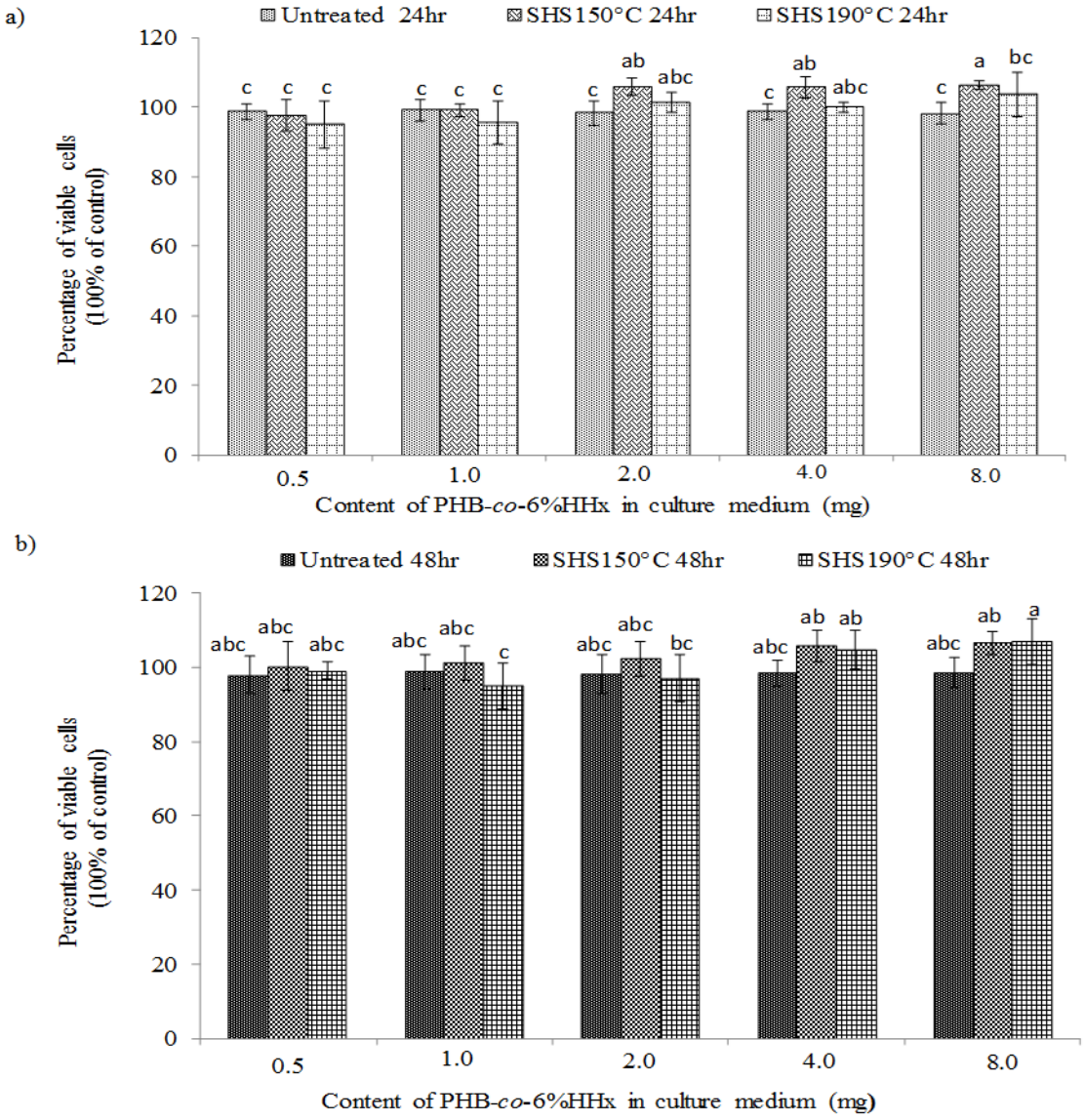

Figure 5.6. Cell viability of NIH 3T3 cells incubated with untreated and SHS treated P(HB-*co*-6%HHx) samples. (a) Cell cultured for 24 hr (b) Cell cultured for 48 hr. The mean data denoted by different superscript letters are significantly different (Duncan's multiple range test, $p < 0.05$)

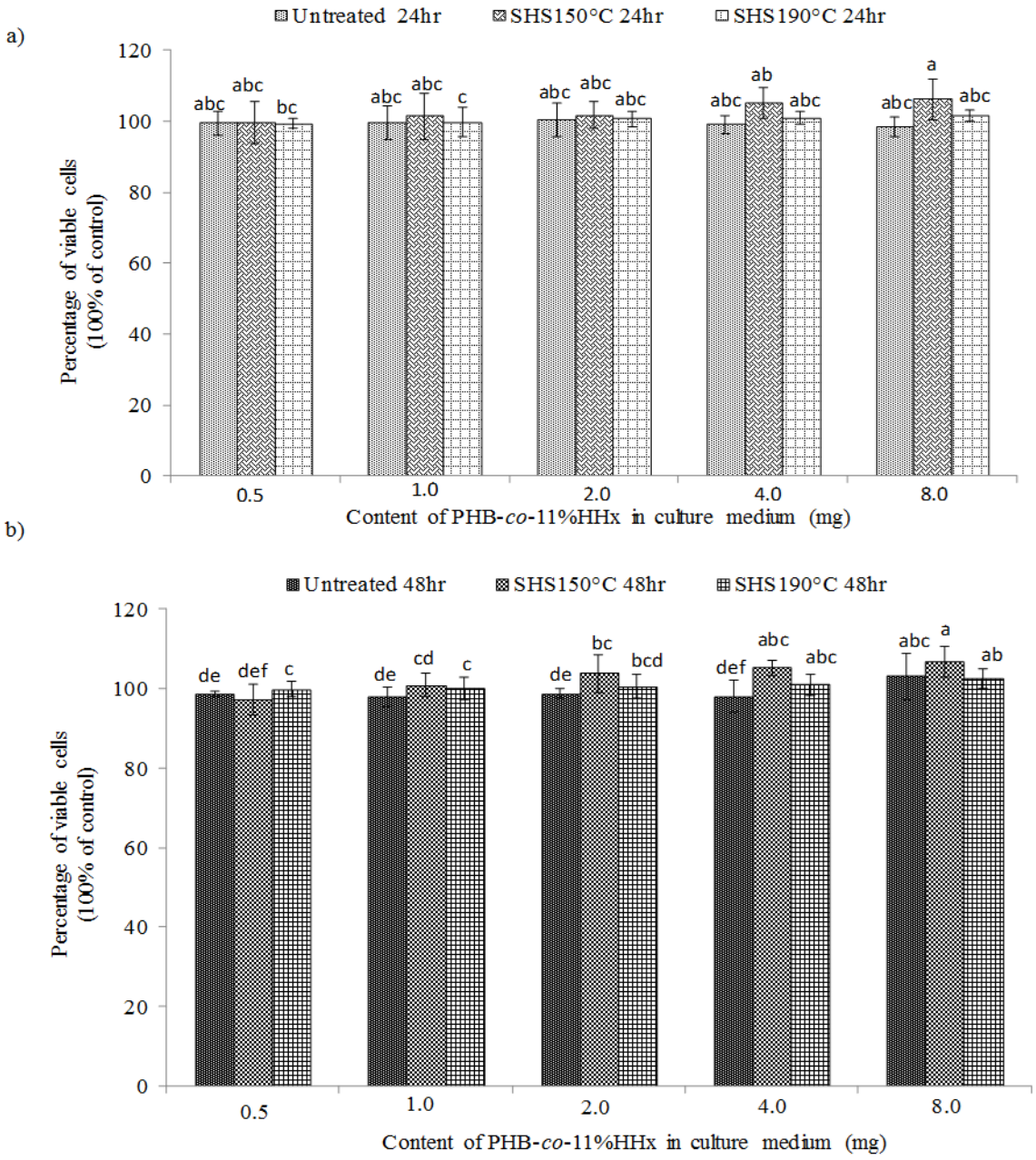

Figure 5.7. Cell viability of NIH 3T3 cells incubated with untreated and SHS treated P(HB-*co*-11%HHx) samples. (a) Cell cultured for 24 hr (b) Cell cultured for 48 hr. The mean data denoted by different superscript letters are significantly different (Duncan's multiple range test, $p < 0.05$)

As shown in Figure 5.6 and Figure 5.7, the NIH 3T3 cells were viable up to 48 hr in the presence of untreated and SHS treated PHBHHx samples with low and high percentage of unsaturated chain ends. The typical spindle morphology of the mouse fibroblast cell line NIH 3T3 remained unchanged during the incubation period of 24 and 48 hr in the presence of different ranges of PHBHHx samples. The morphology of cell line was shown in Figure 5.8 and compared with representative SHS treated PHBHHx samples at 150 °C. The cell viability percentage was found to be almost similar with the control or at least above 95%. Previously, ISO 10993-5 (2009) reported that if the percentage of cell viability exceeds 80%, it is considered non-toxic (Rezvanian *et al*., 2016). Therefore, it can be concluded that the SHS treated PHBHHx samples with crotonoyl and 2-hexenoyl chain ends in the present study did not possess any cytotoxicity effect and can be considered to be used as biomaterial. Moreover, the different weights of the samples also did not significantly affect the cell proliferation rate of the NIH 3T3 cells.

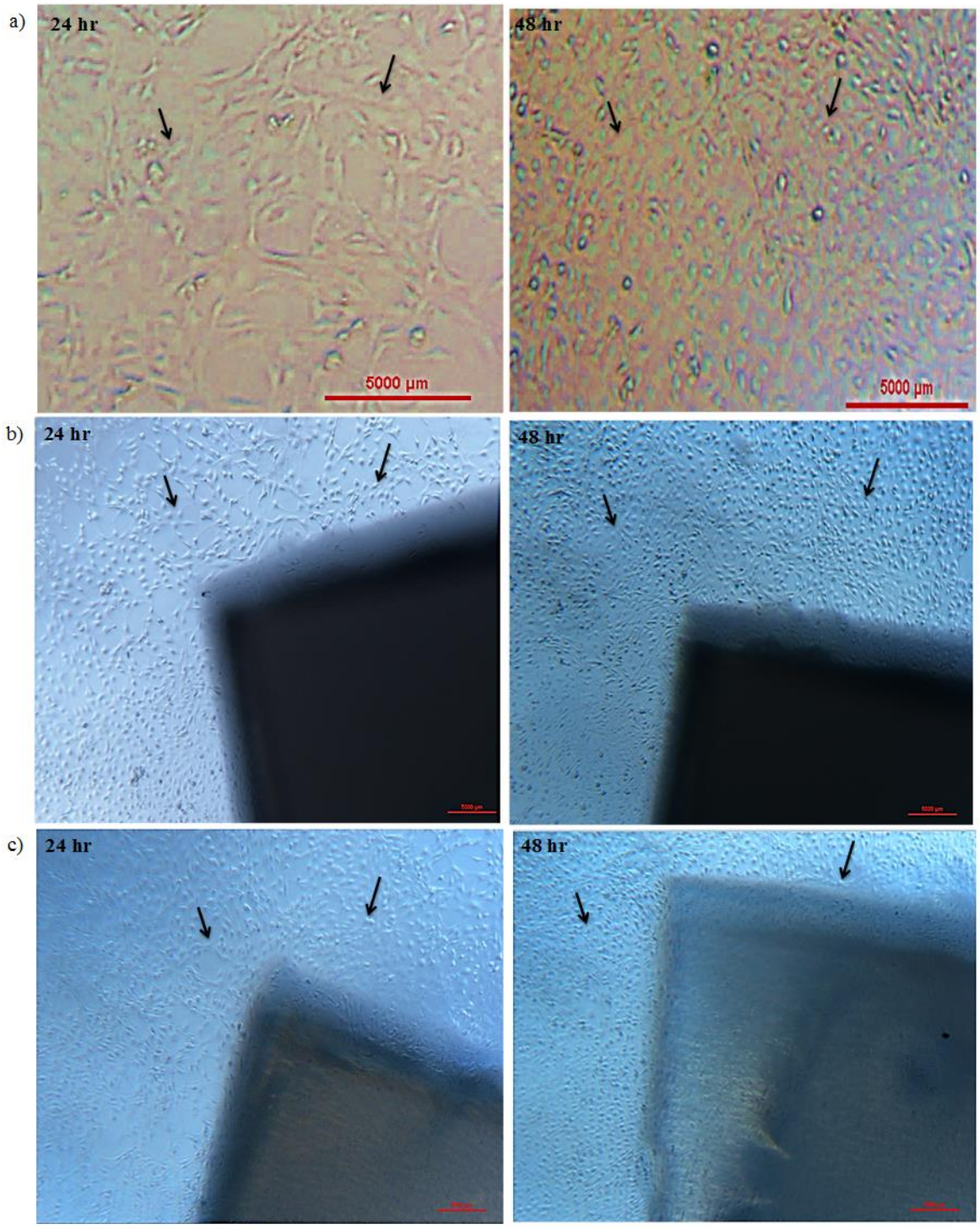

Figure 5.8. Cell morphology of NIH 3T3 cell line (a) Control cell line (b) SHS treated P(HB-*co*-6%HHx) at 150 °C (8mg) (c) SHS treated P(HB-*co*-11%HHx) at 150 °C (8mg). Solid arrows indicate the morphology of mouse fibroblast NIH 3T3 cell lines

5.3.2 Characterization of PHBHHx/PLLA blends

As previously discussed, the SHS treated PHBHHx samples were found to be non-cytotoxic and ideal for the development of functional biomaterial, preferably resorbable surgical sutures. The most important properties of the ideal resorbable sutures are high biocompatibility, smooth surface that prevent injuries on the surrounding tissues, easy to be handle and knot, high tensile strength to close the wounds and absorbed into body after the serving duration (He *et al*., 2014). Generally, fast-degrading sutures required for fast-healing tissues and the usage of PHBHHx oligoester with lower molecular weight aids the fast degradation process *in vivo*. However, the PHBHHx oligoester solely not enough for the production of the medical sutures as it requires polymer with high tensile strength and better elongation to break than PHBHHx oligoester itself. PHBHHx also generally have low crystallization rate that makes the draw of long and thin fibers with uniform texture nearly impossible.

Therefore, the incorporation of second polymer such as PLLA is able to overcome this problem as it is more prone to crystallization (He *et al*., 2014). Moreover, PHBHHx naturally exhibits exceptionally high elongation to break and contrastively lower tensile strength (Zhao *et al*., 2012). Since, PLLA exhibits high mechanical strength the blending of these two polymers (PLLA and PHBHHx) may be able to improve the overall mechanical properties. Thus, in the present study, PHBHHx oligoesters were blended with PLLA in the weight ratio of 20:80 as this ratio was found to remarkably improve the mechanical properties by increasing the toughening and reinforcing effect of the blends (Zhao *et al*., 2012). Moreover, they also reported that PHBHHx/PLLA (20/80)

with the M_w of 624 and 192 kDa, respectively, reflected higher degree of compatibility with one-phase, homogenous pattern based on Fourier transform infrared (FTIR)-microscopic analysis. In order to prepare the PHBHHx/PLLA (20/80) blend, PHBHHx oligoesters that produced by SHS treatment at 170 °C (P(HB-*co*-6%HHx), M_w: 14 kDa; P(HB-*co*-11%HHx), M_w: 21 kDa which were in the preferable molecular weight range of PHA oligomers: 1,200 to 25,000 Da (Scandola *et al*., 2011), were used. For the discussion purpose, SHS treated PHBHHx samples at 170 °C, will be regarded as oligo(PHB-*co*-6%HHx) and oligo(PHB-*co*-11%HHx).

5.3.2.1 Thermal properties of PHBHHx/PLLA blends

The thermal properties of the PHBHHx/PLLA blends were obtained from the heating scan of DSC (Table 5.1 and Figure 5.9). As previously discussed in Chapter 3, the untreated and SHS treated PHBHHx samples had multiple melting peaks. However, after the addition of PLLA, the multiple melting peaks of the PHBHHx was not detected, which could be mainly due to suppression effect of the crystallization of PHBHHx by PLLA. Moreover, the neat PLLA shows a glass transition temperature (T_g) of 67.4 °C. Interestingly, the T_g of neat PLLA was not detected in the PHBHHx/PLLA blends. This suggests that the T_g that mainly depends on the amorphous phase of the material, might have shifted to the lower temperature range. This shift is possible and acceptable as the phase morphology in previous study (Zhao *et al*., 2012) have been showed that the blend ratio of PHBHHx/PLLA (20/80 wt/wt) resulted in the one-phase, as compatible blend, therefore lead to the shift of T_g towards the lower temperature

region. The lower T_g value of the blends also advantageous for further manufacturing in the larger scale.

Moreover, there were observable changes in enthalpy of melting (ΔH_m) of PHBHHx/PLLA blends, which is close to the ΔH_m of the neat PLLA, however, lower than oligo(PHB-*co*-6%HHx) and higher than oligo(PHB-*co*-11%HHx). Therefore, this suggests that the PLLA act as a partial compatibilizable agent with crystal phase of PHBHHx and fully compatible with the amorphous region of the PHBHHx. This can be further supported by the results of crystallinity obtained by WAXD analysis (Table 5.1). As shown in Table 5.1, the percentage of crystallinity of neat PLLA, oligo(PHB-*co*-6%HHx)/PLLA and oligo(PHB-*co*-11%HHx)/PLLA were 70.0, 52.5 and 39.9%, respectively. The crystallinity of original oligo(PHB-*co*-6%HHx) (SHS at 170 °C, 300 min) and oligo(PHB-*co*-11%HHx) (SHS at 170 °C, 300 min) were 43.9 and 28.3% based on DSC measurement as previously reported in section 3.3.2.4 of Chapter 3. Therefore, it is evident that the addition of PLLA not only affects the amorphous phase, but also the crystalline phase of PHBHHx significantly.

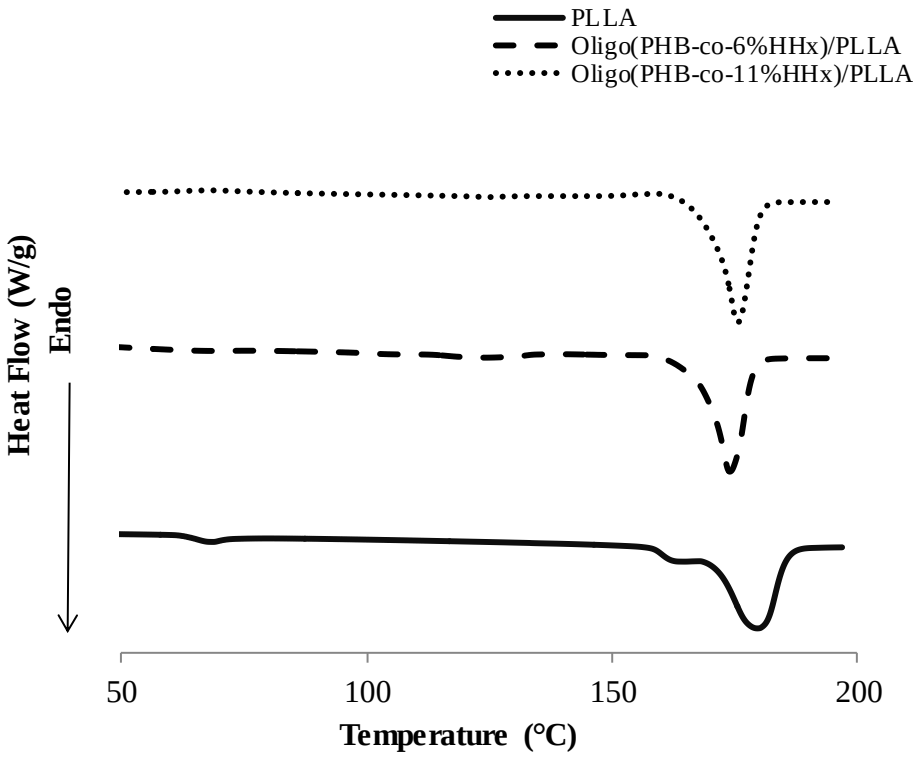

Figure 5.9. DSC thermograms of neat PLLA and PHBHHx/PLLA blends

Table 5.1. Thermal and physical properties of neat PLLA and PHBHHx/PLLA blends

Sample	T_m [a] (°C)	ΔH_m [a] (J/g)	T_g [a] (°C)	X_c [b] (%)
Neat PLLA	179.6	54.1	67.4	70.0
Oligo(PHB-*co*-6%HHx)	123.8, 138.7	64.4	n.d	43.9
Oligo(PHB-*co*-11%HHx)	95.2, 125.1, 144.1	41.5	n.d	28.3
Oligo(PHB-*co*-6%HHx)/PLLA	174.0	48.4	n.d	52.5
Oligo(PHB-*co*-11%HHx)/PLLA	175.6	48.2	n.d	39.9

[a]determined by DSC
[b]determined by WAXD
*****n.d - not detected

5.3.2.2 Mechanical properties of PHBHHx/PLLA blends

Mechanical properties are important characteristics for the production of medical sutures. The desirable range of Young's modulus, tensile strength and elongation at break (%) for medical sutures were ~850 MPa, 37 ± 10 MPa and ~70%, respectively (Manavitehrani *et al*., 2016). Based on Table 5.2, it was found that the tensile strength values of neat PLLA, oligo(PHB-*co*-6%HHx)/PLLA and oligo(PHB-*co*-11%HHx)/PLLA were 54.2, 28.6 and 33.8 MPa, respectively, where the stress-strain curves are shown in Figure 5.10. Based on Figure 5.10, oligo(PHB-*co*-6%HHx)/PLLA showed a brittle fracture, meanwhile the oligo(PHB-*co*-11%HHx)/PLLA which had higher percentage of 3HHx unit in the backbone structure of PHBHHx showed improvement in the ductility. This observation can be explained by the presence of higher portion of bulky side group (3HHx) which interfere the polymer arrangement, caused lower crystallinity (Table 5.1) and hence, a more ductile copolymer. Nevertheless, it is interesting to note that PLLA which had the highest crystallinity showed a partially ductile fracture, as observed in Figure 5.10. Despite the fact that PHBHHx is a more ductile polymer than PLLA due to its low T_g (Zhao *et al*., 2012), the lamella structure might be more developed in highly crystalline, small sized PLLA–rich region during the crystallization, that could have provided resistance towards tilting that leads to the plastic fracture or deformation of the blends as shown in Figure 5.10.

The mechanical properties obtained are close to the desired range of medical sutures, which is obvious in the case of oligo(PHB-*co*-11%HHx)/PLLA. The results show that as

the percentage of HHx unit increased, the tensile strength was increased as well and there were no significant differences in the Young's modulus. PHBHHx is generally regarded as soft and flexible polyester with low tensile strength and Young's modulus, however possesses good elongation at break. Previously, Zhao *et al*. (2012) reported that the PHBHHx/PLLA (20/80) blend exhibited exceptional Young's modulus, tensile strength and elongation at break (%) as 1.32 ± 0.04 (GPa), 29.5 ± 0.9 (MPa) and 99.6 ± 69.4 (%), respectively and Young's modulus, tensile strength and elongation at break (%) for neat PLLA were 1.39 ± 0.09 (GPa), 36.4 ± 3.9 (MPa) and 13.8 ± 5.7 (%), respectively. Similar to the previous study, the mechanical properties for neat PLLA obtained in the present study, were slightly higher than the properties of PHBHHx/PLLA (20/80) blends.

The elongation at break (%) of the blends in the present study was much lower, which can be explained by the difference in % of HHx unit in the PHBHHx samples. In the previous study, PHBHHx with 20% 3-HHx unit was used (Zhao *et al*., 2012), while in this study PHBHHxs with 6% and 11% 3-HHx unit were used. It has been reported that the increasing content of 3-HHx unit will lead to more flexible polymer (Doi *et al*., 1995). The results suggest that the increasing percentage of 3-HHx comonomer unit leads to the increasing percentage of elongation at break, where it is obvious that oligo(PHB-*co*-11%HHx)/PLLA exhibited higher elongation at break (%) than that of oligo(PHB-*co*-6%HHx)/PLLA. Therefore, based on the obtained mechanical properties in the present study, it can be concluded that the addition of PLLA into PHBHHx oligoesters resulted in the improvement in Young's modulus and tensile strength due to

the fine distribution of the small sized stiff PLLA molecules and domains into the continuous phase of PHBHHx matrix.

Table 5.2. Mechanical properties of neat PLLA and PHBHHx/PLLA blends

Samples	Tensile strength (MPa)	Young's modulus (GPa)	Elongation at break (%)	References
Neat PLLA (Toyota Ecoplastic)	54.2 ± 0.0	1.7 ± 0.0	5.6 ± 3.3	This study
Oligo(PHB-*co*-6%HHx)/PLLA	28.6 ± 1.2	1.4 ± 0.0	2.6 ± 1.3	This study
Oligo(PHB-*co*-11%HHx)/PLLA	33.8 ± 2.0	1.2 ± 0.1	3.6 ± 0.7	This study
Neat PLLA (Shimadzu Co.)	36.4 ± 3.9	1.4 ± 0.1	13.8 ± 5.7	Zhao *et al*. (2012)
(PHB-*co*-20%HHx)/PLLA (20/80)	29.5 ± 0.9	1.3 ± 0.0	99.6 ± 69.4	Zhao *et al*. (2012)

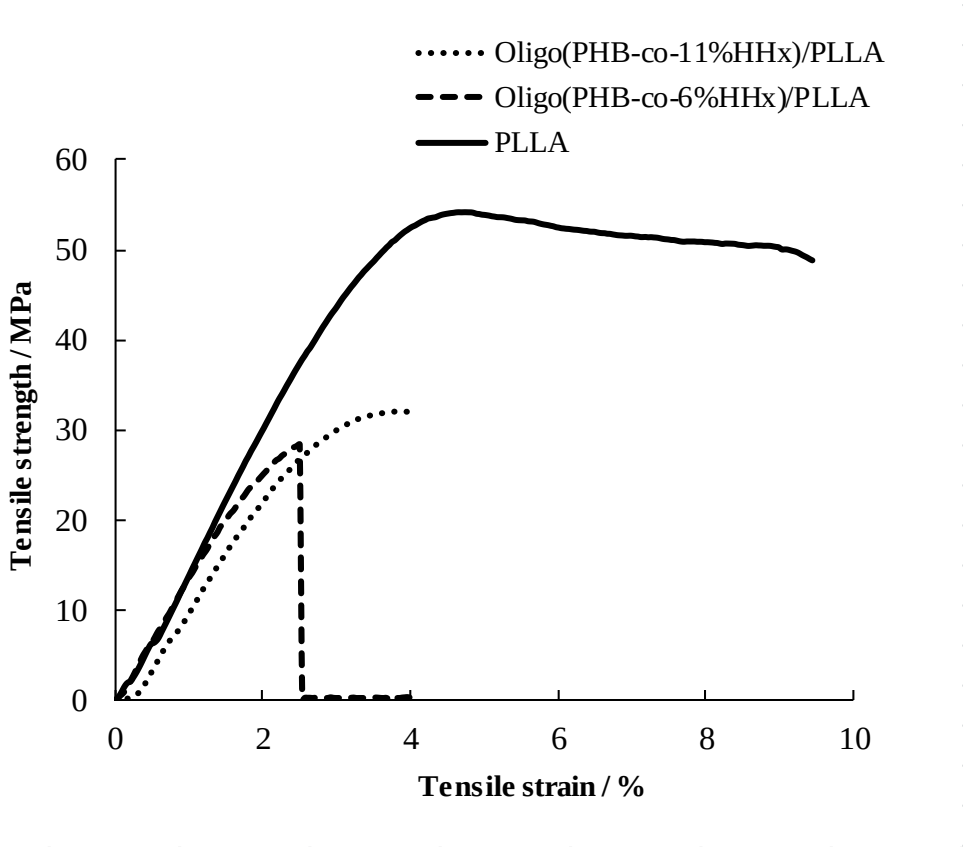

Figure 5.10. Stress-strain curves for neat PLLA and PHBHHx/PLLA blends

5.3.2.3 Surface wettability of PHBHHx/PLLA blends

Surface wettability of the neat PLLA, neat PHBHHx, SHS treated PHBHHx samples and PHBHHx/PLLA blends were determined using the measurement of contact angle. The characteristics of the surface wettability would provide the information on hydrophilic characteristics of polymer surface, which is also important for the cell attachment and cell proliferation. In Table 5.3, the contact angle values of the neat and blend samples were shown. In general, the surface with contact angle of $0<\theta<90°$ is regarded as good wetting with hydrophilicity and surface with contact angle of $180>\theta>$

90° is regarded as incomplete or no wetting due to its hydrophobicity. Therefore, both neat and blend samples used in the present study are slightly hydrophilic, where the contact angle is <90°. The oligomers of PHBHHx exhibited lower contact angle value than the neat PHBHHx. This could be due to the higher ratio of oligoesters with hydroxyl chain-end compared to the polymer after the SHS treatment (Figure 5.11). Therefore, the hydroxyl groups interact with water molecules to form hydrogen bonds that lead to the decrease in the interfacial free energy of the polymer surface which then increases the overall surface hydrophilicity. Moreover, the increase of contact angle value in the blend could be resulted from the compatible blend with PLLA. The contact angle of oligo(PHB-*co*-11%HHx) was slightly higher than the oligo(PHB-*co*-6%HHx), probably could be attributed by the surface roughness.

In general, surfaces that are too hydrophilic or too hydrophobic have been reported to be non-optimal for cell adhesion. Wang *et al*. (2005) reported that among PHBHHx samples with HHx content from 5 to 20% with a contact angle of 85°, PHBHHx with 20% HHx showed the highest cell density of fibroblast proliferation and PHBHHx with 12% HHx showed the highest cell density of osteoblast proliferation. Later, Xu and Siedlecki, (2007) reported that low density polyethylene (LDPE) surfaces with contact angle range of 60-65° showed stronger protein adhesion of bovine serum albumin, fibrinogen and human FXII than for the surfaces with θ<60°. On the other hand, Chinese hamster ovary (CHO), fibroblasts and endothelial cells showed maximum adhesion on LDPE surfaces with contact angle of 55° (Lee *et al*., 1998). Tamada and Ikada (1993) reported that for other polymer surfaces, which includes polyethylene,

polytetrafluoroethylene, poly(ethylene terephthalate), polystyrene and polypropylene, the optimal water contact angle for cell adhesion (mice fibroblast) was around 70°. As reported by previous studies, the cell adhesion varies for different polymer surfaces and cell lines. Generally, the preferable water contact angle values for cell adhesion were found to be in the range of 55–85° as abovementioned. Therefore, contact angle range of 65<θ<70° that obtained in the present study for PHBHHx oligoesters and oligo(PHBHHx)/PLLA blend samples could provide desirable cell adhesion when used as a biomaterial.

Table 5.3. Contact angle measurements of neat PLLA, neat PHBHHx and PHBHHx/PLLA blends

Samples	Contact angle (°)
Neat PLLA	67.1 ± 0.5
Neat P(HB-*co*-6%HHx)	73.3 ± 1.9
Neat P(HB-*co*-11%HHx)	77.5 ± 1.3
Oligo(PHB-*co*-6%HHx)	64.8 ± 1.2
Oligo(PHB-*co*-11%HHx)	65.5 ± 1.9
Oligo(PHB-*co*-6%HHx)/PLLA	67.8 ± 0.9
Oligo(PHB-*co*-11%HHx)/PLLA	68.5 ± 1.7

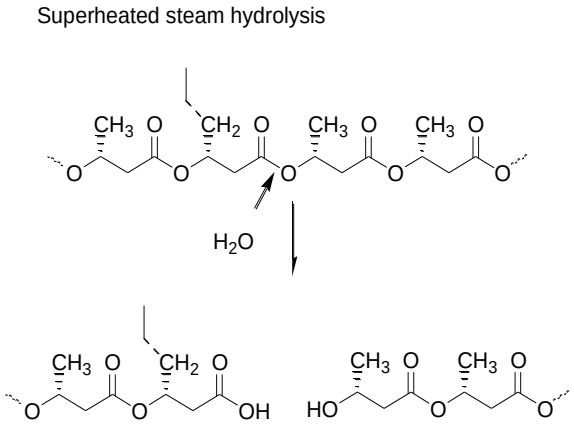

Figure 5.11. Oligoesters with hydroxyl chain-end

5.4 Conclusion

In overall, the present study evaluated the *in-vitro* cytotoxicity effect of superheated steam treated PHBHHx samples for the development of functional biomaterial, preferably resorbable medical sutures. Untreated and SHS treated (150 and 190 °C) PHBHHX samples with low and high percentage of unsaturated chain ends were found to be non-cytotoxic for the growth of mouse fibroblast cell line NIH 3T3 with cell viability percentage of more than 95.0%. Since, the SHS hydrolyzed PHBHHx oligoesters were found to exhibit high biocompatibility, it was further evaluated to be potentially used as resorbable medical sutures. Natural biodegradable polyester PLLA was used to blend with PHBHHx matrix with the weight ratio of (80/20) in order to improve mechanical properties of the films. The combined effect of increased toughening and reinforcing effect of PLLA, and the faster degradation rate resulted from low molecular weight of PHBHHx oligoesters, would be an ideal choice for the fabrication of resorbable medical sutures that requires rapid-healing.

CHAPTER 6

SUMMARY, GENERAL CONCLUSIONS AND RECOMMENDATION FOR FUTURE RESEARCH

6.1 Summary

Poly(3-hydroxybutyrate-*co*-3-hydroxyhexanoate) (PHBHHx) from the PHA family that possess good biodegradability, biocompatibility and improved mechanical properties similar to low density polyethylene, is an emerging biomaterial with many potential applications. In general, the present study was conducted to introduce a controlled depolymerization method for the hydrolysis of PHBHHx to produce biocompatible, low molecular weight PHBHHx for various applications, particularly in biomedical field. The currently existing degradation studies of PHBHHx have mainly focused on enzymatic degradation, thermal degradation, hydrothermal degradation as well as acid and alkaline hydrolysis, which have their own shortcomings for the production of PHBHHx oligoesters. Therefore, the present study introduced an alternative, greener, yet cost effective degradation method by utilizing the super-heated steam (SHS) for the production of biocompatible PHBHHx oligoesters in the preferable range of molecular weight.

The first objective of this study was to depolymerize high molecular weight PHBHHx into low molecular weight PHBHHx, preferably in the range of 1, 200 to 25, 000 Da to make it favorable for biomedical applications such as drug delivery and medical sutures. The molecular weight reduction was clearly observed for both type of PHBHHx samples used, P(HB-*co*-6%HHx) and P(HB-*co*-11%HHx) for all the SHS treatment temperatures of 130, 150, 170, and 190 °C in the order of P(HB-*co*-6%HHx) > P(HB-*co*-11%HHx). The SHS hydrolysis of PHBHHx was preferentially occurred at amorphous phase via bulk erosion and beyond the critical point, heterogeneous degradation was observed. The preferable range of low molecular weight was obtained at the SHS treatment temperature of 170 and 190 °C. At the highest SHS treatment temperature of 190 °C, PHBHHx oligoesters had molecular weight in the range of 4-5 kDa and mainly consists of hydroxyl, crotonoyl and 2-hexenoyl chain-ends. Therefore, the currently introduced SHS degradation method, succefully hydrolyzed PHBHHx polymers into oligomers in the desirable range of molecular weight for biomedical applications.

In the second objective, the effect of HHx unit in HB unit sequence during hydrothermal degradation of PHBHHx samples with different content of HHx unit: P(HB-*co*-6%-HHx) and P(HB-*co*-11%-HHx) was clarified for the employed SHS treatment temperature of 130-190 °C. The obtained results showed a contradictory scission behavior of HB*HHx sequence among the PHBHHx samples due to suppression effect of HHx unit on HB-HHx linkage that responsible for the hydrophobicity and steric hindrance of propyl group during the hydrolysis. Therefore, changes in diad sequence distribution of P(HB-*co*-11%-HHx) showed no preferential chain scission among the

HHx*HB and HB*HHx sequences, compare to P(HB-*co*-6%-HHx). Moreover, the rapid formation of crotonoyl chain-end group at higher temperatures suggests a shift to thermal degradation from thermal hydrolysis as a main reaction. Thermal degradation using TG resulted in apparent E_a values: 138±1.9 and 121±1.8 kJ·mol^{-1} for P(HB-*co*-6%-HHx) and P(HB-*co*-11%-HHx), respectively. The differences in E_a values basically due to the content of HHx unit that acts as a suppressing factor of the thermal degradation from T_{d50}-T_m values; however, the increase in flexibility of polymer sequence promoted the thermal chain cleavage. Therefore, the complex hydrothermal degradation behaviors were considered to be due to the combined results of the suppression effects by hydrophobicity and steric hindrance of propyl group in HHx unit as well as the promotive effects of lower crystallinity and easier steam diffusion into more flexible amorphous region of PHBHHx.

In the third objective, the *in-vitro* cytotoxicity effect of superheated steam treated PHBHHx samples were evaluated for biomaterial applications, preferably resorbable medical sutures. Untreated and SHS treated (150 and 190 °C) PHBHHX samples with low and high percentage of unsaturated chain ends were found to exhibit no cytotoxicity effects towards the growth of mouse fibroblast cell line NIH 3T3. Since the SHS hydrolyzed PHBHHx oligoesters possesses good biocompatibility with cell viability percentage of more than 95.0%, it was further evaluated to be potentially used as resorbable medical sutures. The PHBHHx oligoesters were blend with another type of natural biodegradable polyester, PLLA with the weight ratio of (20/80) in order to improve the overall mechanical properties of the films. The final blend film exhibited

relatively high tensile strength due to toughening and reinforcing effect of PLLA, and expected to have faster degradation rate resulted from low molecular weight of PHBHHx oligoester for the fabrication of resorbable medical sutures that requires rapid-healing.

6.2 Conclusion

From the present study, it can be concluded that the high molecular weight PHBHHx polymers can be hydrolyzed into biocompatible oligoesters with preferable range of molecular weight (1, 200 to 25, 000 Da) using SHS at the temperature range of 170 and 190 °C. The proposed SHS hydrolysis mechanism is foreseen to contribute to the understanding of thermal hydrolysis behavior of the bio-copolyester. Moreover, the good biocompatibility with mouse fibroblast cell line NIH 3T3 and improved mechanical properties of PHBHHx/PLLA blend appears to be an ideal choice for further fabrication of bioresorbable medical sutures and other PHBHHx based medical devices.

6.3 Suggestions for future work

1. The SHS hydrolysis degradation behavior and mechanism of PHBHHx can be further explored for time-dependent changes instead of temperature-dependent changes for higher percentage of HHx unit on HB unit sequence than those used in the present study for the determination of chain-end structure and changes in

diad-sequence. Therefore, the effect of increasing percentage of HHx unit towards the SHS hydrolysis mechanism can be further evaluated.

2. In the present study, *in vitro* cytotoxicity effect of SHS treated degradation products toward the growth of the mouse fibroblast cell lines were determined for different weight contents. However, the *in vitro* cytotoxicity study would be more reliable when the cell lines were grown on the films to precisely evaluate the cell attachment and proliferation. Therefore, in future, sterilized thin films of the SHS treated degradation products need to be prepared and the intended cell lines should be grown on the polymer film surface to study the cell attachment and proliferation. After the desired treatment period, weight loss of the polymer films also need to be taken into consideration in order to determine the degradability of the films.
3. The research should be extended towards the advanced characterization such as the surface properties of blend film of PHBHHx oligoesters and PLLA for intended biomaterial application due to its direct interaction to *in vivo* and *in vitro* environments.
4. The blend film of PHBHHx oligoesters and PLLA need to be fabricated and the *in vitro* biodegradation study of the blend films, either using real animal model or simulating human body conditions in a controlled laboratory environment would be interesting to determine the estimated degradation rate of the PHBHHx/PLLA based medical sutures in real human body conditions for further commercialization.

REFERENCES

Abe, H. (2006). Thermal degradation of environmentally degradable poly(hydroxyalkanoic acid)s. *Macromolecular Bioscience* 6: 469-486.

Alejandra, R.-C., Margarita, C.M. and María Soledad, M.C. (2012). Enzymatic degradation of poly(3-hydroxybutyrate) by a commercial lipase. *Polymer Degradation and Stability* 97: 2473–2476.

Antheunis, H., Van der Meer, J.C., De Geus, M., Heise, A. and Koning, C. E. (2010). Autocatalytic equation describing the change in molecular weight during hydrolytic degradation of aliphatic polyesters. *Biomacromolecules* 11: 1118–1124.

Ariffin, H., Nishida, H., Shirai, Y. and Hassan, M.A. (2008). Determination of multiple thermal degradation mechanisms of poly(3-hydroxybutyrate). *Polymer Degradation and Stability* 93: 1433-1439.

Ariffin, H., Nishida, H., Shirai, Y., Hassan, M.A. (2010a). Chemical recycling of polyhydroxyalkanoates as a method towards sustainable development. *Biotechnology Journal* 5:484-492.

Ariffin, H., Nishida, H., Shirai, Y., Hassan, M.A. (2010b). Highly selective transformation of poly[(R)-3-hydroxybutyric acid] into trans-crotonic acid by catalytic thermal degradation. *Polymer Degradation and Stability* 95: 1375–1381.

Bahrin, E.K., Baharuddin, A.S., Ibrahim, M.F., Razak, M.N.A., Sulaiman, A., Aziz, S.A., Hassan, M.A., Shirai, Y. and Nishida, H. (2012). Physicochemical property changes and enzymatic hydrolysis enhancement of oil palm empty fruit bunches treated with superheated steam. *BioResources* 7: 1784-1801.

Brigham, C. J. and Sinskey, A.J. (2012). Applications of polyhydroxyalkanoates in the medical industry. *International Journal of Biotechnology for Wellness Industries* 1:53-60.

Burkersrodaa, F., Schedlb, L. and Gopferich, A. (2002). Why degradable polymers undergo surface erosion or bulk erosion. *Biomaterials* 23: 4221–4231.

Cai, H. and Qiu, Z. (2009). Effect of comonomer content on the crystallization kinetics and morphology of biodegradable poly(3-hydroxybutyrate-*co*-3-hydroxyhexanoate). *Physical Chemistry Chemical Physics* 11: 9569-9577.

Cam, D., Suong-Hyu, H. and Ikada, Y. (1995). Degradation of high molecular weight poly(L-lactide) in alkaline medium. *Biomaterials* 16: 833–843.

Cavalheiro, J.M.B.T., Almeida, M.C.M.D., Grandfils, C. and Fonseca,M.M.R. (2009). Poly(3-hydroxybutyrate) production by Cupriavidus necator using waste glycerol. *Process Biochemistry* 44: 509-515.

Chanprateep, S. (2010). Current trends in biodegradable polyhydroxyalkanoates. *Journal of Bioscience and Bioengineering* 110: 621-632.

Chen, C., Cheung, M. K. and Yu, P. H. (2005b). Crystallization kinetics and melting behaviour of microbial poly(3-hydroxybutyrate-co-3-hydroxyhexanoate). *Polymer International* 54: 1055–1064.

Chen, G. Q. and Wu, Q. (2005a). The application of polyhydroxyalkanoates as tissue engineering materials. . *Biomaterials* 26: 6565-6578.

Chen, G. Q., Zhang, G., Park, S. J. and Lee, S. Y. (2001). Industrial scale production of poly(3-hydroxybutyrate-co-3-hydroxyhexanoate). *Applied Microbiology and Biotechnology* 57: 50-55.

Chen, G.Q. (2009). A microbial polyhydroxyalkanoates (PHA) based bio- and materials industry. *Chemical Society Reviews* 38: 2434–2446.

Chen, G.Q. (2010). Plastics completely synthesized by bacteria: polyhydroxyalkanoates. *Microbiology Monographs* 14: 17-37.

Contreras, A. R., Monfort, M. C. and Calvo, M. S. (2012). Enzymatic degradation of poly(3-hydroxybutyrate-co-4-hydroxybutyrate) by comercial lipases. *Polymer Degradation and Stability* 97: 597-604.

Corre, Y.M., Bruzaud, S., Audic, J.L. and Grohens, Y. (2012). Morphology and functional properties of commercial polyhydroxyalkanoates: A comprehensive and comparative study. *Polymer Testing* 31: 226-235.

Correa, M. C., Rezende, M. L., Rosa, D. S., Agnelli, J. A. and Nascente, P. A. (2008). Material Behaviour: Surface composition and morphology of poly(3-hydroxybutyrate) exposed to biodegradation. *Polymer Testing* 27: 447–452.

Djonlagic, J. and Nikolic, M.S. (2011). Biodegradable polyesters: synthesis and physical properties. *RSC Green Chemistry* 12: 149-196.

Doi, Y., Kitamura, S. and Abe, H. (1995). Microbial synthesis and characterization of poly(3-hydroxybutyrate-co-3-hydroxyhexanoate). *Macromolecules* 28: 4822-4828.

Faler, G. (2006). Methods for converting linear polyesters to macrocyclic oligoester compositions and macrocyclic oligoesters. PCT/US2001/027332.

Furukawa, T. and Nishida, H. (2016). Adhesion behavior of the marine mussel Mytilus galloprovincialis and effects of poly(L-lactic acid). *Sessile Organisms* 33: 1-6.

Gajjar, C. R.. and King, M. W. (2014). Degradation process. *Resorbable Fiber-Forming Polymers for Biotextile Applications*. New York: Springer.pp. 7-10.

Gomes, M.E. and Reis, R.L. (2004). Biodegradable polymers and composites in biomedical applications: from catgut to tissue engineering. Part 1: Available systems and their properties. *International Material Review* 49: 261-273.

Gonzalez, A., Irusta, L., Fernandez-Berridi, M.J., Iriate, M. and Iruin, J.J. (2005). Application of pyrolysis/gas chromatography/ Fourier transform infrared spectroscopy and TGA techniques in the study of thermal degradation of poly(3–hydroxybutyrate). *Polymer Degradation and Stability* 87: 347-354.

Gopferich, A. (1996). Mechanisms of polymer degradation and erosion. *Biomaterials* 17: 103–114.

Gopferich, A. and Langer, R. (1993). Modeling of polymer erosion. *Macromolecules* 26: 4105–4112.

Gumel, A.M., Annuar, M.S.M. and Heidelberg, T. (2013). Current application of controlled degradation processes in polymer modification and functionalization. *Journal of Applied Polymer Science* 129: 3079–3088.

Hablot, E., Bordes, P., Pollet, E. and Averous, L. (2008). Thermal and thermo-mechanical degradation of poly(3-hydroxybutyrate)-based multiphase systems. *Polymer Degradation and Stability* 93: 413-421.

Hassan, M.A., Yee, L.N., Yee, P.L., Ariffin, H., Raha, A.R., Shirai, Y. and Sudesh, K. (2013). Sustainable production of polyhydroxyalkanoates from renewable oil-palm biomass. *Biomass and Bioenergy* 50: 1-9.

Hazer, B. (2010). Amphiphlic poly(3-hydroxyalkanoate)s: potential candidates for medical applications. *International Journal of Polymer Science* 2010: 1-8.

He, Y., Hu, Z., Ren, M., Ding, C., Chen, P., Gu, Q. and Wu, Q. (2014). Evaluation of PHBHHx and PHBV/PLA fibers used as medical sutures. *Journal of Material Science: Materials in Medicine* 25: 561-571.

Jendrossek , D., Schirmer , A. and Schlegel, H.G. (1996). Biodegradation of polyhydroxyalkanoic acids. *Applied Microbiology and Biotechnology* 46: 451-463.

Kai, Z., Ying, D. and Guo-Qiang, C. (2003). Effects of surface morphology on the biocompatibility of polyhydroxyalkanoates. *Biochemical Engineering Journal* 16: 115-123.

Kaihara, S., Osanai, Y., Nishikawa, K., Toshima, K., Doi, Y. and Matsumura, S. (2005). Enzymatic transformation of bacterial polyhydroxyalkanoates into repolymerizable oligomers directed towards chemical recycling. *Macromolecular Bioscience* 5: 644–652.

Karlsson, S., Sares, C., Renstad, R., & Albertsson, A. C. (1994). Gas chromatographic, liquid chromatorgraphic and gas chromatographicemass spectrometric identification of degradation products in accelerated aged microbial polyhydroxyalkanoates. *Journal of Chromatography A* 669: 97-102.

Kawalec, M., Sobota, M., Scandola, M., Kowalczuk, M. and Kurcok, P. (2010). A Convenient route to PHB macromonomers via anionically controlled moderate temperature degradation of PHB. *Journal of Polymer Science: Part A: Polymer Chemistry* 48: 5490–5497.

Keshavarz, T. and Roy, I. (2010). Polyhydroxyalkanoates: bioplastics with a green agenda. *Current Opinion in Microbiology* 13: 321-326.

Khanna, S. and Srivastava, A.K. (2005). Recent advances in microbial polyhydroxyalkanoates. *Process Biochemistry* 40: 607–619.

Kim, K.J., Doi, Y. and Abe, H. (2008). Effect of metal compounds on thermal degradation behavior of aliphatic poly(hydroxyalkanoic acid)s. *Polymer Degradation and Stability* 93: 776-785.

Kopinke, F. D., Remmler, M. and Mackenzie, K. (1996). Thermal decomposition of biodegradable polyesters – I: poly(b-hydroxybutyric acid). *Polymer Degradation Stability* 52: 25–38.

Kruse, A. and Dinjus, E. (2007). Hot compressed water as reaction medium and reactant. *The Journal of Supercritical Fluids* 41: 361-379.

Kulkarni, A., Reiche, J., Hartmann, J., Kratz, K. and Lendlein, A. (2008). Selective enzymatic degradation of poly(ε-caprolactone) containing multiblock copolymers. *European Journal of Pharmaceutics and Biopharmaceutics* 68: 46-56.

Kunasundari, B. and Sudesh, K. (2011). Isolation and recovery of microbial polyhydroxyalkanoates. *Express Polymer Letters* 5: 620-634.

Lauzier, C., Revol, J. F., Debzi, E. and Marchessault, R. H. (1994). Hydrolytic degradation of isolated poly(β-hydroxybutyrate) granules. *Polymer* 35: 4156-4162.

Lee, J.H., Lee, J.W., Khang, G. and Lee, H.B. (1998). Interaction of different types of cells on polymer surfaces with wettability gradient. *Journal of Colloid and interface science* 205: 323-330.

Lee, S. H., Oh, D. H., Ahn, W. S., Lee, Y., Choi, J. and Lee, S. Y. (2000). Production of poly(3-hydroxybutyrate-*co*-3-hydroxyhexanoate) by high-cell-density cultivation of *Aeromonas hydrophila*. *Biotechnology and Bioengineering* 67: 240-244.

Leja, K. and Lewandowicz, G. (2010). Polymer biodegradation and biodegradable polymers – a review. *Polish Journal of Environmental Studies* 19: 255-266.

Li, S. and McCarthy, S. (1999). Further investigations on the hydrolytic degradation of poly (DL-lactide). *Biomaterials* 20: 35-44.

Lim, J. and Kim, J. (2016). UV-photodegradation of poly(3-hydroxybutyrate-*co*-3-hydroxyhexanoate) (PHB-HHx). *Macromolecular Research* 24: 9-13.

Liu, Q., Shyr, T.W., Tung, C.H., Liu, Z., Shan, G., Zhu, M. and Deng, B. (2012). Particular thermal properties of poly(3-hydroxybutyrate-*co*-3-hydroxyvalerate) oligomers. *Journal of Polymer Research* 19: 9756.

Loo, C. and Sudesh, K. (2007). Polyhydroxyalkanoates: Bio-based microbial plastics and their properties. *Malaysian Polymer Journal* 2: 31-57.

Loredo-Trevino, A., Gutierrez-Sanchez, G., Rodriguez-Herrera, R. and Aguilar, C.N. (2012). Microbial enzymes involved in polyurethane biodegradation: a review. *Journal of Polymer and Environment* 20: 258-265.

Lyu, S. P. and Untereker, D. (2009). Review: Degradability of polymers for implantable biomedical devices. *International Journal of Molecular Sciences* 10: 4033-4065.

Manavitehrani, I., Fathi, A., Badr, H., Daly, S., Shirazi, A.N. and Dehghani, F. (2016). Biomedical applications of biodegradable polyesters. *Polymers* 8: 1-32.

Marchesault, R. H., Monasterios, C. J., Jesudason, J. J., Ramsay, B., Saracovan, I., Ramsay, J., et al. (1994). Chemical, enzymatic and microbialdegradation of bacteria and synthetic poly-beta-hydroxyalkanoates. *Polymer Degradation and Stability* 45: 187-196.

Mohd-Adnan, A.-F., Nishida, H. and Shirai, Y. (2008). Evaluation of kinetics parameters for poly(L-lactic acid) hydrolysis under high-pressure steam. *Polymer Degradation and Stability* 93: 1053–1058.

Montoro, S.R., Medeiros, S.F., Santos, A.M., Silva, M.B. and Tebaldi, M.L. (2013). Application of 2K experimental design and response surface methodology in the optimization of the molar mass reduction of poly (3-hydroxybutyrate-*co*-3-hydroxyvalerate) (PHBHV). *InTech* 6: 94-120.

Morikawa, H. and Marchessau, R. H. (1981). Pyrolysis of bacterial polyalkanoates. *Canadian Journal of Chemistry* 59: 2306-2313.

Mudhoo, A., Mohee, R., Unmar, G.D. and Sharma, S.K. (2011). Degradation of biodegradable and green polymers in the composting environment. *RSC Green Chemistry* 12: 332-362.

Muller, H. and Seebach, D. (1993). Poly(hydroxyalkanoates): A Fifth Class of Physiologically Important Organic Biopolymers? *Angewandte Chemie International Edition* 32: 477-502.

Nair, L.S. and Laurencin, C.T. (2007). Biodegradable polymers as biomaterials. *Progress in polymer Science* 32: 762-798.

Nguyen, S., Yu, G. and Marchessault, R.H. (2002). Thermal degradation of poly(3-hydroxyalkaoates): preparation of well-defined oligomers. *Biomacromolecules* 3: 219-224.

Nishida, H., Ariffin, H., Shirai, Y. and Hassan, M.A. (2010). Precise depolymerization of poly(3-hydroxybutyrate) by pyrolysis. *Biopolymers* 19: 370-386.

Nishida, H., Yamashita, M., Nagashima, M., Hattori, N., Endo, T. and Tokiwa, Y. (2000a). Theoretical prediction of molecular weight on autocatalytic random hydrolysis of aliphatic polyesters. *Macromolecules* 33: 6595-6601.

Nishida, H., Yamashita, M., Nagashima, M., Hattori, N., Endo, T. and Tokiwa, Y. (2000b). Thermal decomposition of poly(1,4-dioxan-2-one). *Polymer Degradation and Stability* 70: 485-496.

Nordin, N.I.A.A., Ariffin, H., Andou, Y., Hassan, M.A., Shirai, Y., Nishida, H., Yunus, W.M.Z.W., Karuppuchamy, S. and Ibrahim, N.A. (2013). Modification of oil palm mesocarp fiber characteristics using superheated steam treatment. *Molecules* 18: 9132-9146.

Ojumu, T., Yu, J. and Solomon, B. (2004). Minireview: Production of polyhydroxyalkanoates, a bacterial biodegradable polymer. *African Journal of Biotechnology* 3: 18-24.

Park, T. G. (1995). Degradation of poly(lactic-co-glycolic acid) microspheres: Effect of copolymer composition. *Biomaterials* 16: 1123-1130.

Parra, D.F., Fusaro, J., Gaboardi, F. and Rosa, D.S. (2006). Influence of poly (ethyle glycol) on the thermal, mechanical, morphological, physical-chemical and biodegradation properties of poly(3-hydrobutyrate). *Polymer Degradation and Stability* 91: 1954-1959.

Piddubnyak, V., Kurcok, P., Matuszowicz, A., Glowala, M., Fiszer-Kierzkowska, A., Jedlinski, Z., Juzwa, M. and Krawczyk, Z. (2004). Oligo-3- hydroxybutyrates as potential carriers for drug delivery. *Biomaterials* 25: 5271-5279.

Prieto, M.A., Eugenio, L.I., Galan, B., Luengo, J.M. and Witholt, B. (2007). Synthesis and degradation of polyhydroxyalkanoates. *Pseudomonas* 14: 397-428.

Qadariyah, L., Mahfud., Sumarno., Machmudah, S., Wahyudiono., Sasaki., M. and Goto, M. (2011). Degradation of glycerol using hydrothermal process. *Bioresource Technology* 102: 9267-9271.

Qu, X. H., Wu, Q., Liang, J., Zou, B., & Chen, G. Q. (2006a). Effect of 3-hydroxyhexanoate content in poly(3-hydroxybutyrate-*co*-3-hydroxyhexanoate) on *in vitro* growth and differentiation of smooth muscle cells. *Biomaterials* 27: 2944–2950.

Qu, X. H., Wu, Q., Zhang, K. Y., & Chen, G. Q. (2006b). *In vivo* studies of poly(3-hydroxybutyrate-*co*-3-hydroxyhexanoate) based polymers: biodegradation and tissue reactions. *Biomaterials* 27: 3540-3548.

Rai, R. and Roy, I. (2011). Polyhydroxyalkanoates: The emerging new green polymers of choice. *RSC Green Chemistry* 12: 80-101.

Rameshwari, R. and Meenakshisundaram, M. (2013). A review on bacterial polyester-polyhydroxyalkanoate. *International Journal of Recent Scientific Research* 4: 1781-1788.

Ramier, J., Grande, D., Langlois, V. and Renard, E. (2012). Toward the controlled production of oligoesters by microwave-assisted degradation of poly(3-hydroxyalkanoate)s. *Polymer Degradation and Stability* 97: 322-328.

Ramis, X., Cadenato, A., Salla, J.M., Morancho, J.M., Valles, A., Contat, L. and Ribes, A. (2004). Thermal degradation of polypropylene/starch-based materials with enhanced biodegradability. *Polymer Degradation and Stability* 86: 483-491.

Ravenelle, F. and Marchessault, R. H. (2002). One-step synthesis of amphiphilic diblock copolymers from bacterial poly ([R]-3-hydroxybutyric acid). *Biomacromolecules* 3: 1057–1064.

Reddy, C.S.K., Ghai, R., Rashmi, Kalia, V.C. (2003). Polyhydroxyalkanoates: an overview. *Bioresource Technology* 87: 137-146.

Reich, L. (1964). A rapid estimation of activation energy from thermogravimetric traces. *Polymer Letter* 2: *621-3.*

Rezvanian, M., Amin, M.C.I.M. and Ng, S.F. (2016). Development and physicochemical characterization of alginate composite film loaded with simvastatin as a potential wound dressing. *Carbohydrate Polymers* 137: 295-304.

Rodriguez-Conteras, A., Calafell-Monfort, M. and Marques-Calvo, M.S. (2012). Enzymatic degradation of poly(3-hydroxybutyrate-*co*-4-hydroxybutyrate) by commercial lipses. *Polymer Degradation and Stability* 97: 597-604.

Saeki, T., Tsukegi, T., Tsuji, H., Daimon, H. and Fujie, K. (2005). Hydrolytic degradation of poly[(R)-3-hydroxybutyric acid] in the melt. *Polymer* 46: 2157-2162.

Scandola, M., Mazzocchetti, L., Focarete, M. L., Kawalec, M., Kurcok, P., Adamus, G and Kowalezuk, Z. (2011). *Process for controlled degradation of polyhydroxyalkanoates and products obtainable therefrom*. United States Patent, PCT/IT2008/000646.

Schroeter, M., Wildermann, B. and Lendlein, A. (2011). Biodegradable materials. *Regenerative Medicine* 20: 469-492.

Shimamura, E. and Kasuya, K. (1994). Physical properties and biodegradability of microbial poly(3-hydroxybutyrate-*co*-3-hydroxyhexanoate). *Macromolecules* 27: 878-880.

Shrivastav, A., Kim, H.Y. and Kim, Y.R. (2013). Advances in the applications of polyhydroxyalkanoate nanoparticles for novel drug delivery system. *BioMed Research International* 2013: 1-12.

Sin, M.C., Gan, S.N., Annuar, M.S.M. and Tan, I.K.P. (2010). Thermodegradation of medium-chain-length poly(3-hydroxyalkanoates) produced by *Pseudomonas putida* from oleic acid. *Polymer Degradation and Stability* 95: 2334-2342.

Sin, M.C., Tan, I.K.P., Annuar, M.S.M. and Gan, S.N. (2011). Characterization of oligomeric hydroxyalkanoic acids from thermal decomposition of palm kernel oil–based biopolyester. *International Journal of Polymer Analysis and Characterization* 16: 337–347.

Sudesh, K., Abe, H. and Doi, Y. (2000). Synthesis, structure and properties of polyhydroxyalkanoates: biological polyesters. *Progress in Polymer Science* 25: 1503-1555.

Sun, J., Dai, Z., Zhaob, Y. and Chena, G.Q. (2007). *In vitro* effect of oligo-hydroxyalkanoates on the growth of mouse fibroblast cell line L929. *Biomaterials* 28: 3896–3903.

Tamada, Y. and Ikada, Y. (1993). Cell adhesion to plasma-treated polymer surfaces. *Polymer* 34: 2208-2212.

Tian, P.Y., Shang, L., Ren, H., Mi, Y., Fan, D.D. and Jiang, M. (2009). Biosynthesis of polyhydroxydroxyalkanoates: current research and development. *African Journal of Biotechnology* 8: 709-714.

Tokiwa, Y. and Suzuki, T. (1978). Hydrolysis of polyesters by Rhizopus delemar lipase. *Agricultural and Biological Chemistry* 42: 1071–1072.

Tripathi, L., Wu, L. P., Chen, J. C. and Chen, G. Q. (2012). Synthesis of Diblock copolymer poly-3-hydroxybutyrate–block-poly-3-hydroxyhexanoate [PHB-b-PHHx] by a β-oxidation weakened Pseudomonas putida KT2442. *Microbial Cell Factories* 11*:* 1-11.

Tsuji, H. (2002). Autocatalytic hydrolysis of amorphous-made polylactides: effects of L-lactide content, tacticity, and enantiomeric polymer blending. *Polymer* 43: 1789-1796.

Tsuji, H. and Miyauchi, S. (2001). Poly(L-lactide): VI. Effects of crystallinity on enzymatic hydrolysis of poly(L-lactide) without free amorphous region. *Polymer Degradation and Stability* 71: 415-424.

Wang, S., Chen, W., Xiang, H., Yang, J., Zhao, Z. and Zhu, M. (2016). Modification and potential application of short-chain-length polyhydroxyalkanoate (SCL-PHA). *Polymers* 8: 273.

Wang, W. C., Turner, T. L., Roberts, W. L. and Stikeleather, L. F. (2012). Direct injection of superheated steam for continuous hydrolysis reaction. *Chemical Engineering and Processing* 59: 52–59.

Wang, Y. W., Mo, W. K., Yao, H. L., Wu, Q., Chen, J. C. and Chen, G. Q. (2004). Biodegradation studies of poly(3-hydroxybutyrate-co-3-hydroxyhexanoate. *Polymer Degradation and Stability* 85: 815-821.

Wang, Y., Inagawa, Y., Saito, T., Kasuya., K., Doi, Y. and Inoue, Y. (2002). Enzymatic hydrolysis of bacterial poly(3-hydroxybutyrate-*co*-3-hydroxypropionate)s by poly(3-hydroxyalkanoate) depolymerase from *Acidovorax Sp*. TP4. *Biomacromolecules* 3: 828-834.

Wang, Y.W., Yang, F., Wu, Q., Cheng, Y.C., Yu, P.H.F., Chen, J. and Chen, G.Q. (2005). Effect of composition of poly(3-hydroxybutyrate-*co*-3-hydroxyhexanoate) on growth of fibroblast and osteoblast. *Biomaterials* 26: 755-761.

Watanabe, M., Matsuo, Y., Matsushita, T., Inomata, H., Miyake, T. and Hironaka, K. (2009). Chemical recycling of polycarbonate in high pressure high temperature steam at 573 K. *Polymer Degradation and Stability* 94: 2157–2162.

Xu, L.C. and Siedlecki, C.A. (2007). Effects of surface wettability and contact time on protein adhesion to biomaterial surfaces. *Biomaterials* 28: 3273-3283.

Yang, H. X., Sun, M. and Zhou, P. (2009). Investigation of water diffusion in poly(3-hydroxybutyrate-*co*-3-hydroxyhexanoate) by generalized two-dimensional correlation ATR-FTIR spectroscopy. *Polymer* 50: 1533-1540.

Yang, Q. X., Wang, J., Zhang, S., Tang, X., Shang, G., Peng, Q., Wang, R. and Cai, X. (2014). The properties of poly(3-hydroxybutyrate-*co*-3-hydroxyhexanoate) and its applications in tissue engineering. *Current Stem Cell Research and Theraphy* 9: 215-222.

Yang, X. S., Zhao, K. and Chen, G. Q. (2002). Effect of surface treatment on the biocompatibility of microbial polyhydroxyalkanoates. *Biomaterials* 23: 1391-1397.

Ye, H.M., Wang, Z., Wang, H.H., Chen, G.Q. and Xu, J. (2010). Different thermal behaviors of microbial polyesters poly(3-hydroxybutyrate-*co*-3-hydroxyvalerate-*co*-3-hydroxyhexanoate) and poly(3-hydroxybutyrate-*co*-3-hydroxyhexanoate). *Polymer* 51: 6037-6046.

Yezza, A., Halasz, A., Levadoux, W. and Hawari, J. (2007). Production of poly-β-hydroxybutyrate (PHB) by *Alcaligenes latus* from maple sap. *Applied Microbiology and Biotechnology* 77: 269–274.

Yoon, J. S., Jin, H.-J., Chin, I.-J., Kim, C. and Kim, M.-N. (1997). Theoretical prediction of weight loss and molecular weight during random chain scission degradation of polymers. *Polymer* 38: 3573–3579.

Yu, G. and Marchessault, R.H. (2000). Characterization of low molecular weight poly(β -hydroxybutyrate)s from alkaline and acidic hydrolysis. *Polymer* 41: 1087-1098.

Yu, J., Plackett, D. and Chen, L.X.L. (2005). Kinetics and mechanism of the monomeric products from abiotic hydrolysis of poly[(*R*)-3-hydroxybutyrate] under acidic and alkaline conditions. *Polymer Degradation and Stability* 89: 289-299.

Zahari, M.A.K.M., Abdullah, S.S.S., Roslan, A.M., Ariffin, H., Shirai, Y. and Hassan, M.A. (2014). Efficient utilization of oil palm fond for bio-based products and biorefinery. *Journal of Cleaner Production* 65: 252-260.

Zahari, M.A.K.M., Zakaria, M.R., Ariffin, H., Mokhtar, M.N., Salihon, J., Shirai, Y. and Hassan, M.A. (2012). Renewable sugars from oil palm frond juice as an alternative novel fermentation feedstock for value-added products. *Bioresource Technology* 110: 566-571.

Zhao, K., Deng, Y., Chen, J.C. and Chen, G.Q. (2003). Polyhydroxyalkanoate (PHA) scaffolds with good mechanical properties and biocompatibility. *Biomaterials* 24, 104-1045.

Zhao, Q., Wang, S., Kong, M., Geng, W., Li, R.K.Y., Song, C. and Kong, D. (2012). Phase morphology, physical properties, and biodegradation behavior of novel PLA/PHBHHx blends. *Journal of Biomaterial Research Part B*: 100: 23-31.

Zheng, Z., Bei, F.-F., Tian, H.-L. and Chen, G.Q. (2005). Effects of crystallization of polyhydroxyalkanoate blend on surface physicochemical properties and interactions with rabbit articular cartilage chondrocytes. *Biomaterials* 26: 3537– 3548.

Zinn, M., Witholt, B. and Egli, T. (2001). Occurrence, synthesis and medical application of bacterial polyhydroxyalkanoate. *Advanced Drug Delivery Reviews* 53: 5-21.

Zulkifli, F.H., Hussain, F.S.J., Rasad, M.S.B.A. and Yusoff, M.M. (2014). *In vitro* degradation study of novel HEC/PVA/collagen nanofirous scaffold for skin tissue engineering applications. *Polymer Degradation and Stability* 110: 473-481.

Appendix A

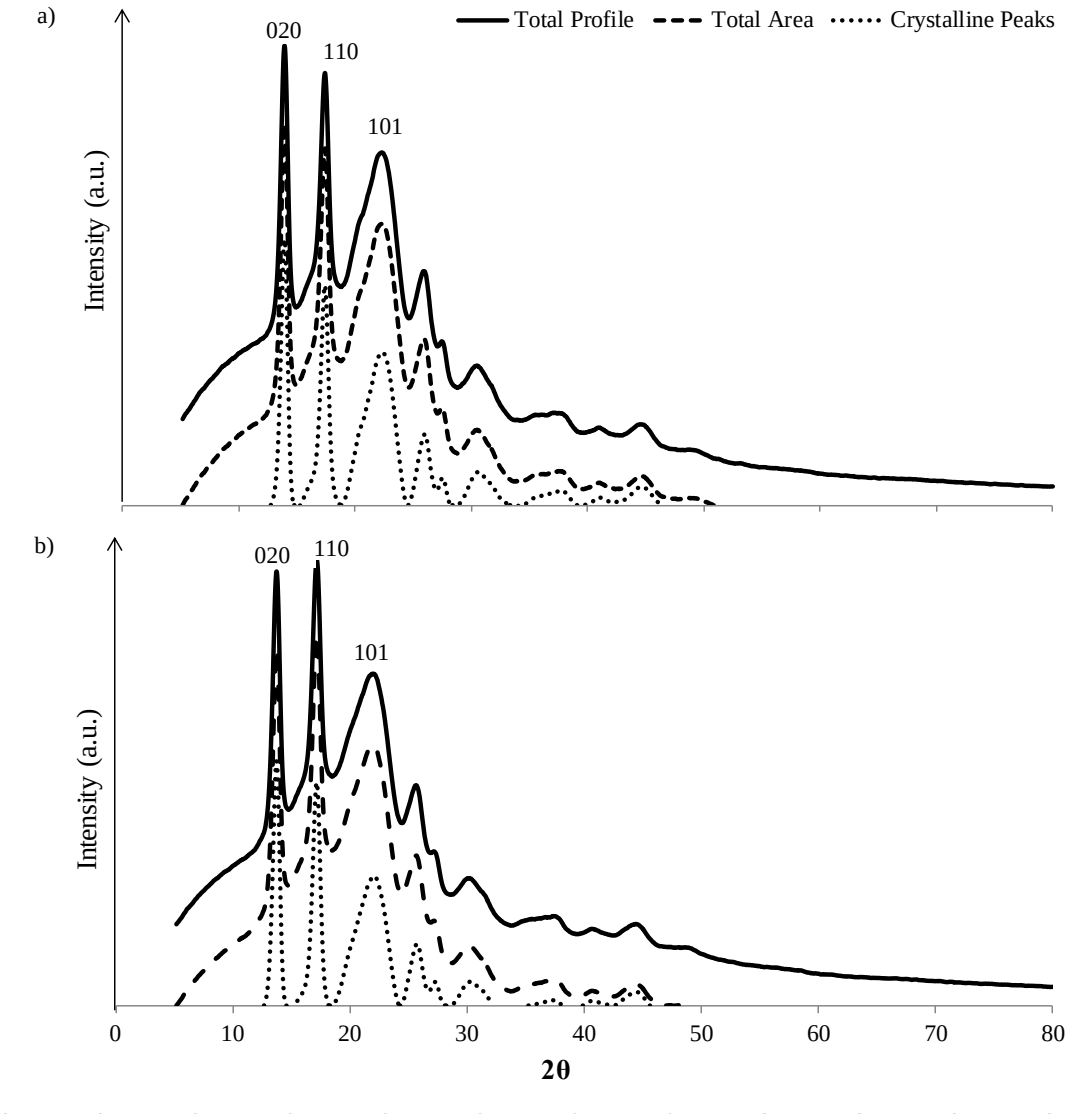

Appendix A1. X-ray diffraction profiles of (a) P(HB-*co*-6%HHx) and (b) P(HB-*co*-11%HHx)

Appendix A2. Crystallographic parameters of PHBHHx

PHBHHx	Crystallographic parameters								
	[020]			[110]			[101]		
	2θ[a] (°)	*d*[020][b] (nm)	*D*[c] (nm)	2θ (°)	*d*[110] (nm)	*D* (nm)	2θ (°)	*d*[101] (nm)	*D* (nm)
P(HB-*co*-6%HHx)	13.96	0.632	12.89	17.44	0.506	11.16	22.38	0.394	2.65
P(HB-*co*-11%HHx)	13.74	0.642	12.61	17.20	0.514	11.05	22.04	0.400	2.25

[a]Calculated from X-ray diffraction profiles
[b]Calculated by Bragg equation from 2θ values
[c]Represents the depth of crystalline direction

Appendix A3. Percentage of weight loss (%) for PHBHHx film strips at SHS treatment temperature of 130 °C

Sampling time (minutes)	Percentage of weight loss (%) at SHS treatment of 130 °C	
	P(HB-*co*-6%HHx)	P(HB- *co*-11%HHx)
60	0.092 ± 0.001	0.096 ± 0.008
120	0.111 ± 0.032	0.070 ± 0.035
180	0.112 ± 0.096	0.155 ± 0.033
240	0.154 ± 0.035	0.135 ± 0.129
300	0.242 ± 0.032	0.210 ± 0.116
360	0.240 ± 0.030	0.198 ± 0.035
420	0.233 ± 0.088	0.202 ± 0.034
480	0.289 ± 0.034	0.230 ± 0.069
540	0.310 ± 0.014	0.230 ± 0.016
600	0.336 ± 0.180	0.252 ± 0.027

Note: Values are expressed as mean and standard deviation (n =2)

Appendix A4. Percentage of weight loss (%) for PHBHHx film strips at SHS treatment temperature of 150 °C

Sampling time (minutes)	Percentage of weight loss (%) at SHS treatment of 150 °C	
	P(HB-*co*-6%HHx)	P(HB- *co*-11%HHx)
40	0.173 ± 0.005	0.069 ± 0.034
80	0.194 ± 0.035	0.086 ± 0.004
120	0.258 ± 0.061	0.090 ± 0.064
160	0.260 ± 0.001	0.114 ± 0.032
200	0.333 ± 0.028	0.216 ± 0.004
240	0.296 ± 0.107	0.270 ± 0.130
280	0.337 ± 0.045	0.265 ± 0.066
320	0.336 ± 0.129	0.276 ± 0.081
360	0.364 ± 0.082	0.255 ± 0.007
400	0.367 ± 0.068	0.292 ± 0.103

Note: Values are expressed as mean and standard deviation (n =2)

Appendix A5. Percentage of weight loss (%) for PHBHHx film strips at SHS treatment temperature of 170 °C

Sampling time (minutes)	Percentage of weight loss (%) at SHS treatment of 170 °C	
	P(HB-*co*-6%HHx)	P(HB- *co*-11%HHx)
30	0.200 ± 0.033	0.173 ± 0.056
60	0.265 ± 0.118	0.238 ± 0.034
90	0.378 ± 0.035	0.331 ± 0.015
120	0.420 ± 0.025	0.375 ± 0.042
150	0.423 ± 0.018	0.384 ± 0.037
180	0.452 ± 0.320	0.358 ± 0.002
210	0.584 ± 0.087	0.556 ± 0.180
240	0.682 ± 0.152	0.591 ± 0.168
270	0.658 ± 0.412	0.624 ± 0.037
300	0.699 ± 0.011	0.675 ± 0.097

Note: Values are expressed as mean and standard deviation (n =2)

Appendix A6. Percentage of weight loss (%) for PHBHHx film strips at SHS treatment temperature of 190 °C

Sampling time (minutes)	Percentage of weight loss (%) at SHS treatment of 190 °C	
	P(HB-*co*-6%HHx)	P(HB- *co*-11%HHx)
20	0.309 ± 0.071	0.271 ± 0.129
40	0.459 ± 0.351	0.285 ± 0.081
60	0.582 ± 0.145	0.356 ± 0.208
80	0.830 ± 0.024	0.430 ± 0.242
100	1.087 ± 0.385	0.505 ± 0.278
120	1.196 ± 0.161	0.791 ± 0.073
140	2.235 ± 0.694	1.083 ± 0.195
160	2.270 ± 0.399	1.303 ± 0.598
180	2.520 ± 1.360	2.295 ± 0.141
200	3.131 ± 1.595	2.631 ± 0.005

Note: Values are expressed as mean and standard deviation (n =2)

Appendix A7. Molecular weight reduction data of PHBHHx film strips at SHS treatment temperature of 130 °C

Sampling time (minutes)	Molecular weight reduction data at SHS treatment of 130 °C					
	P(HB-*co*-6%HHx)			P(HB- *co*-11%HHx)		
	M_w (kDa)	M_n (kDa)	PDI	M_w (kDa)	M_n (kDa)	PDI
0	304.5 ± 5.0	111.5 ± 2.1	2.73	351.5 ± 29.0	125.5 ± 0.7	2.80
60	333.0 ± 0.0	128.0 ± 0.0	2.60	347.0 ± 5.7	137.5 ± 0.7	2.52
120	257.5 ± 34.6	90.5 ± 27.6	2.85	305.0 ± 2.8	122.0 ± 0.0	2.50
180	266.0 ± 5.7	105.0 ± 2.8	2.53	295.5 ± 0.7	117.0 ± 0.0	2.53
240	240.5 ± 7.8	96.5 ± 2.1	2.49	260.0 ± 4.2	104.0 ± 1.4	2.50
300	205.0 ± 2.8	86.0 ± 2.8	2.38	242.0 ± 9.9	98.0 ± 2.8	2.47
360	200.5 ± 5.0	82.5 ± 0.7	2.43	235.0 ± 8.5	94.5 ± 2.1	2.49
420	166.0 ± 2.8	73.0 ± 1.4	2.27	206.5 ± 0.7	83.5 ± 0.7	2.47
480	165.0 ± 5.7	70.5 ± 2.1	2.34	213.5 ± 7.8	87.0 ± 2.8	2.45
540	188.0 ± 0.0	79.0 ± 0.0	2.38	179.5 ± 5.0	76.0 ± 1.4	2.36
600	138.5 ± 0.7	56.5 ± 0.7	2.45	180.0 ± 8.5	76.5 ± 3.5	2.35

Note: Values are expressed as mean and standard deviation (n =2)

Appendix A8. Molecular weight reduction data of PHBHHx film strips at SHS treatment temperature of 150 °C

Sampling time (minutes)	Molecular weight reduction data at SHS treatment of 150 °C					
	P(HB-*co*-6%HHx)			P(HB- *co*-11%HHx)		
	M_w (kDa)	M_n (kDa)	PDI	M_w (kDa)	M_n (kDa)	PDI
0	304.5 ± 5.0	111.5 ± 2.1	2.73	351.5 ± 29.0	125.5 ± 0.7	2.80
40	314.5 ± 7.8	123.5 ± 3.5	2.55	354.0 ± 2.8	157.0 ± 25.5	2.25
80	260.0 ± 0.0	100.5 ± 0.7	2.59	277.5 ± 0.7	113.0 ± 0.0	2.46
120	216.5 ± 5.0	81.5 ± 2.1	2.66	237.0 ± 4.2	91.5 ± 2.1	2.59
160	180.5 ± 0.7	69.5 ± 0.7	2.60	196.0 ± 7.1	91.5 ± 26.2	2.14
200	135.5 ± 0.7	54.5 ± 0.7	2.49	170.5 ± 3.5	67.5 ± 2.1	2.53
240	128.5 ± 2.1	51.5 ± 0.7	2.50	162.0 ± 2.8	65.0 ± 1.4	2.49
280	99.0 ± 4.2	42.0 ± 1.4	2.36	122.5 ± 0.7	49.0 ± 0.0	2.50
320	94.5 ± 2.1	40.0 ± 1.4	2.36	141.0 ± 1.4	57.0 ± 1.4	2.47
360	95.5 ± 17.7	39.5 ± 5.0	2.42	102.5 ± 2.1	42.5 ± 0.7	2.41
400	72.5 ± 7.8	30.5 ± 3.5	2.38	107.0 ± 5.7	44.5 ± 2.1	2.40

Note: Values are expressed as mean and standard deviation (n =2)

Appendix A9. Molecular weight reduction data of PHA film strips at SHS treatment temperature of 170 °C

Sampling time (minutes)	Molecular weight reduction data at SHS treatment of 170 °C					
	P(HB-*co*-6%HHx)			P(HB-*co*-11%HHx)		
	M_w (kDa)	M_n (kDa)	PDI	M_w (kDa)	M_n (kDa)	PDI
0	304.5 ± 5.0	111.5 ± 2.1	2.73	351.5 ± 29.0	125.5 ± 0.7	2.80
30	265.0 ± 21.2	103.5 ± 5.0	2.56	279.0 ± 14.1	107.0 ± 4.2	2.61
60	147.5 ± 3.5	62.5 ± 0.7	2.36	162.5 ± 5.0	69.0 ± 1.4	2.36
90	62.5 ± 31.8	17.5 ± 6.4	3.57	112.5 ± 10.6	48.5 ± 3.5	2.32
120	58.0 ± 2.9	27.5 ± 0.7	2.11	65.5 ± 3.5	30.5 ± 0.7	2.15
150	32.5 ± 2.1	15.0 ± 1.4	2.17	36.5 ± 2.1	19.5 ± 0.7	1.87
180	29.0 ± 0.0	13.0 ± 0.0	2.23	45.5 ± 0.7	21.5 ± 0.7	2.12
210	19.0 ± 1.4	9.5 ± 0.7	2.00	20.5 ± 0.7	10.0 ± 0.0	2.05
240	16.5 ± 0.7	7.0 ± 0.0	2.36	26.0 ± 4.2	12.0 ± 1.4	2.17
300	14.1 ± 1.3	7.5 ± 0.5	1.87	21.0 ± 0.0	10.0 ± 0.0	2.10

Note: Values are expressed as mean and standard deviation (n =2)

Appendix A10. Molecular weight reduction data of PHA film strips at SHS treatment temperature of 190 °C

Sampling time (minutes)	Molecular weight reduction data at SHS treatment of 190 °C					
	P(HB-*co*-6%HHx)			P(HB- *co*-11%HHx)		
	M_w (kDa)	M_n (kDa)	PDI	M_w (kDa)	M_n (kDa)	PDI
0	304.5 ± 5.0	111.5 ± 2.1	2.73	351.5 ± 29.0	125.5 ± 0.7	2.80
20	192.5 ± 2.1	72.0 ± 1.4	2.67	209.0 ± 14.1	76.5 ± 5.0	2.73
40	63.5 ± 2.1	28.5 ± 0.7	2.23	69.0 ± 5.7	30.0 ± 2.8	2.30
60	34.0 ± 5.7	17.0 ± 2.8	2.00	47.5 ± 0.7	22.0 ± 0.0	2.16
80	23.5 ± 0.7	8.0 ± 1.4	2.94	18.5 ± 0.7	7.5 ± 0.7	2.47
100	10.0 ± 0.0	4.0 ± 0.0	2.50	15.0 ± 4.2	6.0 ± 1.4	2.50
120	10.0 ± 1.4	4.0 ± 0.0	2.50	11.5 ± 0.7	5.0 ± 0.0	2.30
140	5.0 ± 0.0	2.0 ± 0.0	2.50	5.0 ± 0.0	2.0 ± 0.0	2.50
160	5.5 ± 0.7	2.5 ± 0.7	2.20	8.0 ± 1.4	3.5 ± 0.7	2.29
200	4.0 ± 0.0	2.0 ± 0.0	2.00	5.5 ± 0.7	2.5 ± 0.7	2.20

Note: Values are expressed as mean and standard deviation (n =2)

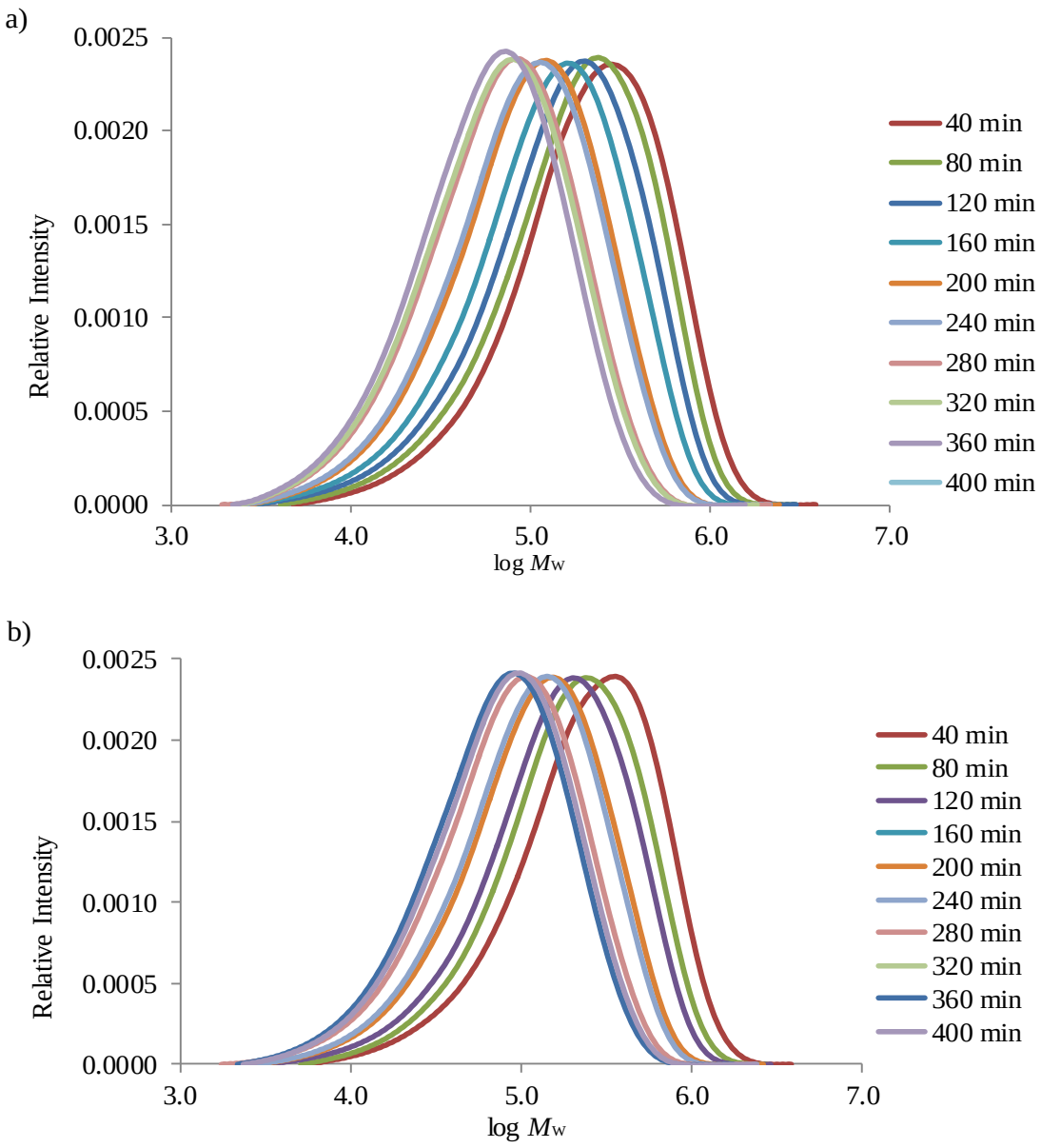

Appendix A11. Time-dependent changes in SEC profile of (a) P(HB-*co*-6%HHx) (b) P(HB-*co*-11%HHx) during superheated steam hydrolysis treatment at 150 °C

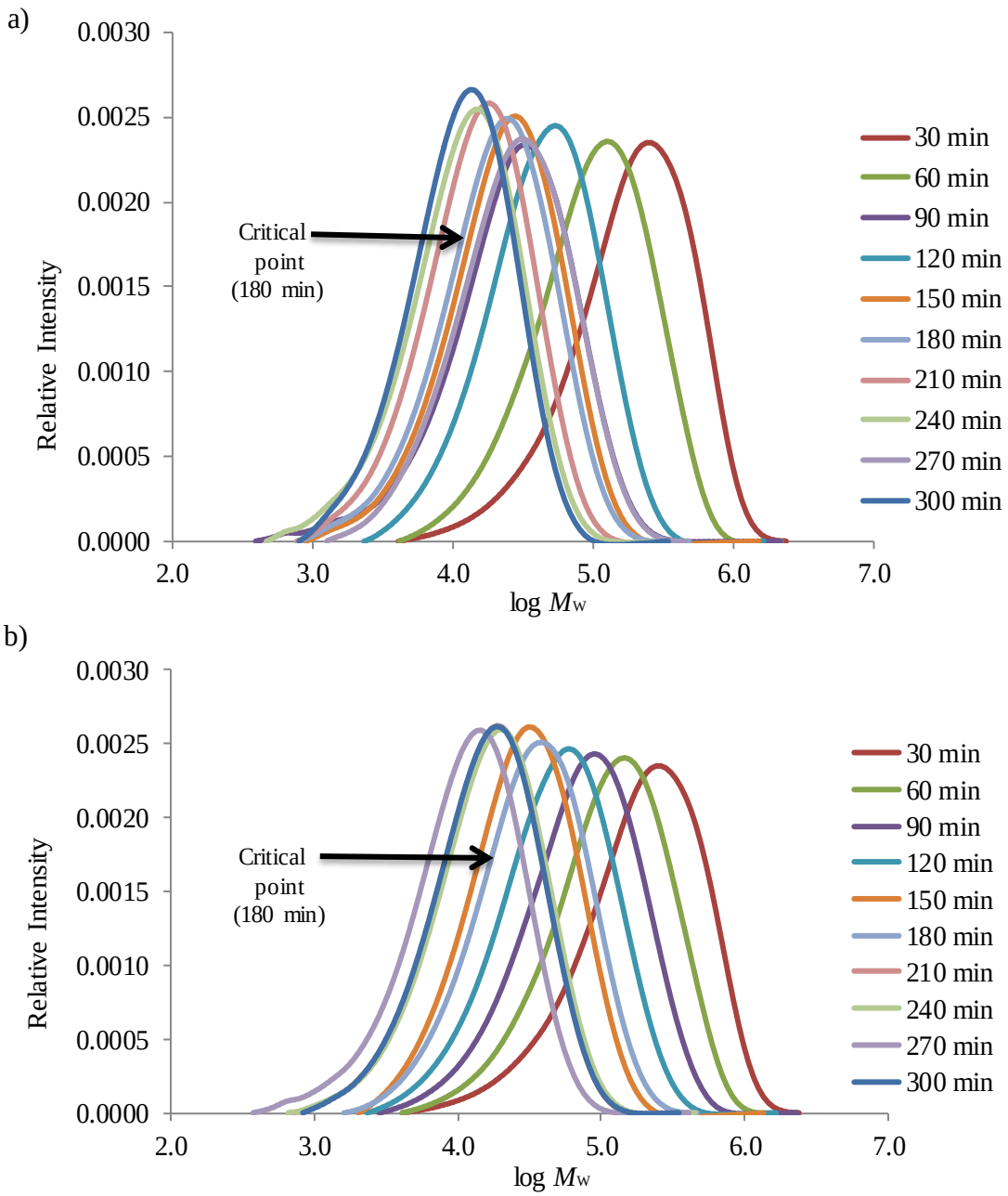

Appendix A12. Changes in SEC profile of (a) P(HB-*co*-6%HHx) (b) P(HB-*co*-11%HHx) during superheated steam hydrolysis treatment at 170 °C

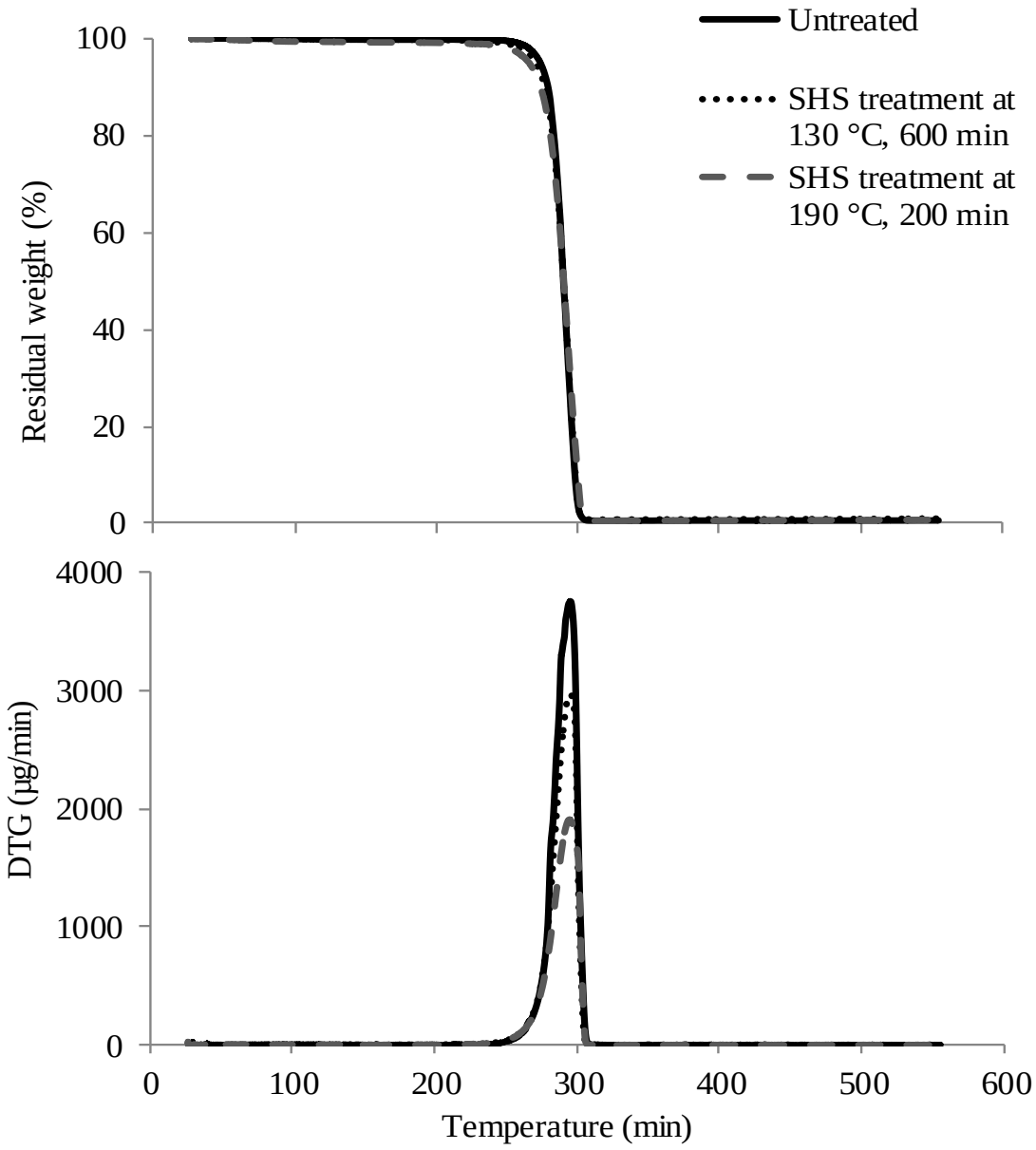

Appendix A13. Thermogravimetric (TG) and differential thermogravimetric (DTG) profiles of P(HB-*co*-6%HHx)

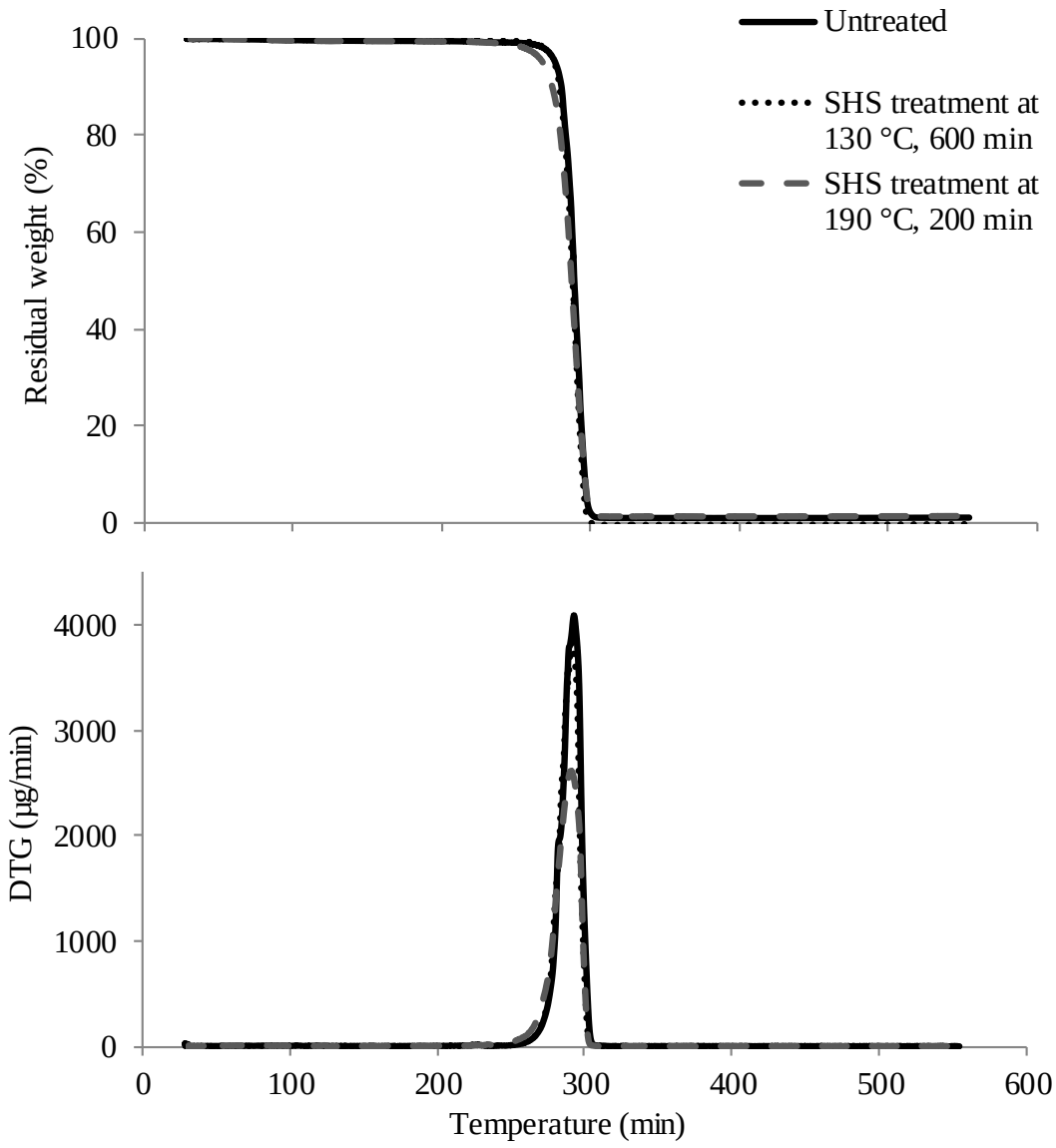

Appendix A14. Thermogravimetric (TG) and differential thermogravimetric (DTG) profiles of P(HB-*co*-11%HHx)

Appendix A15. Changes in co-monomer unit of SHS treated PHBHHx samples based on ^{1}HNMR spectra for treatment temperature range of 130 – 190 °C

PHA sample	SHS treatment		Relative Intensity		Composition (%)	
	Temperature (°C)	Time (min)	HHx, A	HB, B	HHx unit	HB unit
P(HB-*co*-6%HHx)	Untreated	0	0.0612	1.0	6.0	94.0
	130	60	0.0607	1.0	6.0	94.0
		600	0.0594	1.0	6.0	94.0
	150	40	0.0594	1.0	6.0	94.0
		400	0.0598	1.0	6.0	94.0
	170	30	00604	1.0	6.0	94.0
		300	0.0623	1.0	6.0	94.0
	190	20	0.0616	1.0	6.0	94.0
		200	0.0603	1.0	6.0	94.0
P(HB-*co*-11%HHx)	Untreated	0	0.1142	1.0	11.0	89.0
	130	60	0.1146	1.0	11.0	89.0
		600	0.1149	1.0	11.0	89.0
	150	40	0.1151	1.0	11.0	89.0
		400	0.1152	1.0	11.0	89.0
	170	30	0.1142	1.0	11.0	89.0
		300	0.1147	1.0	11.0	89.0
	190	20	0.1142	1.0	11.0	89.0
		200	0.1143	1.0	11.0	89.0

Calculation method:

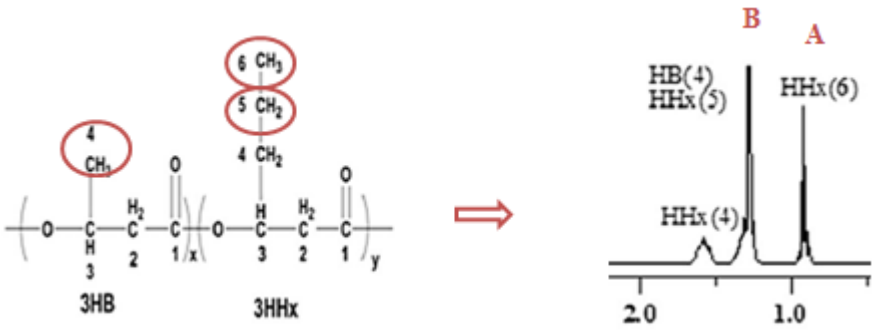

Based on above assumption,

The formula that can be used to calculate percentage of HHx is derived.

Let

x = composition of HB (assumed to be 1); y = composition of HHx

Thus,

$\%\ HHx = y/(1+y) \times 100\%$ [1]

A : B = (3 H at C_6 of HHx) : (3 H at C_4 of HB + 2 H at C_5 of HHx)

A : B = (3y) : (3 + 2y)

(3y)B = (3 + 2y)A

$y = 3A/(3B-2A)$ [2]

By substitute the value of y from [2] into [1], the percentage of HHx was determined.

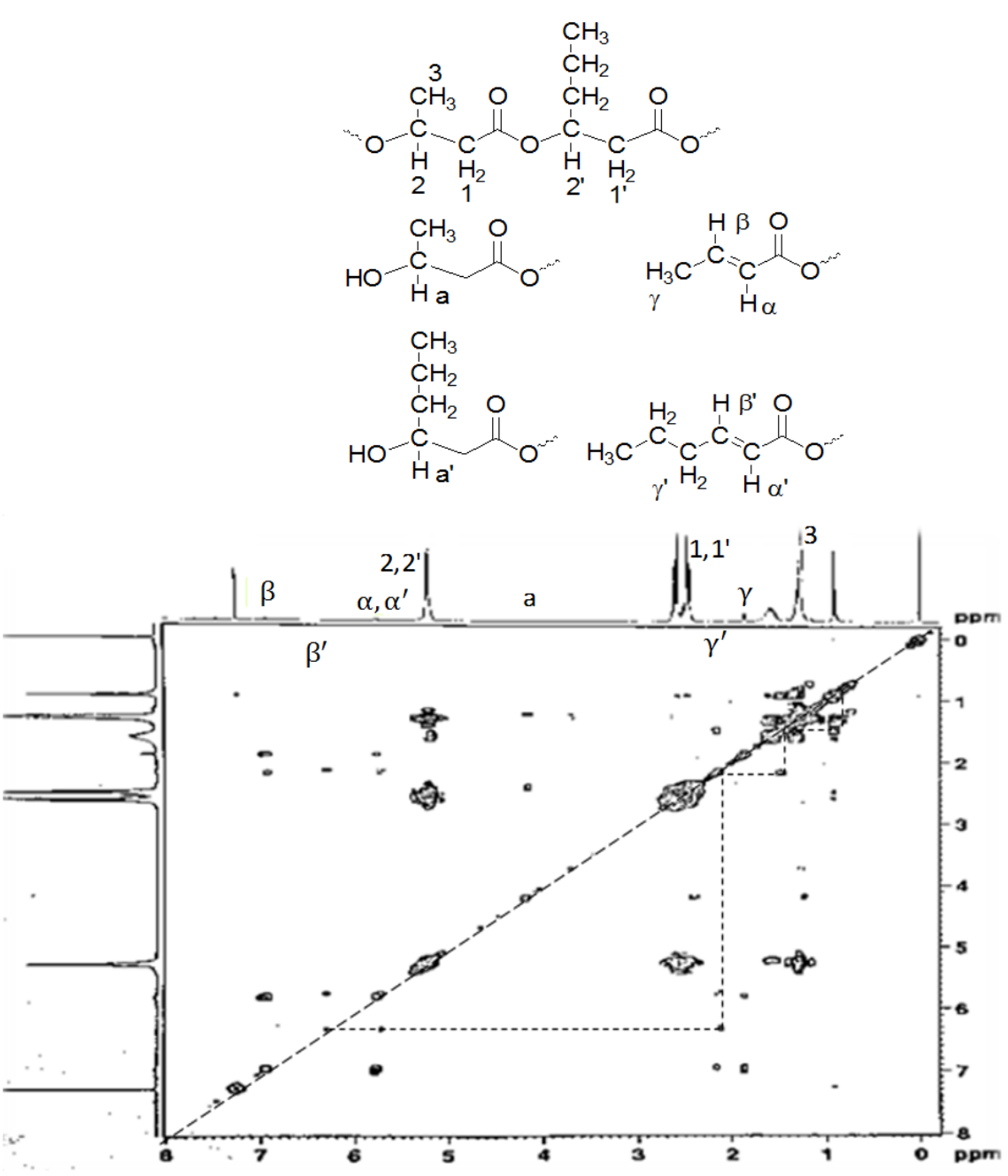

Appendix A16. ^{1}H–^{1}H COSY of P(HB-*co*-11%HHx) hydrolyzates at the end of SHS treatment of 190 °C

Appendix B

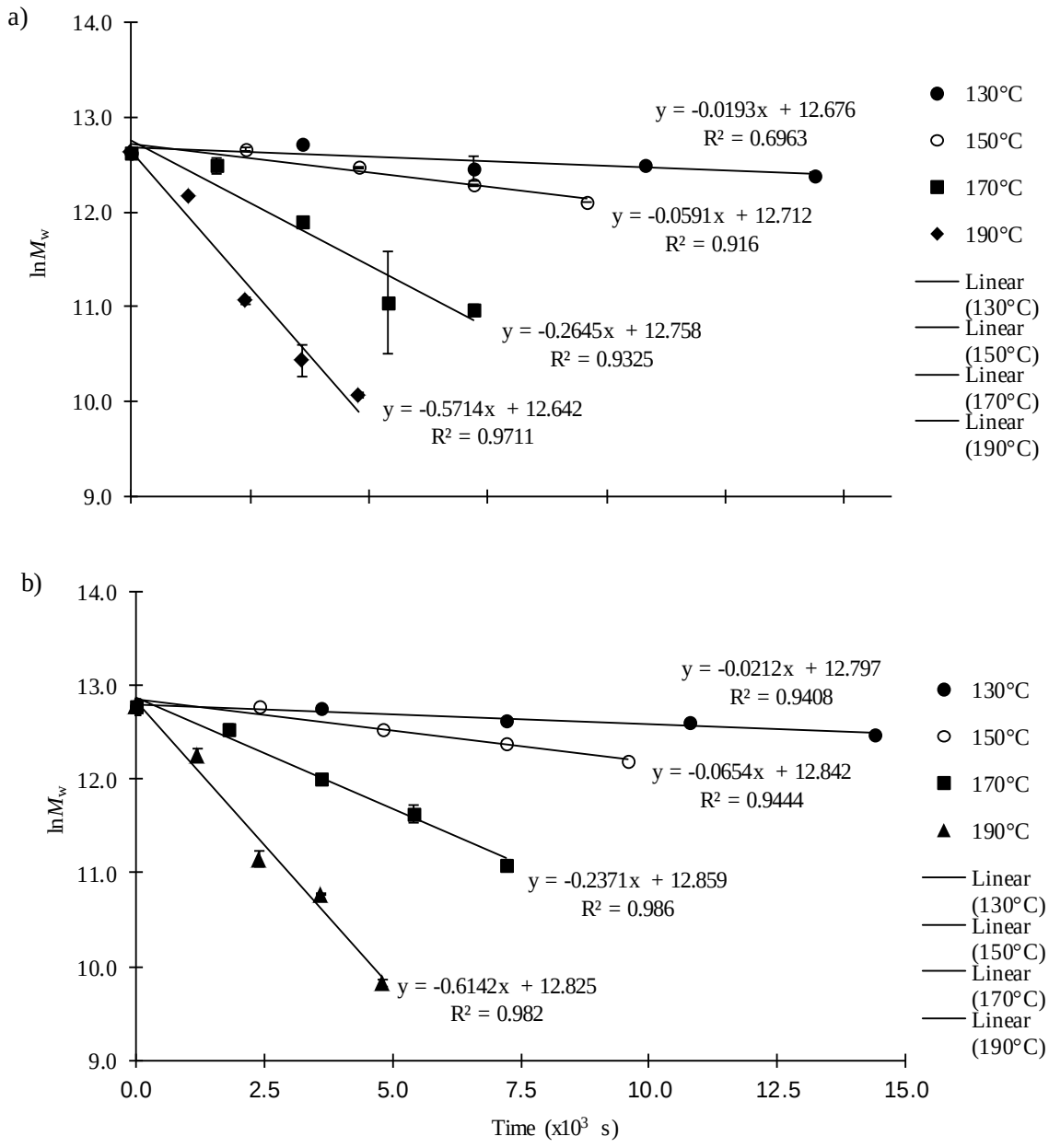

Appendix B1. Plots of 1/M_w versus time for (a) P(HB-*co*-6%HHx) (b) P(HB-*co*-11%HHx) during SHS hydrolysis treatment temperature range of 130 - 190 °C

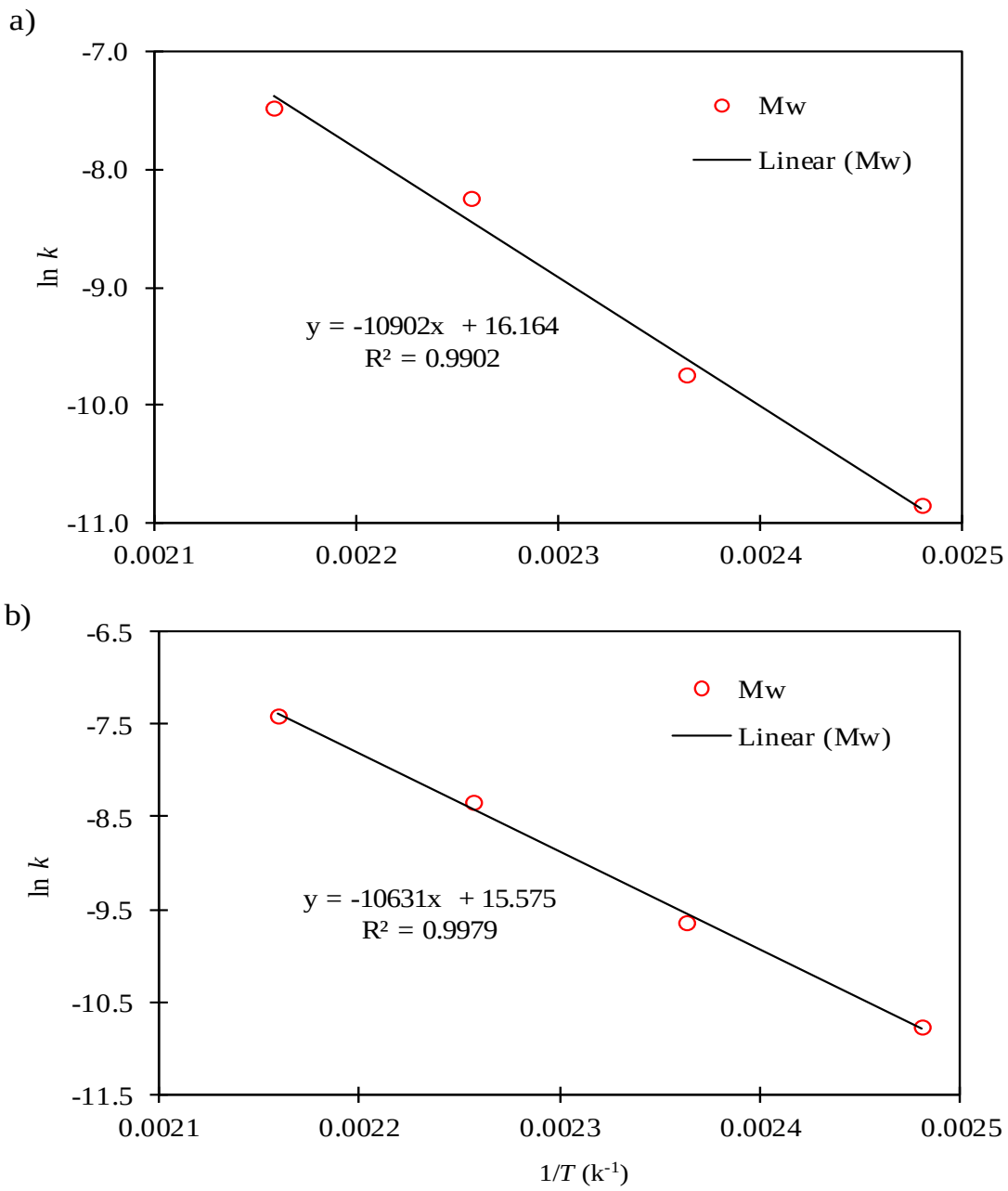

Appendix B2. Plots of ln *k* versus 1/*T* for (a) P(HB-*co*-6%HHx) (b) P(HB-*co*-11%HHx) during SHS hydrolysis treatment temperature range of 130 - 190 °C

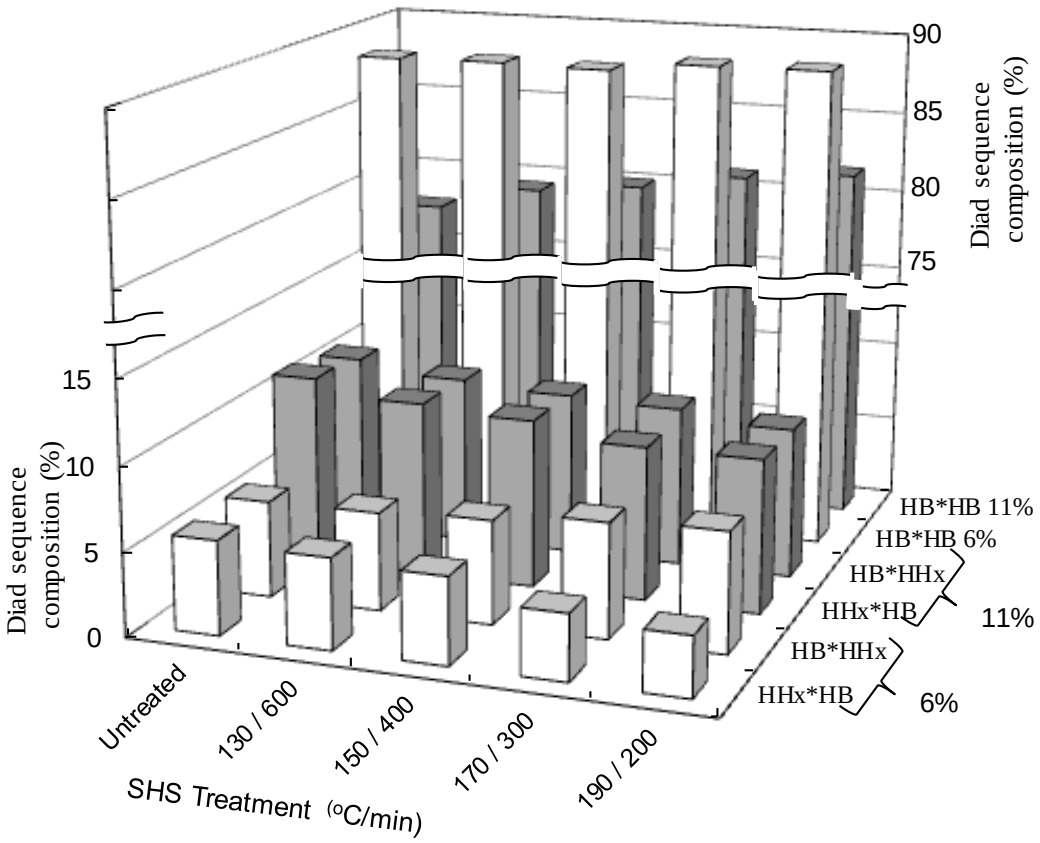

Appendix B3. Changes in diad sequence distribution of SHS treated PHBHHx samples: P(HB-*co*-6%HHx) and P(HB-*co*-11%HHx)

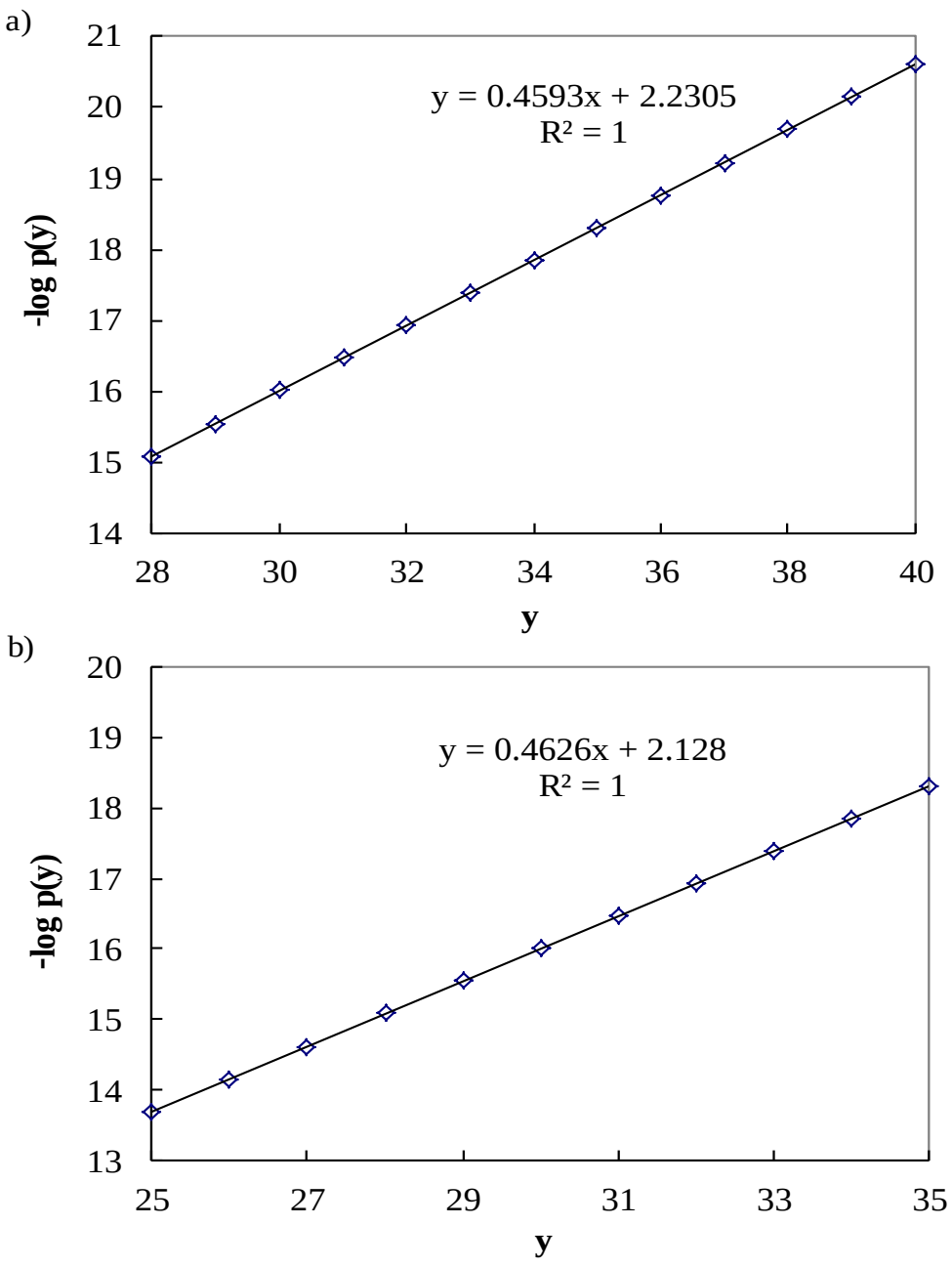

Appendix B4. Recalculated values of *a* and *b* constants (a) P(HB-*co*-6%HHx) (b) P(HB-*co*-11%HHx)

Appendix C

Appendix C1

Preparation of DMEM media (g/L)

1) DMEM media powder (Gibco)	1 pack	dissolved in 1L of sterile deionized water and filtered using media filter ↓
2) Sodium bicarbonate, $NaHCO_3$	1.5g	
3) Glucose	4.5g	
4) 10mM Hepes	2.383mL	
5) 10mM Sodium pyruvate	0.11mL	after filtration, 1% penicillin-streptomycin and 10% fetal bovine serum was added
6) Penicillin-Streptomycin	1% (10mL)	
7) Fetal bovine serum	10% (100mL)	

Preparation of 10mM hepes stock solution

Volume of stock solution to be prepared = 10mL (0.01L)

Molecular weight = 238.3012 g/mol

Molarity, M =10mM (10mmol/L)

Calculation:

$0.01L \times 10mmol/L = 0.1mmol$

0.1×10^{-3} mol $\times$ 238.3012 g/mol

$0.0238301g \approx 0.0238g$

Thus, 0.0238g of hepes was dissolved in 10mL of deionized water to prepare 10mL of stock solution.

Preparation of 10mM sodium pyruvate stock solution

Volume of stock solution to be prepared = 5mL (0.005L)

Molecular weight = 110.0 g/mol

Molarity, M =10mM (10mmol/L)

Calculation:

0.005L × 10mmol/L = 0.05mmol

0.05×10^{-3} mol × 110.0 g/mol

0.0055g

Thus, 0.0055g of sodium pyruvate was dissolved in 5mL of deionized water to prepare 5mL of stock solution.

Preparation of 1× phosphate buffer saline solution

1) Sodium chloride, NaCl 8.0g
2) Potassium chloride, KCl 0.2g
3) Sodium hydrogen phosphate, Na_2HPO_4 1.44g
4) Potassium dihydrogen phosphate, KH_2PO_4 0.24g

dissolved in 800mL of sterile deionized water, the pH was adjusted to 7.4 with HCl, then the total final volume of was bought to 1L

↓

stored at 4 °C